MSc Thesis

Combined Self-Healing Method for Lifetime Extension in Asphalt - A Mechanical and Sustainability Assessment

MS53035
Peter John Recordon

Delft University of Technology

TU Delft

MSc Thesis

Combined Self-Healing Method for Lifetime Extension in Asphalt - A Mechanical and Sustainability Assessment

by

Peter John Recordon

Student Name	Student Number
P.J. Recordon	5621763

Supervisor, TU Delft (Chair):	Prof. dr. ir. J.M.C. (Arjan) Mol
Supervisor, TU Delft:	Prof. dr. ir. E. (Erik) Schlangen
Supervisor, TU Delft:	Dr. S. (Shi) Xu,
Supervisor, TU Delft:	Dr G. (Georgy) Filonenko
Project Duration:	Nov, 2022 - Jul, 2023
Faculties:	MSE & CiTG, Delft

Cover: Porous Asphalt Road through the Swiss Alps
Style: TU Delft Report

TU Delft

Abstract

Over the last 15 years or so, research has revealed the great self-healing prospects possessed by asphaltic mixtures. Researchers have proposed novel methods to harness this capability, aiming to prolong the service life of asphalt pavement, particularly in porous asphalt. To date, the most promising of the healing methods is the combined capsule-induction system. This thesis aims to ascertain whether such a system would show positive results in stone mastic asphalt (SMA). Following that, an optimisation of the composition of self-healing SMA was proposed by assessing the mechanical and healing properties via laboratory testing. Finally, an evaluation of sustainability from an environmental perspective was done using Life Cycle Analysis (LCA) methodology.

Results of the healing assessment revealed that each combined healing system was able to recover between 58-63% of its original fracture strength after 8 healing cycles, while the reference mix (without healing) was only able to regain 10% fracture strength before failure after 2 cycles.

Inclusion of the combined healing system slightly reduced the strength, stiffness and water sensitivity of the SMA mixture compared to the reference. However, improved rutting resistance was observed in each self-healing case. Within the self-healing mixtures, increasing capsule content reduced asphalt density, stiffness and strength and resulted in an increase in asphalt void content.

The LCA results show that the self-healing system had environmental benefits in some facets such as a 14% reduction in fossil fuel resource depletion and a 21% reduction in land use. However, the present total known environmental costs of other impacts are approximately 15% lower in the reference system based on a cradle to gate, and use phase analysis. Almost half of this total cost was attributed to maintenance activities. It was concluded that a 32% increase in maintenance efficiency would ensure environmental viability of a self-healing mixture over a reference mixture within the constraints of the analysis conducted.

Contents

List of Figures

List of Tables

Nomenclature

Nomenclature used in this thesis, in order of appearance.

Abbreviations

Abbreviation	Definition
SMA	Stone Mastic Asphalt
PA	Porous Asphalt
APJ	Asphaltic Plug Joint
SBS	Styrene-Butadiene-Styrene
WMA	Warm-mix asphalt
HMA	Hot-mix asphalt
CRF	Crushed Rock Fine
CIS	Capsule Induction System
A/R	Alginate/Rejuvenator ratio
ITS	Indirect Tensile Stiffness
ITSM	Indirect Tensile Stiffness Modulus
ITT	Indirect Tensile Strength
VC	Void Content
BD	Binder drainage
SCB	Semi-Circular bending
LCA	Life Cycle Assessment
LCI	Life Cycle Inventory
LCIA	Life Cycle Impact Assessment
IC	Impact Category
ECI	Eco-cost Indicator

1

Introduction

Roads, runway and bridge surfaces made using asphalt form the vast majority of critical transport infrastructure on land. They stimulate social and economic development worldwide, and billions of people depend on them to provide access to crucial services and to transport goods. In Europe alone, production of asphalt exceeds 300 million tonnes per year; supporting a road network of over 5.5 million kilometers with an estimated value of over $8 trillion [1]. The improvement of road infrastructure is widely acknowledged as a major challenge in the construction sector today. Rapid population growth and increased vehicle traffic is leading to premature failure of pavement infrastructure worldwide [2].

Self-healing is a phenomenon found in many aspects of nature. In recent times, the scientific community has looked to harness some of the concepts used in nature to improve the functionality and sustainability of many man-made material solutions. Among the materials studied for this phenomenon is asphalt. The interest in self-healing asphalt comes from its manifold benefits. Asphalt mixtures can be designed to self-heal damages within the material prolonging its service life, reducing the need for replacement. Moreover, its application to road surfaces can also diminish the need for road closure for maintenance activities, reducing disruption for road users and the associated secondary economic costs arising from traffic diversion. In order to realise the optimum benefits, self-healing mixtures need to be optimised in terms of their compositions. Healing additives in the form of capsules for insitu rejuvenation and crack healing alongside steel fibres for induction healing are the basis for the healing mechanism discussed in this research.

This thesis aims to gain a better understanding of the mechanical viability of self-healing stone mastic asphalt (SMA) and ascertain whether or not it is a sustainable alternative to conventional SMA in pavement and joint applications. Initially, a literature review will be conducted, covering failure mechanisms experienced by asphalt mixtures and joints in particular, and an overview of the current state of the art in self-healing asphalt technology. Based on the review, research questions are formulated to assess the mechanical and sustainability aspects of self-healing SMA. Following that, research methodologies for each aspect are given. Results and discussions for the mechanical assessment are then presented followed by the conclusions of the study and recommendations for future research.

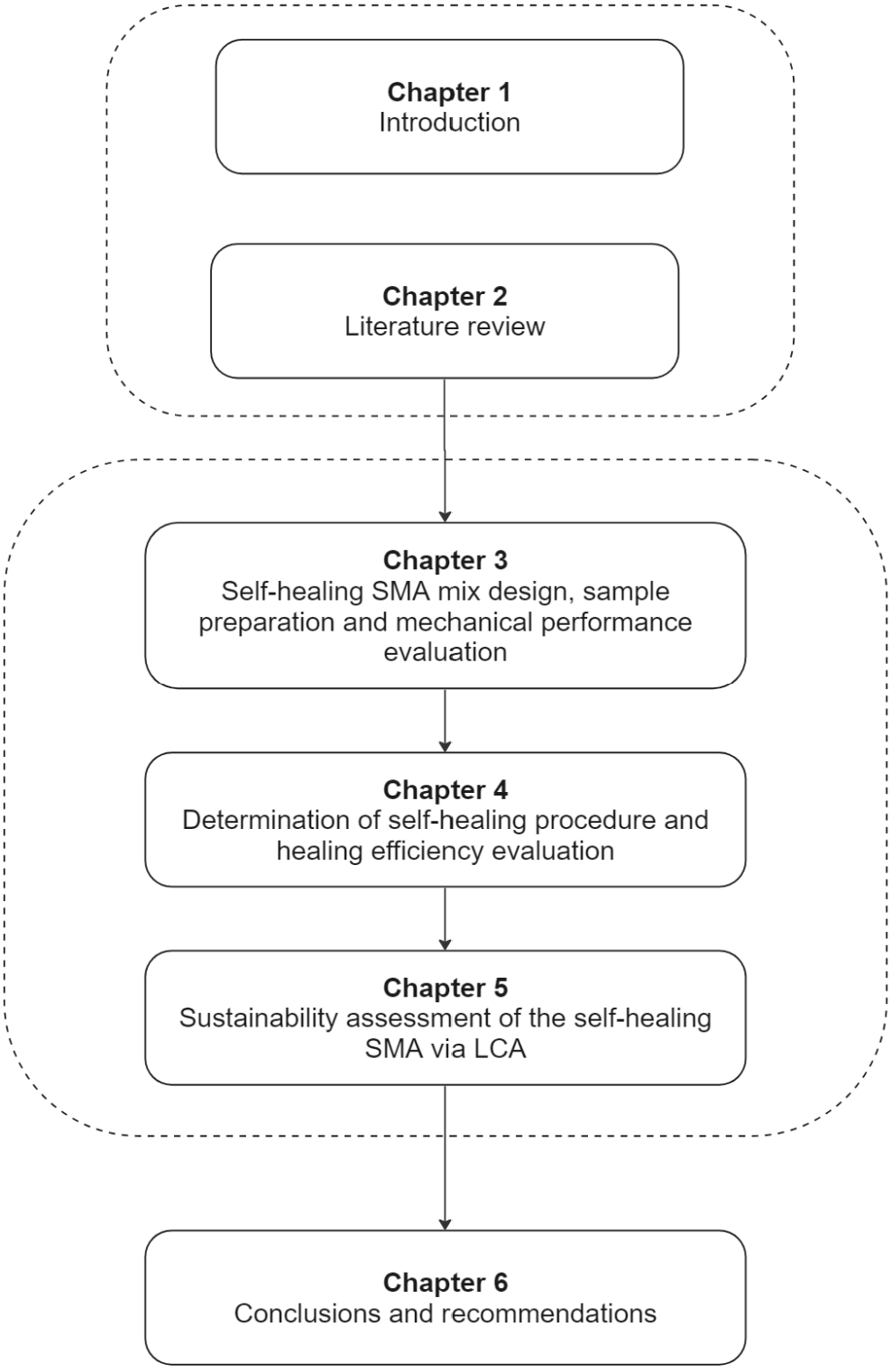

Figure 1.1: Thesis outline

2

Literature Review

This literature review will aim to cover the concepts of self-healing that can be applied to asphalt, and focus on the current state-of-the-art of asphalt plug joints (APJs) as a case study to apply these concepts. Failure mechanisms of asphalt mixtures will be discussed as well as the effects of intrinsic and extrinsic factors. Self-healing methods such as induction heating and encapsulation for rejuvenative healing, as well as a combination of the two methods will then be discussed in depth. Following that, the current literature focusing on the sustainability of the above self-healing solutions and the necessary frameworks will be covered to inform the conceptualisation of the final research question.

2.1. Overview of the problem

The modern world has an extreme techno-socio-economic dependency on road networks. This high level of dependency has far-reaching effects. Analysis by the European Union indicates that maintaining the quality of this infrastructure is an essential prerequisite to maximising the socio-economic benefits that can be obtained from it. Failure to do so properly will hinder economic and social development over the medium to long term [3].

The use of asphalt pertains to many advantages as a binding material for pavement surfaces. It provides a low cost, low noise and comfortable driving experience for road users the world over. However, after extended periods of service, the layers of asphalt are subject to degradation due to variable factors such as cyclical loading and environmental conditions [4] [5].

Certain parts of the transport infrastructure network are especially prone to failure. In bridges, natural expansion and contraction of the concrete superstructure occurs due to changes in temperature and load over time. Asphaltic plug joints (APJs) are a type of expansion joint used to accommodate such movements while maintaining a smooth driving surface [6]. Its primary purpose is to reduce the amount of cracking and separation by mitigating the formation of stress concentrations at the most susceptible parts of the structure. They are cheap, easy to install, and help to provide a smooth driving experience in transition between the bridge and the connecting road. As a result, they are numerous across the global infrastructure network.

Despite the benefits APJs provide, they have a significantly lower average lifetime compared to the rest of the asphalt road surface [7]. Frequent maintenance checks are required to monitor ageing and mitigate the risk of failure. Despite this, many experience premature failure, costing UK councils over £30 million per year adjusted for inflation [8]. This figure fails to consider lost revenues from road closures, traffic delays and other indirect economic costs arising from wear and tear of vehicles, for example and is replicated in other countries worldwide.

Component	APJ	Porous Asphalt Surface	Dense Asphalt Surface
Expected lifetime	5-7 years	10-12 years	20 years

Table 2.1: Expected lifetimes of APJs vs Porous and Dense Asphalt pavement surfaces

The exact number of APJs currently in operation around the world is large but unknown. Sustained global economic growth requires further building and repair of roads to connect more people and goods. Therefore, it is estimated that the world road network length will have increased by 14-23% in 2050 [9]. This will see many airfields and thousands of bridges built, thereby increasing the number of APJs in operation and the ensuing need for repairs. One can therefore infer, that APJs are a potential performance limiting factor when it comes to transport infrastructure, and will continue to be into the future. Consequently a targeted approach to increasing the lifetime of these joints is required.

2.2. Current state of the art

In order to propose an approach to improving joint lifetime, we must first understand the current state of the art of APJs, followed by the failure mechanisms. Due to large variation in climate, available materials and construction limitations per country, standards for APJs per country/department of transport are not fixed. Nevertheless, it is useful to have an overview as to what the different standards may have in common. Each organisation considered delivers specifications through open and transparent processes by committees of relevant industry professionals. Figure 2.1 shows the ASTM standard specification for the joint mix used in APJs for bridges. It represents the recommended material property standards necessary for joint mixtures. While the constituent materials are subject to quality tests, the final joint mixture composition is not subject to stringent regulation as there are multiple ways to achieve these properties and can be adjusted depending on the required conditions.

	ASTM standards	Required physical properties
Softening point, min	D 36	83 °C
Tensile adhesion, min	D 5329	700%
Ductility, min at 25 °C (77°F)	D 113	400 mm
Penetration, Max at 25 °C, (77°F),150 g, 5 s	D 3407	7.5 mm
Low temperature penetration, min at −18 °C (0°F), 200 g,60 s		1.0 mm
Flow, max 5 h, at 60 °C (140°F)	D 3407	3.0 mm
Resiliency, min–max at 25 °C (77°F)	D 3407	40–70%
Asphalt compatibility	D 3407	Pass
Recommended installation temperature range		182–199 °C
Safe heating temperature range		199–216 °C
Bond 3 Cycles at −7 °C (+20°F), 100% Elong	D 3405	Pass
Flexibility, at −23 °C (−10°F)	D 5329	Pass

Figure 2.1: ASTM Specification Standards for APJs [10]

In Europe, the European Organisation for Technical Assessment (EOTA) provides a design specification framework for APJ materials and their properties as outlined in EAD 120093-00-0107 [11]. Based on these design specifications, APJ systems are typically around 500mm wide and between 70-160mm thick. They must be able to accommodate bridge movements of up to 50mm and have a working temperature range of between -25°C and +45°C. The gap plate is made using structural steel with corrosion protection, and covers the gap between the decks, preventing asphalt from entering the gap. Furthermore, caulking (a backing material which is placed in the structural gap to provide support for sealant in an expansion joint) is used as a compressible material to fill the gap and prevent leakage of the asphaltic binder during installation. The caulking material must be heat resistant to withstand the high temperatures experienced when the binder is being poured [12]. Below the steel plate sits a backer rod which is typically waterproofed using a polymer foam.

The asphaltic binder mixture used in each standard is one of bitumen with polymer modifier, either waste rubber or SBS. The aggregate mixed with the binder is graded, washed, crushed rock from trade groups such as granite, basalt, or dolerite [6]. The aggregate must meet the appropriate standards for flakiness, abrasion value and crushing value such as those described by standard BS 812, to ensure structural integrity [13] [7]. Figure 2.2 shows a typical APJ construction.

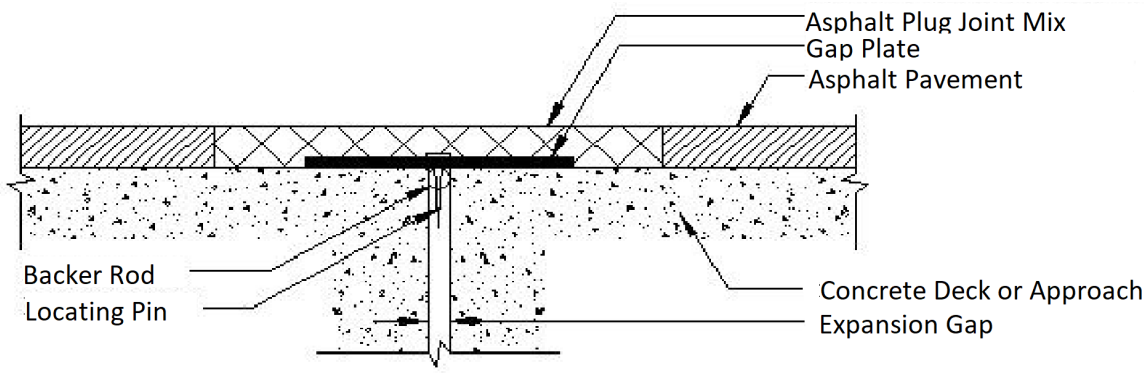

Figure 2.2: Basic schematic of a typical Asphaltic Plug Joint [14].

APJs installed according to the European standards have an expected lifetime of 5 to 7 years depending on the environment of operation according to Liang et al [15].

In colder climates, cracking was observed within two years of installation with APJs of similar composition [16]. Similar timeframes of failure were reported in the US, the vast majority of failures in joints were attributed to material failure of the asphaltic plug according to data from the Department of Transport in Ohio, Illinois, Michigan and Kentucky [17].

2.3. Main failure mechanisms of APJs

Although they have many benefits, the harsh physical and chemical environments that APJs are subjected to, make them one of the most susceptible areas to failure within transport infrastructure. Failure of an APJ is defined as the point at which the asphaltic binder is no longer impervious to water and other contaminants, which then penetrate the underlying super structure. The following is a breakdown of the main failure mechanisms, how they occur, and associated visual observations that are typical of each mechanism. Many of these failure mechanisms also apply to regular asphalt pavement, although the timescales for failure are shorter (see Table 2.1).

2.3.1. Ravelling

Ageing of the asphaltic binder causes a reduction of relaxation capacity and an increase in stiffness. This usually happens as a result of progressive binder oxidation over its lifespan. As a result, stresses induced by loading in tension or compression may cause microcracks to form within the binder. Over time and further loading, these microcracks grow and aggregate particles are progressively separated from the binder, exacerbating the problem due to the subsequent reduced load bearing capacity and loss of adhesion. In the early stages of ravelling, finer aggregate particles separate, followed by progressively larger ones. The surface of the joint is left with an appearance typical of surface erosion (see figure 2.3) [7] [18].

Ravelling occurs more readily within porous asphalt compositions due to its higher void content. Progressive ravelling can contribute towards other failure mechanisms such as cracking due to the reduction in mechanical properties resulting from the loss of aggregate. Besides the obvious loss in ride quality, loose aggregate can damage vehicles and reduce ride efficiency by increasing the friction coefficient of the surface [19]. In the most severe cases, if left untreated, ravelling can result in pothole formation in asphalt pavement, detracting from road quality and safety, though it is unlikely to reach this extreme in the case of APJs due to their structural importance and frequent maintenance [6].

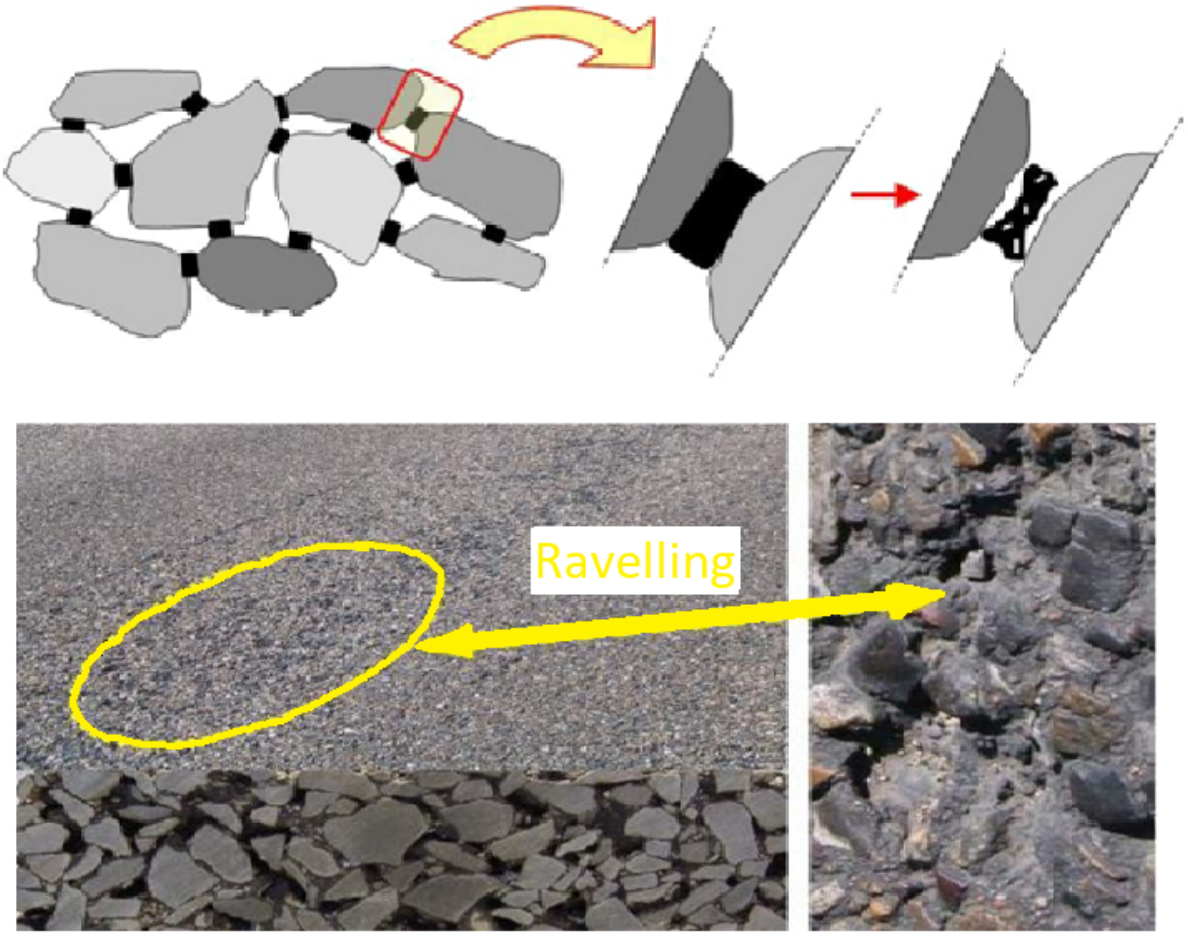

Figure 2.3: Mechanism leading to ravelling, including an example [19].

2.3.2. Cracking

Cracking or splitting due to excessive tensile stresses or strains is another potential mechanism. This mode of failure is mainly induced via joint motion over time due to movement of the concrete super structure, and material fatigue from cyclical loading. Both transverse and longitudinal cracks will propagate over time with sustained loading, and act as a route for water to infiltrate the joint, increasing the risk of failure [14]. This is the most common failure mechanism and is affected by many intrinsic and extrinsic factors. Cracking is not necessarily visible, making it difficult to ascertain whether or not a joint is in need of repair. An example of this is **reflective cracking**.

In an APJ, the steel gap plate covers the expansion gap, however the reflective cracking does not occur across the gap. Using finite element analysis, a mesoscale simulation model developed by Liu et al [20] aimed to understand the behaviour of the joint form a stress concentration perspective. The analysis showed that the joint pavement interface and the edges of the steel gap plates are two critical locations that are more sensitive to cracking due to bridge movements or traffic loads. In figure 2.4, this is clearly demonstrated, with the binder experiencing high levels of stress between aggregate particles near the edges of the steel gap plates. As a result, the red zones are the regions where reflective cracking is most prominent. Many of the

failure mechanisms discussed lead to some form of cracking, which is the leading failure mode for APJs.

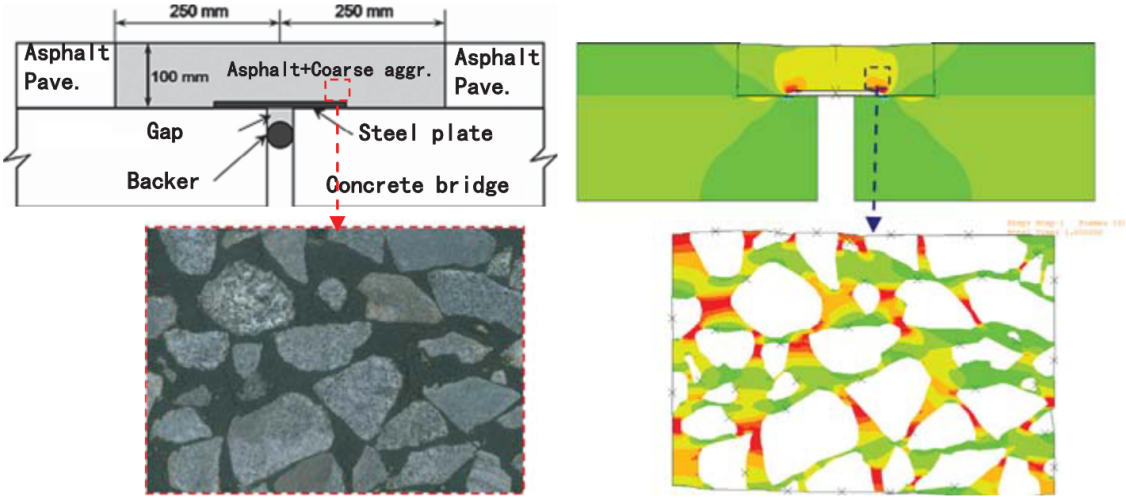

Figure 2.4: Finite element analysis giving an insight into stress concentrations within the asphalt mastic in an APJ [20].

2.3.3. Debonding

Debonding between the APJ and the adjacent pavement interface occurs due to adhesion failure between the two materials. This has been theorised to take place via different methods in the literature. For example, it can arise due to variance in glass transition between the APJ and the adjacent pavement. Temperature change may cause one side of the interface to become brittle and crack, causing subsequent loss of adhesion [7]. An alternative theory, posed by Partl et al [21] suggests that the ingression of water is to blame. If the matrix becomes saturated and water can no longer drain, water build up in voids within the asphalt matrix may freeze and expand at the interface, resulting in debonding.

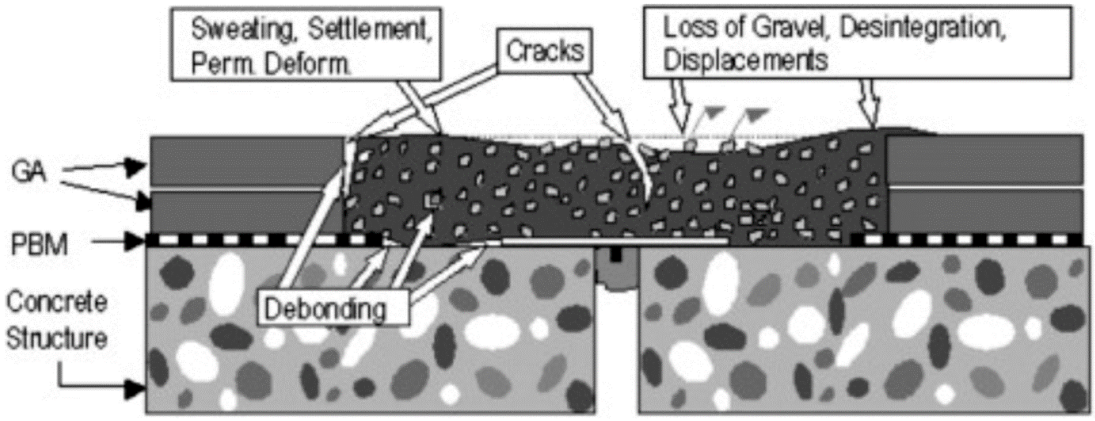

Figure 2.5: Debonding within an APJ, alongside other damage mechanisms previously mentioned [6].

As shown in figure 2.5 debonding is most likely to happen at the pavement-joint

interface, but may also occur at the steel plate interface, and between aggregate and binder within the asphalt mix due to the presence of voids.

2.3.4. Rutting and shoving

The surface of asphaltic materials are subject to short-term loading from vehicles. After many repetitions, loading may induce permanent deformation of the material surface [22]. The repetitive loading may be localised due to the road layout and result in shear flow of material and an uneven surface, detracting from ride quality and safety.

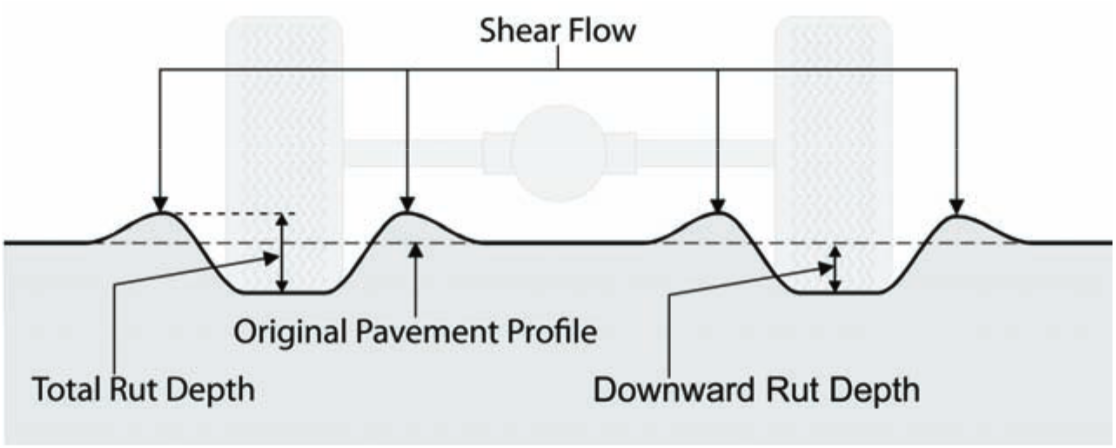

Figure 2.6: Rutting of a pavement surface due to vehicle loading, from a cross-sectional point of view [23].

Shoving refers to the displacement of asphaltic material in the joint caused by lateral shifting of material due to the component of horizontal force applied by wheel motion. Rutting and shoving are exacerbated at high temperatures due to the decrease in viscosity of the bituminous binder. They are also highly dependent on volume and magnitude on traffic load [23]. Unlike the other failure mechanisms, shoving and rutting do not have a significant effect on water intrusion into the underlying structure. This will only occur if the profile is profoundly altered such that large stress concentrations form, which can induce cracking after ageing of the asphalt mastic when it becomes more brittle.

2.4. Effects of asphalt design parameters on properties

There are many factors influencing the mechanical properties of APJs, and therefore their failure. Firstly, the intrinsic properties such as bitumen grading, aggregate types, mix design and modifier will be addressed.

2.4.1. Binder and aggregate chemistry

Within the asphalt, the bitumen content is key in determining the final mechanical properties of the mix. Higher bitumen content results in a more flexible asphalt, improving

formability and pliability of the final mix at the expense of strength. As a result, the asphalt is less stiff and cannot withstand large mechanical loads as effectively. A balance must therefore be struck between flexibility and strength in order to optimise the mechanical properties [24]. Binder-aggregate interaction also plays an important role in defining the properties of the mix. A greater degree of adhesion between the binder and aggregate will increase stiffness, but an inherent time-dependence will lead to a decrease in interaction over time. The interaction parameter defined by Guo et al. established that limestone aggregate typically showed an increased the magnitude of adhesion with the bituminous binder compared to granite [25]. It is thought that a stronger interaction improves interfacial shear properties of the aggregate and binder leading to an increase in both strength and stiffness of the binder close to the interface.

Cohesion refers to molecular interaction between bitumen molecules. High bitumen cohesion can better distribute stresses throughout the asphalt mixture, reducing the risks of crack propagation and fatigue damage. It also has an effect on flow properties of the binder, as a more cohesive bitumen will reduce flow and reduce potential for deformation by rutting [26].

2.4.2. Void content

Void content is another intrinsic property that affects the lifetime of asphalt. In general, the mechanical properties are detrimentally affected by the presence of voids. Figure 2.7 shows that fatigue and rutting resistance decrease significantly beyond a 5% void content, and that strength decreases linearly with void content. Differences in mechanical properties between porous asphalt and dense asphalt mixtures (e.g. SMA) are substantial, and this can largely be attributed to void content within the mixture. Porous asphalt has a void content of above 10% which contributes positively to noise reduction and act as a drainage mechanism to improve road safety. However, this comes at a cost of durability and strength. SMA mixtures designed with dense aggregate structures and high binder content helps prevent water ingression, and improves strength and rutting resistance. Zaltoum et al [27] also noted that ravelling rate is also increased with a higher void content.

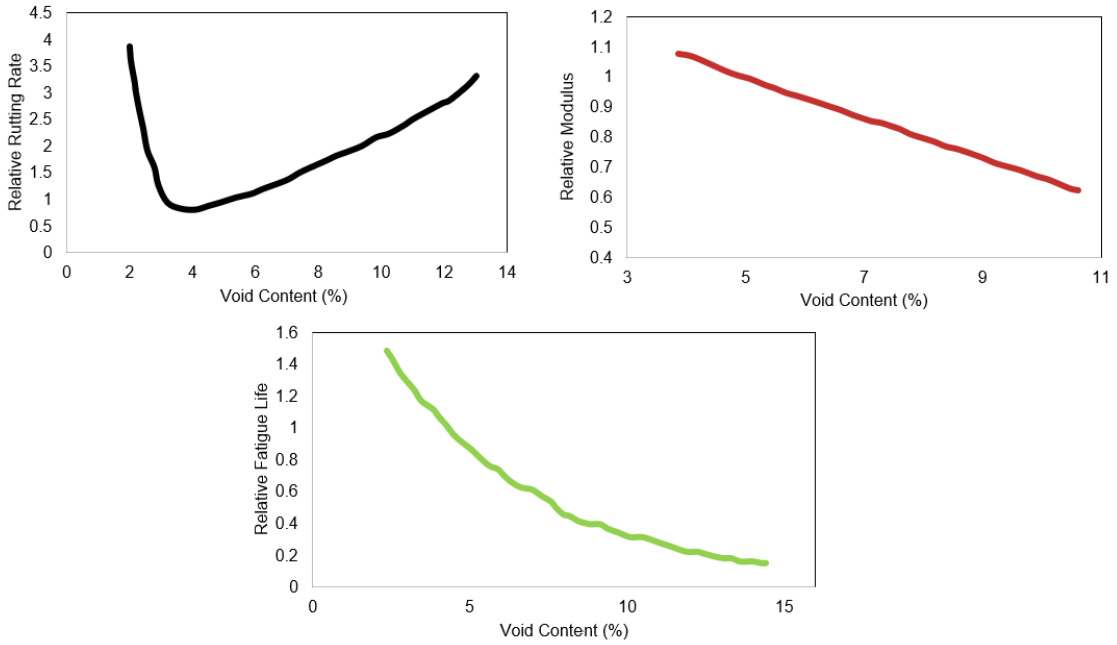

Figure 2.7: Effect of air void content on different mechanical properties. Black line = effect on rutting rate, red line = effect on strength (relative modulus), green line = effect on relative fatigue life [27].

Factors in the construction of asphalt pavements and joints can also influence void content. Compaction procedures in particular, must be controlled to obtain an optimal void content for the desired application.

2.4.3. Additives

Additives can ameliorate properties and extend the lifetime of the asphalt. Extra polymeric materials can be integrated into the asphaltic binder to improve the rheological properties and resistance to permanent deformation. For example, complex modulus and complex viscosity can be altered with the addition of modifiers. For example, rubber will increase these values, while the addition of oil would reduce them [28]. The addition of a crumb rubber modifier helps to reduce moisture sensitivity, but increases the viscosity of the mixture, increasing the energy consumption and greenhouse gas emissions associated with production [29]. Another example of a polymer modifier commonly used is Styrene-Butadiene-Styrene (SBS) which reduces the temperature sensitivity by increasing the softening point of the mastic and is commonly used in APJs [30]. This correlation can clearly be seen in figure 2.8 with an increase in softening point, and hence increased viscosity of the asphalt mastic at a given temperature with the addition of polymer modifier.

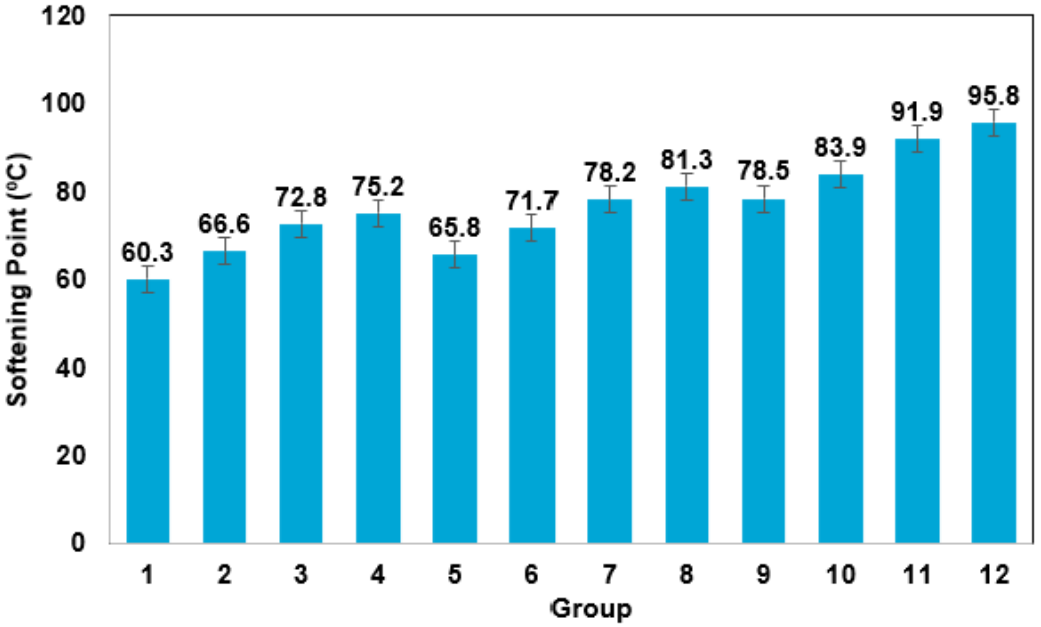

Group	1	2	3	4	5	6	7	8	9	10	11	12
CR Contents (%)	10	10	10	10	15	15	15	15	20	20	20	20
SBS Contents (%)	1	3	5	7	1	3	5	7	1	3	5	7

Figure 2.8: Softening point of different asphalt groups as a function of modifier composition [30].

The reduction of temperature sensitivity also means low temperature performance is improved, with SBS modifier increasing complex modulus at lower temperatures. As can be seen in figure 2.9, the SBS modified asphalt, shows a lower phase angle and higher complex modulus in the temperature range 45-75^{o}C compared to unmodified asphalt, this indicates that the unmodified asphalt mixtures is more susceptible to rutting and exhibit better strength and stiffness properties at low temperature.

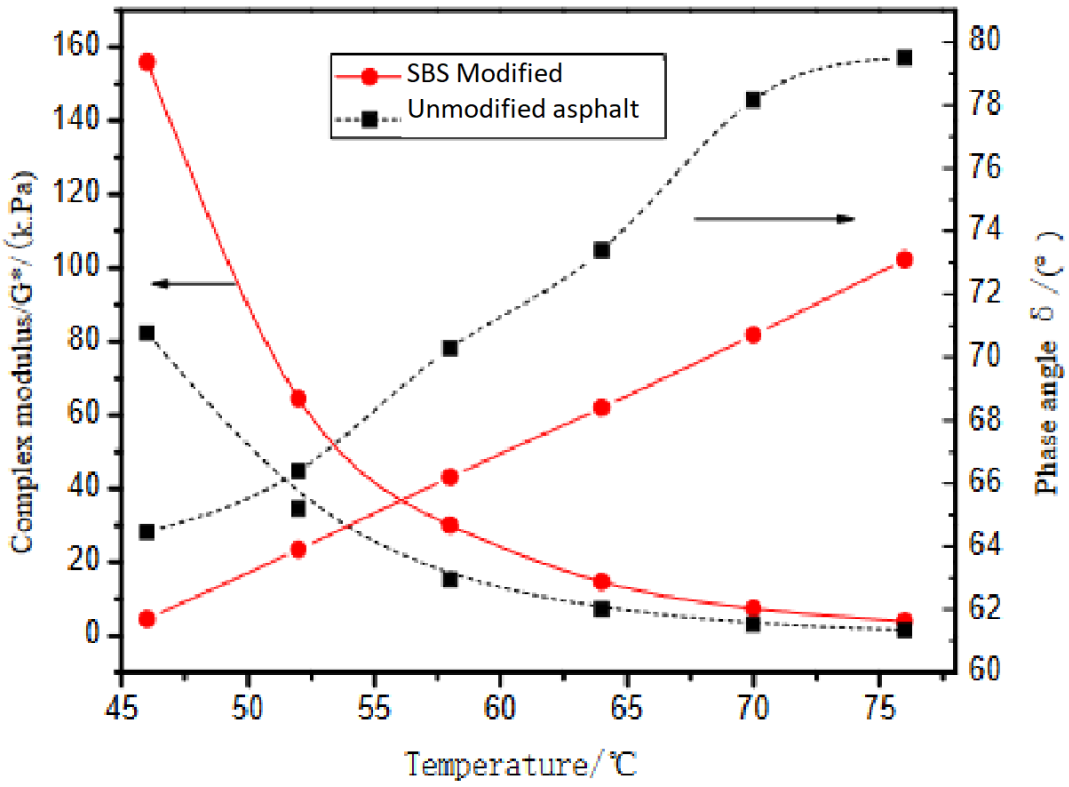

Figure 2.9: Rheological properties of SBS-modified vs unmodified asphalt using DSR [31].

2.5. Extrinsic factors affecting asphalt performance

Whilst the asphalt properties are fundamentally affected by the composition and physical make up of the binder, they are also significantly influenced by the environment that they are subjected to. The effects of the main extrinsic factors will be discussed in this following section.

2.5.1. Temperature

Due to the viscoelastic nature of asphalt, its properties vary with temperature. In summary, peer-reviewed literature suggests that the APJ mixture is soft and pliable at warm temperatures, and stiff and brittle at lower temperatures [7] [6] [5]. Defects in APJs vary with temperature as a result, with greater degrees of rutting and tracking in summer, versus increased cracking, ravelling and debonding at the interface during winter.

An optimal asphaltic binder material will have maximum extensibility at low temperatures, and high flow resistance at high temperatures. This is difficult to achieve, due to the fundamental differences between the two requirements. For example, using a hot mix asphalt with a low softening point will improve fatigue life, but reduce the stiffness of the binder. Therefore, a trade-off must be made when designing the asphalt mixture to optimise the component lifetime. Each of the standards for APJ binders

outlined in section 2.2 opt for a modified bitumen with a higher softening point so as not to compromise the stiffness of the asphalt, but leaves it susceptible for premature failure via fatigue cracking [32]. This trade-off is clearly demonstrated in figure 2.10 with a near opposite variance between the two properties as temperature increases.

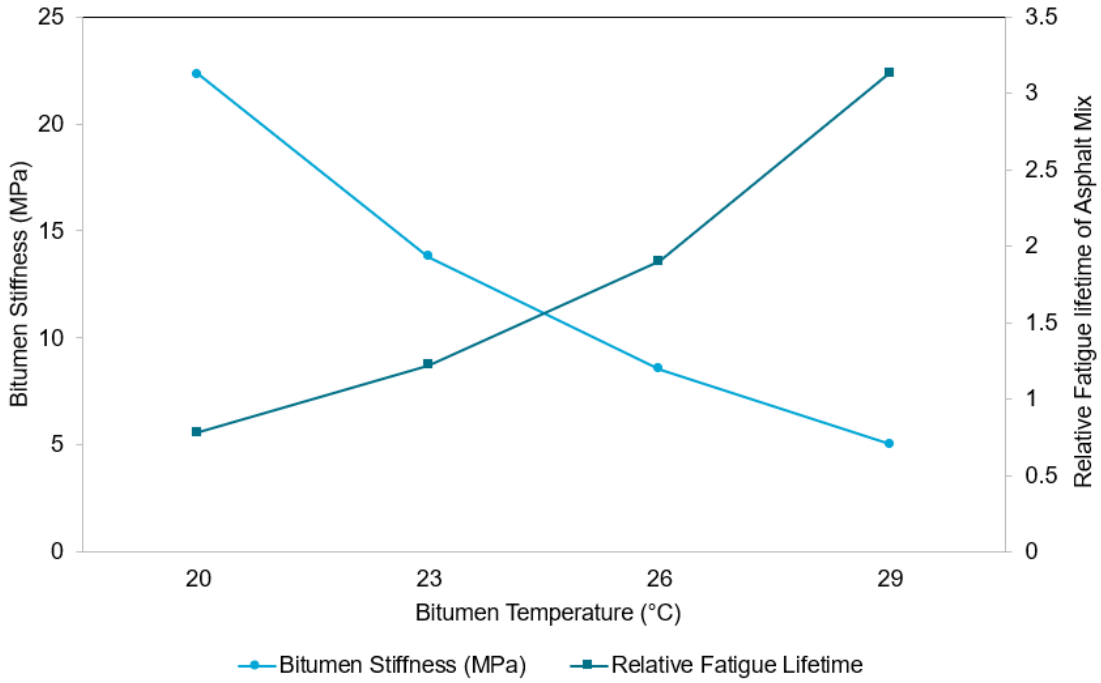

Figure 2.10: Stiffness and Relative Fatigue lifetime of an asphalt concrete wearing course and their respective variance with temperature [32].

2.5.2. Moisture

Adhesion between the aggregate and asphalt binder is negatively affected by moisture. The adhesion is governed partially by the bonds' physio-chemical interaction with water, particularly Van der Waals forces [4]. The adhesion phenomenon is not entirely understood, and there are several proposed theories to help describe it, as outlined in a review by Omar et al [33]. Moisture absorption is heavily dependent on composition of both the aggregate and the asphalt binder, and is interconnected with other preceding factors outlined in this review, such as temperature and void content (porosity). A comprehensive summary can be seen in figure 2.11.

Variable	Influenced property	Desirable feature
First group		
Bitumen	Viscosity	High
	The source	Not defined
	Film thickness	Thick
	Chemical parameters	Phenolic groups and nitrogen bases
	Additive	Hydrated lime, amines, polymer
	Moisture diffusion coefficient	As low as possible
Aggregate particle	Texture of surface	Rough
	Surface cleanliness	No fines or dust
	Porosity	Sufficient pore size to absorb bitumen
	Mineralogy	Basic aggregate type
	Chemical composition	More calcium oxide
		Less silicon dioxide
		Presence of calcium, magnesium and iron
	Surface chemistry	Ability to form hydrogen bonds
	Surface moisture	Dry
	Treatment with hydrated lime	Reduces the acid SFE and increases the base SFE
	Hydrated lime treatment method	Adding dry hydrated lime to wet aggregate
Second group		
Mixture property	Bitumen content	High content
	Void ratio	Less than 6% or more than 15%
	Permeability	Less than 100×10^{-5} cm/s
	Mixing temperature	High sufficiently to coat aggregate surface
	Stiffness	High
	Bitumen-aggregate interaction	High electrostatic forces or hydrogen bonding, or Van der Waals interactions.
		High acid component of bitumen and base component of aggregates
		Calcium ions on aggregate surface with carboxylic acids in a bitumen
	Moisture diffusion coefficient of the mastic	Low
	Gradation	Very dense or open graded
	Filler	
	Mineralogy	Basic
	Treatment	Treated with hydrated lime
Construction condition	Rainfall and/or snow	No rainfall or snow
	Compaction	Depends on mixture design
	Temperature	Warm
	Moisture in site	No moisture
Field factors after construction		
Traffic effect	Traffic load	Minimal traffic load
Drainage effect	Surface drainage	Good drainage
	Subsurface drainage	Increasing the depth for drains at the shoulder edge
	High water table	Low water table
Temperature effect	Freeze-thaw cycle	Minimal
	Cool-warm cycle	Minimal
	Temperature	Moderate
Others	Rainfall and/or snow	Minimal
	pH of field water	Controlled pH

Figure 2.11: A summary of the parameters affecting moisture damage, with the ideal scenario included as outlined by Omar et al [33].

The moisture uptake is directly correlated with adhesive strength loss and subsequent debonding due to chemical interactions, and the ingression of water causing freeze-thaw expansion (see figure 2.12). This strength loss and resulting degradation of the pavement integrity can lead to premature fatigue cracking, ravelling and rutting. The problem is exacerbated by ageing of the asphalt mastic, but can be mitigated by rejuvenation [34]. This will be elaborated upon in later sections.

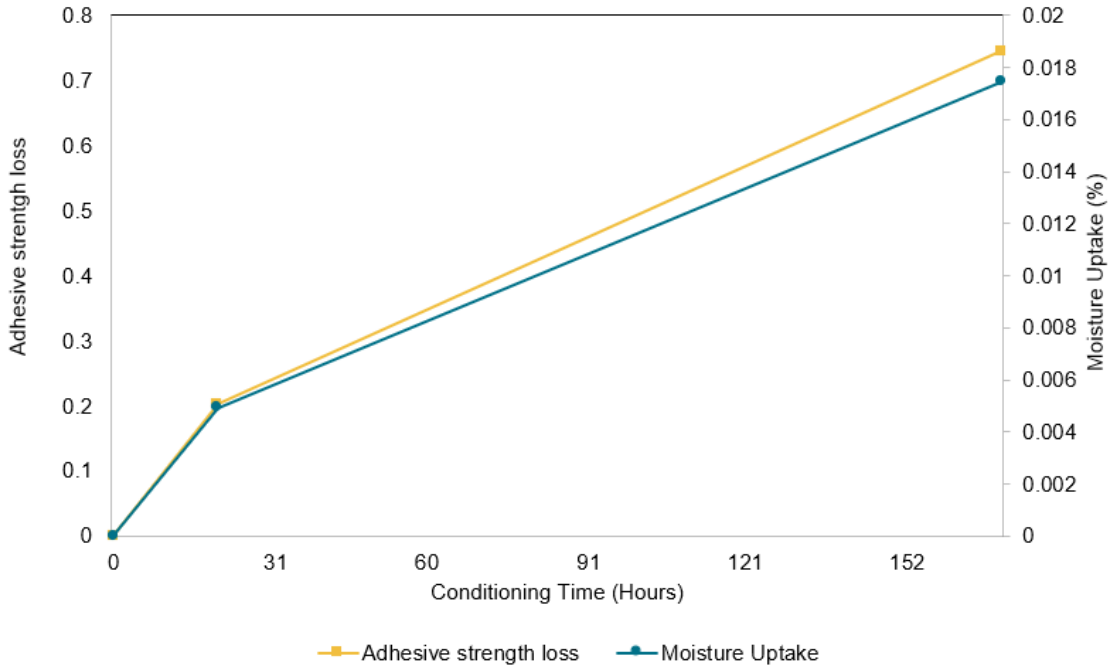

Figure 2.12: Correlation between Adhesive strength loss and moisture uptake [4].

2.5.3. UV light exposure and oxidation

UV radiation of sufficient energy can break down the cross-links in polymer modified binders. The destruction of the network through exposure to sunlight increases the rate of ageing of the binder at the surface. As a result, UV radiation over extended periods can induce shrinkage stresses. Due to ageing, the binder is more brittle and rigid. The combination of these factors make the asphalt mix make cracking after cyclic loading more likely but deformation mechanisms such as rutting are reduced [35]. Oxidation through exposure to air is also detrimental to asphalt properties and shows a strong temperature and time dependency. It is once again a complicated mechanism, but the most common instance is the conversion of resins within the fresh asphalt mixture (such as maltenes) to asphaltenes over time, with oxygen being incorporated as functional group before being eliminated in the form of water [36]. The conversion of resins to asphaltenes is synonymous with ageing and increases the binders' susceptibility to cracking.

2.5.4. Vehicle loading and quality control

Finally, proper installation and adherence to construction standards is key to improving resistance to failure by ensuring the loading is as intended. It is well documented that incorrect installation of APJs results in a significant increase in the rate of failure [7]. If installed improperly APJs are more susceptible to fatigue cracking due to traffic loading. If the loading is not as intended due to poor installation, stress concentrations will occur more readily, cracks will form, and get progressively larger with repeated loading eventually leading to failure. This is perhaps the most important factor, and concludes this section on the different parameters affecting the lifetime of APJs.

2.6. The concept and application of self-healing in asphalt mixtures

2.6.1. Damage prevention vs damage management

Traditionally, materials selection for engineering applications has been based upon the concept of 'damage prevention'. Within this principle, improvement of material performance is achieved by opposing formation and propagation of microcracks through microstructural control. As a result, selection of materials is based upon intrinsic material properties such as stiffness and strength, and the quantum understanding of these properties. Microstructural optimisation generally ensures that the atoms have low mobility, making deformation more difficult [37].

This method of material design has been the subject of successful scientific research and development for thousands of years, but it is not without drawbacks. Namely, once damaging load has been reduced or removed completely, damage will still be present. As such, the rate of damage formation is always greater than zero for materials selected using damage prevention design principles.

$$d(damage)/dt \geq 0 \qquad for \qquad 0 < t < t_{life} \tag{2.1}$$

Damage during service life of a component is an inevitability, therefore current materials must be inspected periodically and maintained to ensure that they continue to meet the necessary mechanical requirements. Cracks induced by mechanical load can mechanical load can propagate and evolve from microscale to macroscale damages, and are the primary source of failure in many applications. If damage levels are sufficient, costs incurred over a component's lifetime can be significant.

Self-healing materials are based upon the 'damage management' principle, which has fundamentally different characteristics to the 'damage prevention' concept. Instead of damage accumulation over time within the material, there is the possibility of damage reduction during an autonomous healing event which can occur at one or more stages over its lifetime. The overall aim of the self-healing process is to reduce damage level and subsequently extend the lifetime and functionality of the material.

$$d(damage)/dt < 0 \qquad for \qquad t_i < t < t_{i+healing} \tag{2.2}$$

Where t_i is the time at which a damage event occurs, and a damage level of 1 equates to failure.

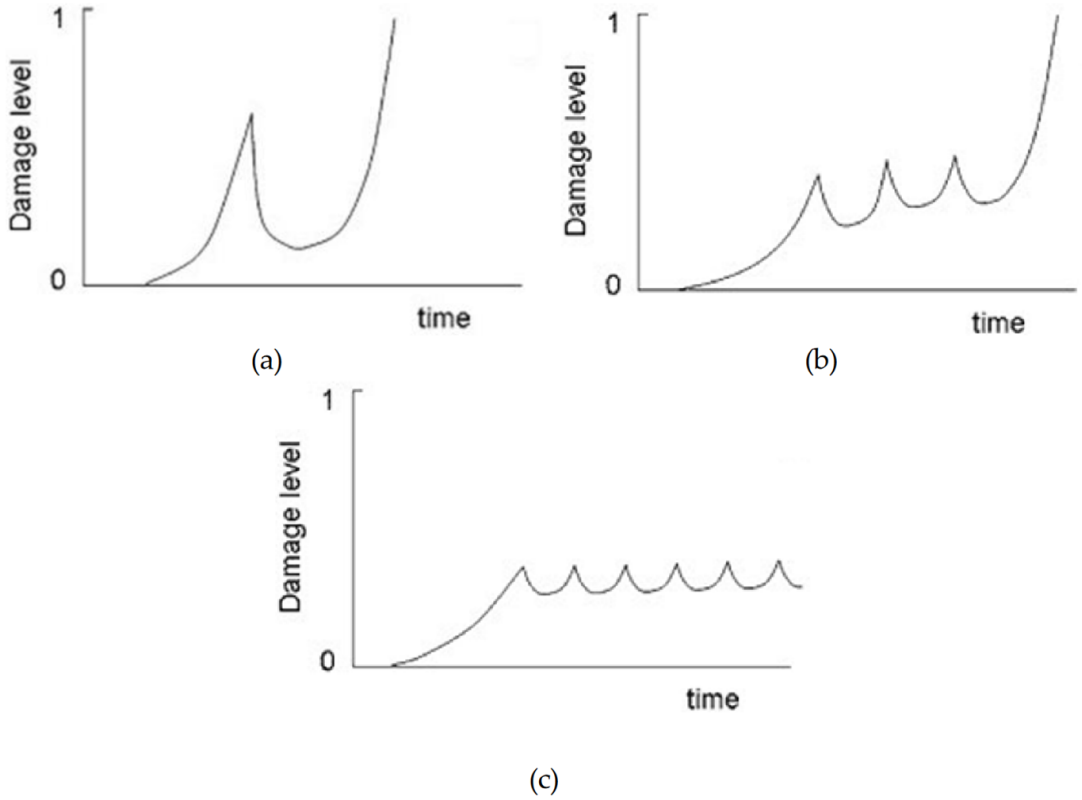

Figure 2.13: 3 potential possibilities of damage level behaviours of a SH material from a single healing event to a an ideal SH material with many healing events [37].

Self-healing materials require a degree of mobility within the structure, over long or short distance to remediate the damage on location, restoring the functional capabilities of the material [38]. In the case of a load-bearing material, mechanical load will inevitably give rise to a crack in the material. To begin the self-healing event, a mobile phase is generated and is activated by the occurrence of damage, or by external stimuli. Targeted mass transport towards the damage site occurs before the mobile phase is immobilised again resulting in (at least partial) restoration of the mechanical properties.

Figure 2.14: Schematic of the basic principle of self-healing materials, with reaction progression from left to right. Mechanical load induces a crack, resulting in activation of a mobile phase. The mobile phase closes the crack and is immobilised post healing event. [38]

Self-healing efficacy can be measured easily using the healing index for any relevant physical property, for example bending or fatigue strength.

$$HI = \frac{C_x}{C_1} \times 100\% \tag{2.3}$$

Where HI is the healing index (%), C_1 = initial physical property measurement and C_x is the physical property measurement from the x testing cycle. Healing efficacy tends to diminish as the number of cycles increases, due to the presence of 'weak-points' within the structure where diffusion and randomisation of the polymer network has not fully occurred.

2.6.2. Self-healing in Asphalt

The bituminous binder in an asphalt mix has intrinsic self-healing properties. The polymeric nature of the structure means that local temporary mobility can be achieved under certain conditions. At elevated temperatures, the polymer chains are more mobile and interdiffusion of two faces of a microcrack can ensue, restoring the properties of the original material through the following process:

1. Wetting of the micro-crack faces.
2. Interdiffusion of molecules between the two crack faces
3. Randomisation of diffused molecules to regain strength of the material

Autogenous healing of the binder is dependent on time and temperature, over periods of reduced loading, and is thought to be a viscosity driven process. [39] Higher temperatures and longer times lead to greater healing, due to the arrhenius dependency of diffusion and temperature dependent kinetics of randomisation. Moreover, the smaller the damage event, the greater the efficacy of the healing event due to this dependency (i.e. a smaller crack will lead to a more successful healing event than a larger one as there is a lower distance for the chains to diffuse across and higher temperatures accelerate the randomisation process) [40]. Other intrinsic and extrinsic factors influencing the autogenous healing process of asphalt depicted in figure 2.15, many of which are similar to the factors affecting failure mechanisms, and will be discussed in this section.

Factors influencing healing	Bitumen properties	Bitumen type
		Chemical compositions
		Viscoelastic properties
		Surface free energy
		Ageing
		Diffusion
		Modifiers
	Asphalt mixture compositions	Bitumen content
		Aggregate structure
		Gradation
		Thickness
	Environmental aspects	Temperature
		Loading history
		Rest period

Figure 2.15: Intrinsic and extrinsic factors affecting healing [5].

A relevant example of the bitumen type affecting self-healing properties is shown in a study by Qiu et al. where bitumen modified with SBS was determined to have a lower healing capability than the standard 70/100 penetration bitumen mixture at a reference temperature of 25°C [41]. This is due to the elevated viscosity associated with SBS modification which has a negative effect on the self-healing mechanism of diffusion and randomisation. This can be seen in figure 2.16 where crack closure is significantly faster, and the degree of healing is better in the case of unmodified 70/100 bitumen asphalt mix.

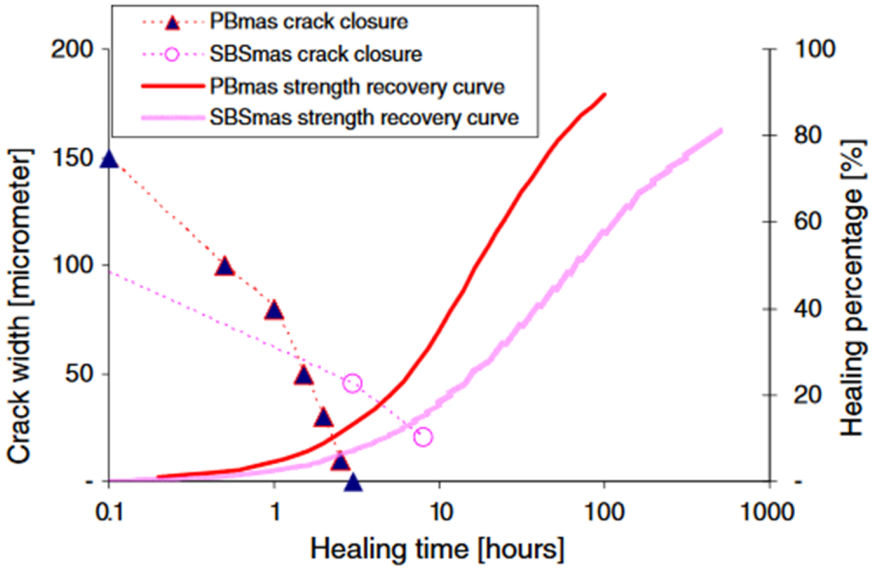

Figure 2.16: Effect of polymer modification on the healing of asphalt. PBmas refers to an asphalt containing 70/100 penetrative bitumen, while SBSmas refers to an asphalt mix containing SBS modified bitumen. [41]

2.6.3. Induction healing

Extrinsic healing methods for asphalt have been well documented in peer-reviewed literature over the last 15 years. Healing through induction heating was developed at Delft University of Technology, to exploit the temperature dependent and intrinsic healing properties of the bituminous binder. The principle is relatively straightforward: Conductive particles are included as a part of the asphalt mixture, along with aggregates and bitumen. Magnetic induction causes the formation of eddy currents within the conductive materials which lead to rapid heating of the mixture. Upon heating, the bitumen melts and is able to fill cracks present in the binder. Particles such as steel fibres, steel wool, carbon fibre and graphite are effective for this application due to their high conduction efficiencies [5].

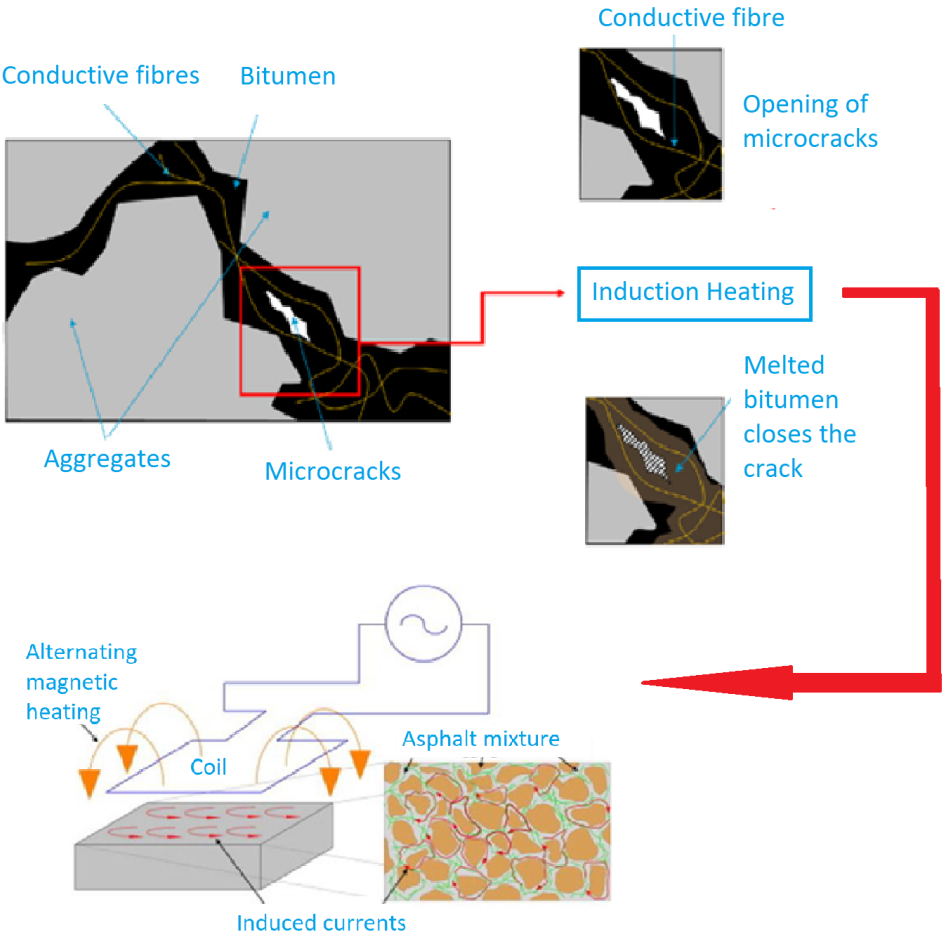

Figure 2.17: A schematic of the induction healing process within an asphaltic mixture [42].

According to recent research by Liu et al [43], short and thick steel wool fibres (diameter: 70-130 μm, length: 1-4mm) yield the best overall results for heating speed, flexural stiffness and bending strength recovery post healing. They are easy to mix into the binder pre-production, and improve mechanical properties such as fatigue and ravelling resistance. They also positively impact low temperature strength. Liu et al. also concluded that induction healing was most effective when combined with a rest

period. If such procedures are followed, the healing index can be improved by 15% if autogenous healing is supported by induction heating [43].

Optimum content of steel wool fibres was hypothesised at 6-8% volume of bitumen by Dinh et al [44] to provide optimum healing and reduce the risk of fibre clustering. However, induction heating is less effective on aged asphalt mixtures, and it was found that induction alone was relatively ineffective as a healing method for oxidised mixtures. The addition of asphalt rejuvenators were able to improve the healing performance by decreasing the binder viscosity. In this case, induction could not fully restore the initial strength of the apshalt mix for the following reasons:

1. The crack represents a weak point within the structure, i.e. full randomisation has not yet taken place, leading to lower physical bond stiffness.
2. The structure experiences some structural damage as a result of induction heating.

Fracture tests are used to simulate the cracking in practice, and therefore can be used to evaluate the healing index of polymeric materials. It should be noted that induction healing is optimised when the crack is smaller as the flow distances are shorter, and thus the cracks are easier to close [42].

Following further analysis using finite element modelling and lab experimentation, two main contributing factors to affect the success of an induction healing cycle. These were the power supplied by the heating system and the speed at which the induction system travelled over the section of material. As with the autogenous healing of asphalt, the longer the time spent at temperature, the greater the degree of healing [43].

Research by Dai et al. [45] confirmed this theory on the temperature dependence of healing using induction. Recovery of fracture strength was assessed at a range of temperatures between 60 and 100°C. Induction heating cycles at 100°C had the greatest strength recovery and therefore was deemed the optimum temperature for healing for a sand-aggregate bitumen asphaltic mixture. However, optimisation is somewhat composition dependent, as the optimum temperature for a limestone aggregate porous asphalt mix is around 85°C [46].

Induction healing efficacy is also dependent on the temperature dependence of asphalt mix. Warm mix asphalt (WMA) has a lower optimal induction heating temperature than hot mix asphalt (HMA). WMA generally will have a lower healing index compared to HMA, but has a marginally higher fatigue resistance. Overall, both mixtures' mechanical properties are highly strain dependent and show a good healing response to induction healing [47] .

2.6.4. Rejuvenative healing via capsules

In the case of asphalt, recovery of properties is also possible through the addition of a rejuvenating agent. A rejuvenator is defined as a product which restores the ratio of asphaltenes to maltenes within the asphalt binder to its original molecular structure [48]. Maltenes within the binder become oxidised over time which can lead to detrimental effects on the mechanical properties, such as reduction in ductility, leading to a higher susceptibility to cracks [36].

The use of rejuvenator to restore aged binder to prolong pavement life is well documented in the literature and has been implemented by the Ministry of Infrastructure

and Environment in the Netherlands in the form of a bituminous spray [49]. However, there are several issues with this method. Firstly, there is a need for road closure to apply the layer of rejuvenator. Once applied, there is a reduction in surface friction of the pavement leading to safety concerns for the road users. Moreover, environmental damage due to inevitable spray depostion away from the target area is unavoidable. Finally, the penetration of the rejuvenator is only 5-10mm in dense asphalt grades, or up to 20mm in porous grades, so the problem of cracks deeper in the matrix is not addressed [5].

The use of microcapsules containing rejuvenator offers a prospective solution to these problems. The principle can be broken down as follows: The capsules are incorporated into the binder at the expense of a small amount of aggregate to ensure mechanical properties are not detrimentally effected. When the stress on the capsules reaches a threshold value, e.g. when a crack begins to propogate through its structure, the capsules break and rejuvenator is released, at least partially restoring the mechanical properties of the asphalt mixture by filling the formed microcrack. Once the capsule is ruptured, it cannot be used again for healing, meaning that it is effective for a one-time healing event. A schematic can be seen below in figure 2.18.

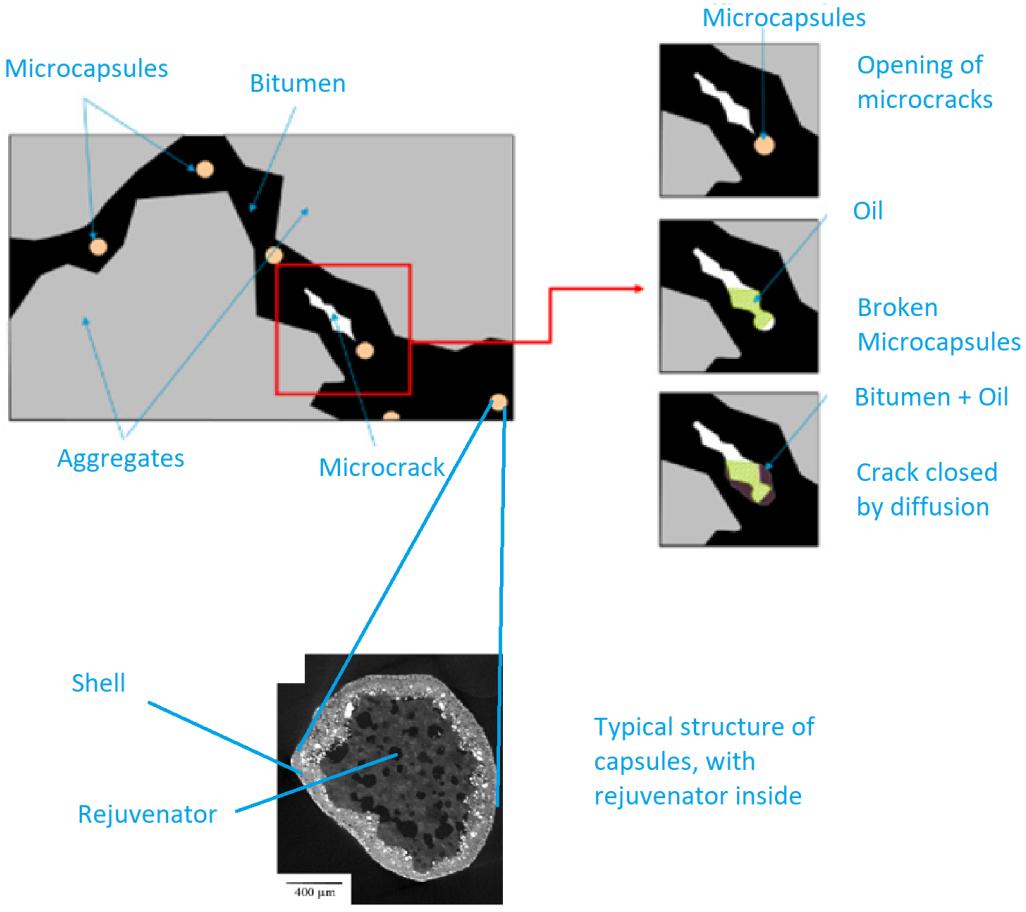

Figure 2.18: A schematic of the rejuvenative healing process within asphalt [50] [51].

A key property of these microcapsules is their ability to withstand the strenuous asphalt production process. This has been demonstrated by Tabakovic et al. [52] and

Xu et al. [53] through the use of calcium alginate capsules as a rejuvenative healing method. Alginates are the metabolic products of bacteria and can be found in brown algae, making them an attractive option for their low economic and environmental cost. Another advantage is that the alginate capsules do not suffer from ageing in the same way as the asphalt mastic [53].

There are other successful instances of rejuvenator encapsulation that have been covered in the literature such as Melamine-formaldehyde (MMF) [54] and Epoxy capsules [51]. However, these capsules exhibit problems with their production or implementation. MMF capsules require high concentrations of formaldehyde during their production which is hazardous for human and environmental health. Epoxy capsules survive mixing and compaction of the asphalt, but the breaking mechanism is difficult to predict and control, leading to variable results. For these reasons only calcium alginate capsules will be considered for the remainder of this section.

Shell material to rejuvenator ratio must be optimised to provide maximum healing capacity while maintaining structural integrity of the system during asphalt production and compaction. Tabaković et al. [55] established that the optimum ratio of alginate to rejuvenator was 30/70. Even at high temperatures, the compressive strength of these capsules exceeded the reference strength necessary for compaction of asphalt (2MPa).

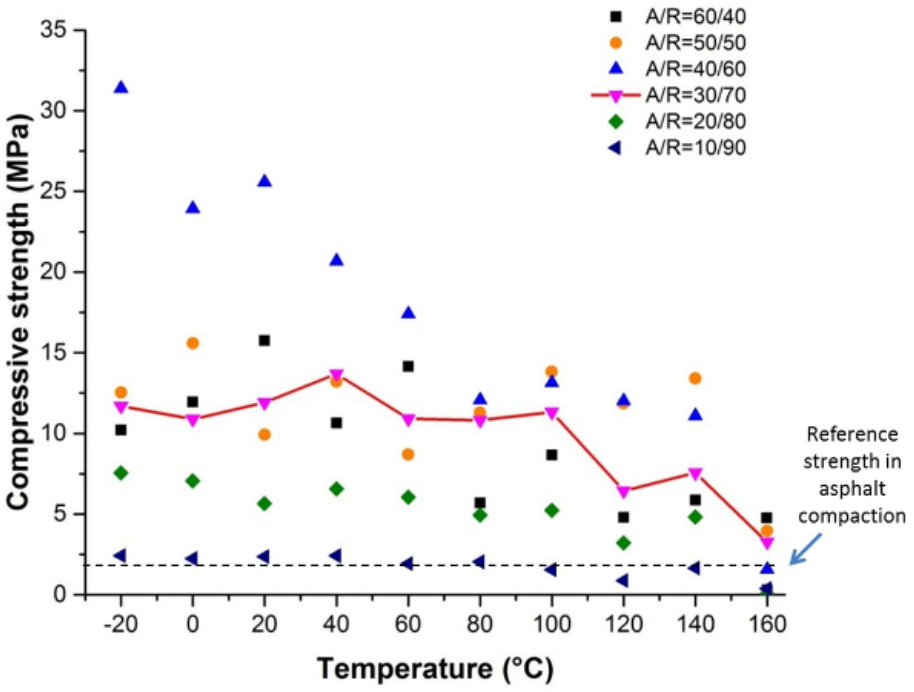

Figure 2.19: Alginate:Rejuvenator (A/R) ratio effect on compressive strength as a function of temperature

Using this capsule composition, when undergoing a three-point bend (3PB) test, it was shown that an aged asphalt mastic containing alginate capsules had a healing index of 90.1% after the first healing event, and 76.4% after the second. A significant improvement on the autogenous healing of the mastic (75.7% and 50% respectively

[53]). Capsules provide a reinforcing effect within porous asphalt beams, showing a higher original bending strength than those without capsules [5].

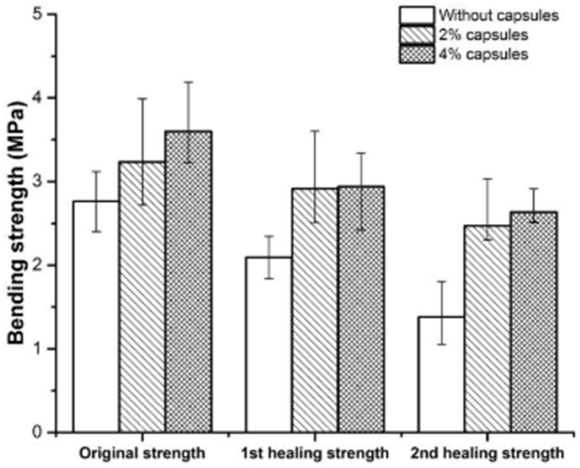

Figure 2.20: Healing efficacy of capsules over the first two healing cycles using aged bitumen [53]

However, when the bituminous material is fresh, the asphalt has a greater autogenous self-healing capacity, and the capsules have minimal effect on improving healing efficiency (see figure 2.21) Therefore, the encapsulated rejuvenator healing method works more significantly on aged bitumen.

These discrepancies in healing effects show that asphalt age and mixture composition have a significant impact on the self-healing capability of the asphalt. In terms of mixture composition, Xu et al. [55] understood that 2% volume by capsules provided better recovery in strength than 4% volume by capsules, but the inclusion of capsules improved the mechanical properties of the mastic. Optimum capsule volume was hypothesised to be 2.6 wt% bitumen of the asphalt mix to make the trade-off between these two factors.

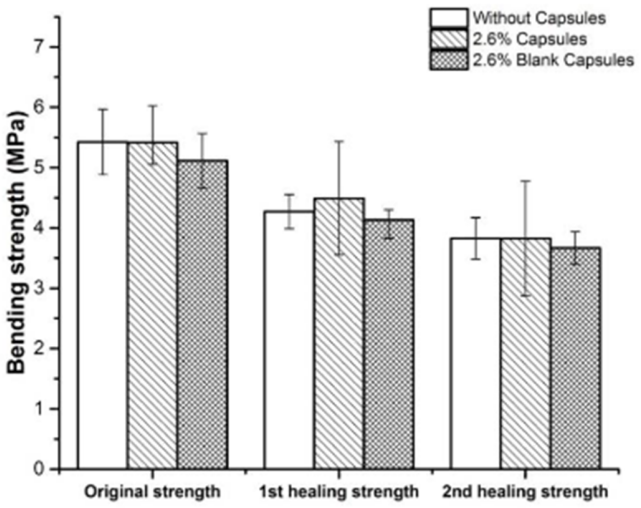

Figure 2.21: Healing efficacy of capsules over the first two healing cycles of asphalt with new bitumen [53]

Type of rejuvenator encapsulated also has an effect on healing efficacy. Wang et al [56] tested different rejuvenators encapsulated using alginate capsules, finding that vegetable oil and waste cooking oil would have a similar healing index for fatigue properties when compared to industrial rejuvenator capsules. Notably, the healing index for each rejuvenative method was greater than the reference mix (see figure 2.22).

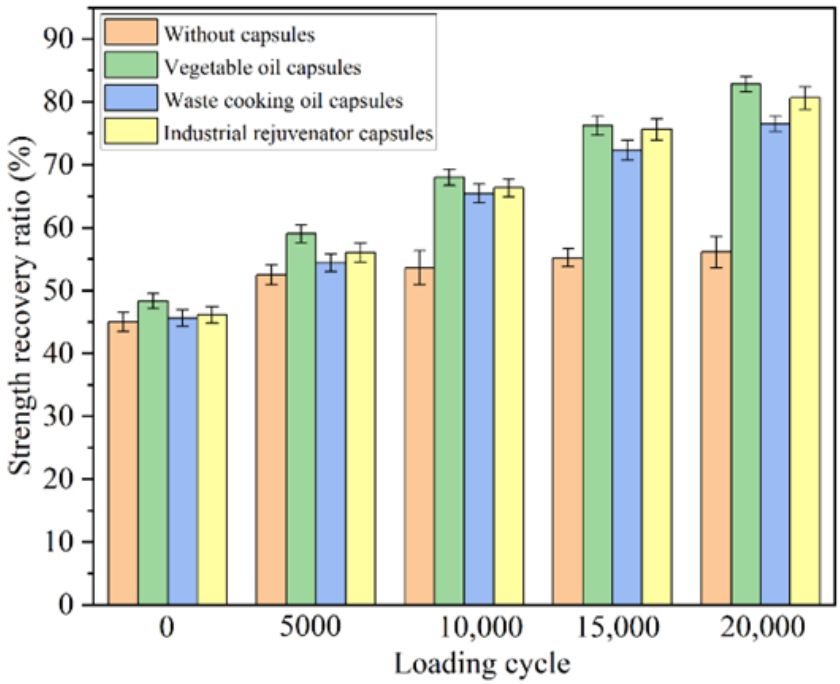

Figure 2.22: Effect of rejuvenator type on healing percentage [56]

2.6.5. Combined healing method

Given the major points associated with both healing methods, namely:

1. Induction - Less effective when the binder is aged, but highly effective on fresh mixture and can be done multiple times.
2. Capsules - Single use, Less efficient at improving property recovery, but effective at restoring properties to some degree in aged mixture.

Xu [5] proposed and tested a combined healing method. The use of 85^{o}C induction healing cycles on a porous asphalt mix containing rejuvenative capsules was achieved and the healing capabilities of PA significantly improved when the pavement was allowed to rest. The release of rejuvenator from the capsules when ruptured, reduces the effect of ageing in the binder and improves the efficacy of the induction healing process. The projected lifetime of the pavement rises significantly when healing events are added at intervals similar to the induction heating only method. The healing effect is not only due to the advantages of both mechanisms, but also coactive effects which assist each mechanism individually. For example, the accelerated diffusion of rejuvenator into the crack during induction heating due to the temperature dependency.

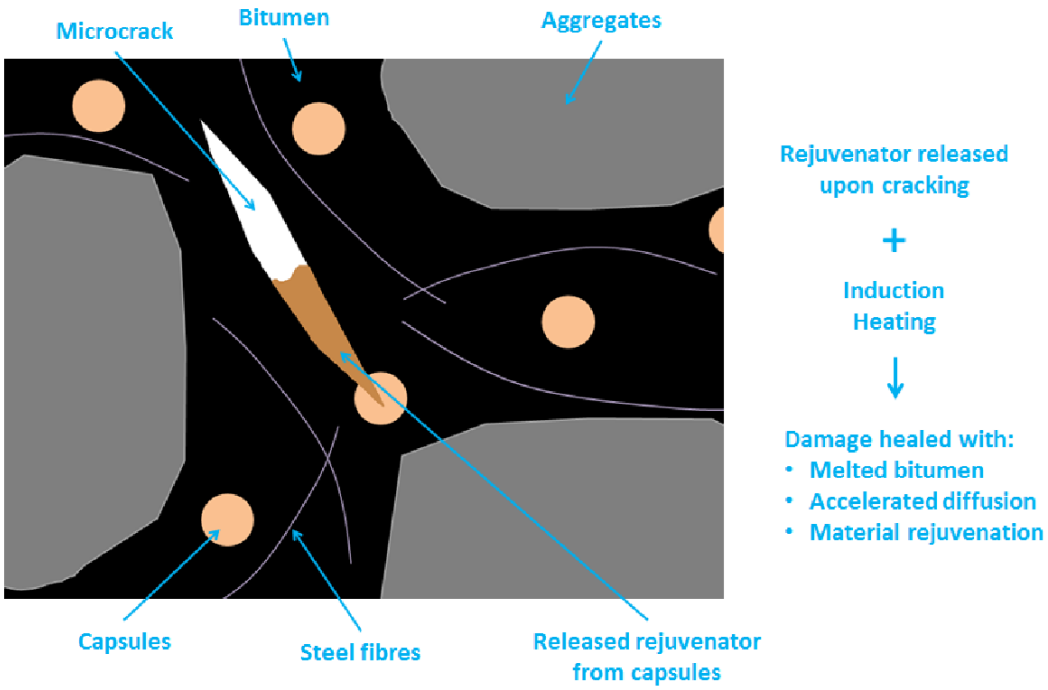

Figure 2.23: Schematic of a combined healing method proposed by Xu [5].

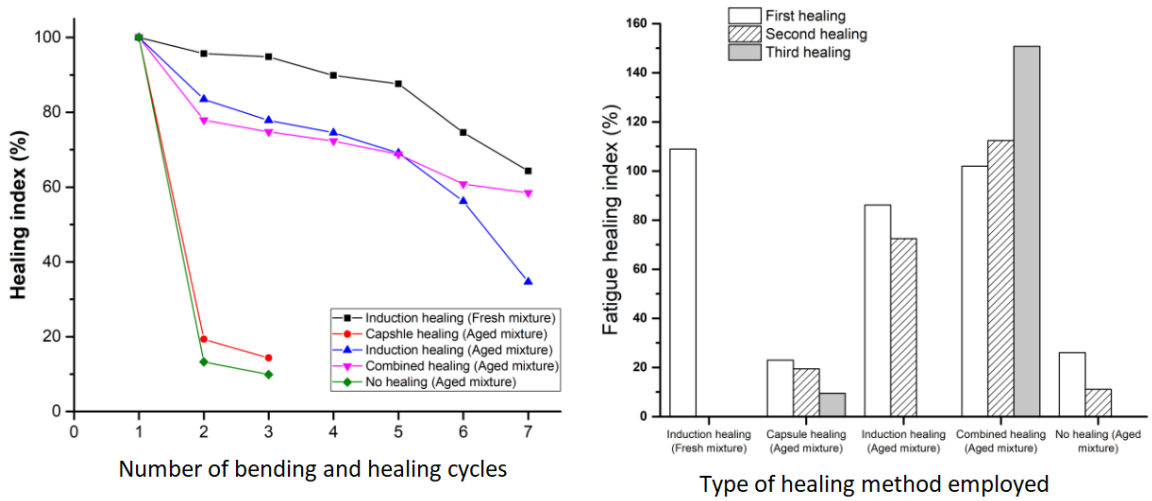

Figure 2.24: Healing index for multiple healing cycles as a function of the type of healing method employed. Left: shows bending strength healing index over 7 healing cycles for different self-healing mechanisms, right: shows the effect of healing method on fatigue healing index over 3 healing cycles [5].

Figure 2.24 highlights the effectiveness of the combined system over multiple healing cycles. Fatigue damage healing effects are markedly improved, even increasing with subsequent healing events. These findings help to reinforce the idea that the gradually released rejuvenator mitigates the ageing of the binder and allows the induction healing to be more effective. The bending strength healing index becomes better than induction heating beyond 5 healing cycles in an aged asphalt mix, showing a significant advantage in service life extension than in a single induction healing system.

There are limitations to the applicability of lab work to in-situ applications. Figures 2.23 and 2.24 indicate the performance of the combined healing event under certain conditions, and do not necessarily accurately represent how such a system would perform in a long-term field application.

2.6.6. Summary of self-healing asphalt and APJ applicability

At the time of writing there is little evidence in the literature of self-healing technology being applied to asphaltic plug joints. Self-healing technology stimulates asphalt crack healing, therefore extends the service life and reduces the maintenance frequency making it an exciting research prospect. The most promising of the mechanisms discussed in this chapter is a combination of induction and capsule healing. Given the failure mechanisms and limited lifetimes of APJs, it makes engineering and scientific sense to apply a combined healing approach to APJs in an attempt to mitigate premature failure and reduce costs. However, the optimal capsule and fibre content in a combined healing mixture is yet to be determined. An assessment of viability in the form of laboratory experiments followed by in-situ field application is needed to understand the efficacy of this system over the long term as well as more accurately quantify potential lifetime extension.

2.7. Sustainability

The environmental pollution due to reparations of road damage in conventional APJs, will undoubtedly lead to greater environmental degradation. Laboratory work and engineering practice has shown that self-healing technology for crack healing is an efficient method for extending lifetime and reducing the frequency of repairs of asphaltic mixtures. Therefore, it is necessary to understand the implications of sustainability on the production and lifetime of such technology to assess viability and quantify these benefits.

2.7.1. Life Cycle Assessment (LCA)

LCA is a calculation tool used to quantify the environmental impact of a product or a process over its life cycle. It takes into account factors such as raw materials, transport, manufacturing, and maintenance to end of life. Inputs such as the energy and resources required, and emission outputs or environmental pollutants can be defined. From this, environmental impact can be determined for a variety of ecological challenges. At present, government bodies and businesses are largely concerned with carbon emissions and the associated global warming potential. However, ecological problems such as eutrophication, human and marine ecotoxicity may be important, and can also be addressed by LCA.

The conduction of LCA can have several benefits, including the informing of decision making based on the environmental impact of activities. Understanding these impacts can help ascertain environmental weak points in supply chains, which can then be optimised. The reduction in environmental impact through saving energy and/or initial resource consumption can lead to economic savings.

Methodological framework

Based on international standards ISO 14040 and ISO 14044 (2006) [57], LCAs are carried out in 4 distinct steps. The steps are shown below in figure 2.25:

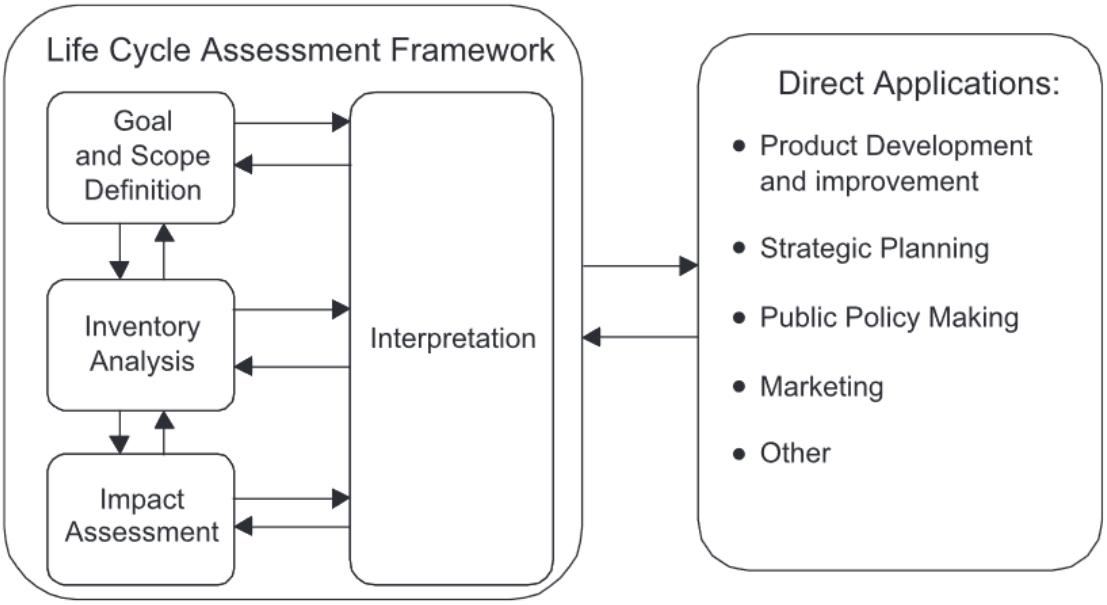

Figure 2.25: Life Cycle Assessment Framework based on ISO 14040 (2006) and ISO 14044 (2006) [58].

Goal and scope definition

The goal of the LCA must be clearly defined to determine the type of study and the approach taken. The target audience and basis of the analysis must also be stated. The scope of any LCA is constrained by the geographical region of relevance, and the boundary conditions of the problem. This step is crucial as it specifies which phases and activities within the lifecycle should be considered and those that fall outside and are surplus to requirement. Once the scope has been established, a functional unit must be determined. The functional unit is considered a normalising step, as all of the LCA results can be expressed against it, leading to straightforward comparison between products and processes. For a pavement related LCA, a functional unit may be a particular length of pavement of a specific geometry. From this, CO_2 equivalent emissions or relative marine toxicity can be measured per meter of pavement for example [59].

Inventory analysis

The second LCA phase is where input and output flows are identified and quantified for the given system called Life Cycle Inventory (LCI). For this, a significant amount of data is required. The majority of the data is obtained from relevant public/commercial databases, or can be collected from the literature or on-site for project specific cases. Depending on the case, a combination of these data collection approaches may be required, depending on quality, availability and scope of the LCA. Inventory analysis is an iterative process. If an issue arises where some data is difficult to obtain or the source is unreliable, the performer of the LCA must make assumptions to account for this discrepancy.

Impact assessment

Following LCI, a Life Cycle Impact Assessment (LCIA) is conducted. In this stage, the results from the inventory analysis can be used to calculate the environmental impact of the inputs and outputs of each stage of the LCA and is used to beter understand the environmental significance of the LCI. Impacts generally fall into the broad categories of resource depletion, human impact, and impact on nature (ecosystems). Depending on the goal and scope of the LCA, the assessment can be narrowly focused on a small subcategory, or extend across multiple impact categories. In the surrounding literature, LCIA impact categories tend to be categorised into midpoints and endpoints. Midpoint approaches look at short term results such as global warming potential, ecotoxicity and resource depletion, whereas the endpoint approaches focus more on general environmental themes such as ecosystem and human health [60]. Generally, the midpoint approach is more relevant to assessing current impact as the analysis can be more easily expressed using indicators. Furthermore, presenting endpoint findings is optional according to ISO standards.

Interpretation

Interpreting the results is the final step of the LCA. Once the LCA objectives have been met, a final evaluation of the process and findings can be carried out. This often includes limitations of the study as well as conclusions drawn.

2.7.2. Current sustainability literature

LCAs for asphalt with self-healing additives, are not abundant in the literature. Butt et al [61] concluded in 2012 that while the use of autogenous self-healing asphalt with wax additives could lead to an increase in the sustainability of asphalt over the long term, there was a lack of fundamental understanding of the healing mechanism and properties of the binder. Research efforts since then have focused on the development of self-healing asphalt technology and its use cases. Given the promising results obtained in research focusing on the mechanism and efficacy of self-healing materials, the scientific community is in a better position to make more accurate predictions as to how the binder will behave and more accurate LCAs can be attempted.

Recently, LCA by Rodriguez-Alloza et al [62] in 2022 showed that many of the environmental impacts for a self-healing asphalt mix for use as road pavement surface were significantly reduced compared to a conventional asphalt mix. In this particular case, a microwave heating procedure (every 10 years) with steel slag additive self-healing technique was used. The study was based on the assumption of a conservative lifetime extension of 25%, which is significantly less than much of the literature suggests (with a 50-100% potential lifetime increase).

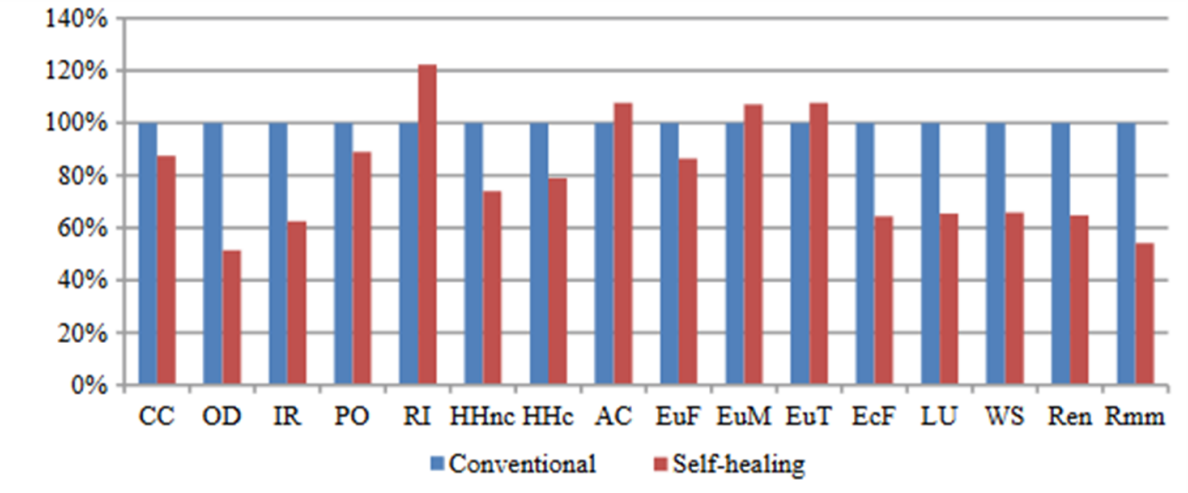

Figure 2.26: Comparative LCA study of self-healing asphalt vs conventional mix. The environmental impact categories covered in the study are listed are as follows: Climate change (CC), Ozone depletion (OD), Ionising radiation (IR), photochemical ozone formation (PO), respiratory inorganics (RI),human toxicity (cancer (HTc) and non-cancer effects (HTnc)), acidification (AC),eutrophication (terrestrial (EuT), fresh water (EuF) and marine (EuM)), freshwater eco toxicity (EcF), land use (LU), water scarcity (WS), resource use, energy carriers (Ren), and resource use, minerals and fossils (Rmm) [62].

As per figure 2.26, there are notable reductions for climate related impacts such as ozone depletion and climate change (GHG emissions) in favour of the self-healing asphalt. Resource use is also lower over the lifecycle in self-healing case.

Given the specific nature of the case-study, and the assumptions used, it is not possible to say with certainty that other self-healing methods will exhibit the same environmental benefits. The distinct lack of literature surrounding the topic has implications on the assumptions made, and causes result variation on a case-by-case basis. Similarly, the literature surrounding the sustainability of APJs over their lifecycle is non-existent at the time of writing.

Fortunately, LCAs have been conducted on other asphalt compositions at various stages of use. Comparative LCAs concerning warm and hot mix asphalt have been achieved [63] as well as a those discussing different modifiers added to improve mechanical properties of RAP such as lignin fibre and diatomite powder as demonstrated by Yue et al [64] and waste plastic addition by Veropalumbo et al [65]. Through these studies, RAP has been deemed advisable for use in road rehabilitation processes from an environmental perspective and the use of WMA instead of HMA is thought to lower environmental impacts at the expense of road quality.

In summary, the use of relevant midpoint and endpoint indicators combined with the appropriate framework and assumptions in an LCA study provide valuable insight into comparing the environmental impacts of different processes/products. With emerging technologies this can be difficult given the lack of available data, but a prospective LCA can be useful in providing a prediction of implementation benefits and the resulting data can aid strategic product development over the long term.

2.8. Concluding remarks

Given the current state of the art, the opinion of the writer is as follows: the use of a combined self-healing method is still a relatively novel concept, and must be further researched as to its capabilities for self-healing in different types of asphalt mixtures. Furthermore, it is necessary to understand the environmental aspects of the combined healing system, and whether or not its implementation does lead to reductions in environmental impacts. While the premature failure of APJs are an important problem to address, the primary goal of present research should be looking at optimising self-healing asphaltic mixtures. This will have an effect on the broader scope of pavement engineering, and their implementation will be relevant for not only joints, but also pavement surfaces, in particular the top layer. Therefore, the focus must remain on more general asphalt properties, with the aim being to understand the suitability of self-healing asphalt mixtures compared to standard SMA mixtures for general pavement applications. These can then be related to key failure points such as joints in discussions and conclusions drawn.

2.9. Research questions and aims

There has been a growing basis of knowledge over the last 10 years surrounding self healing technology. However, the optimum composition of a self-healing asphaltic mixture is yet to be determined. Given the particular promise of the dual-healing method, this thesis aims to understand how the capsule composition can be optimised to obtain the maximum lifetime of SMA mixtures. Alongside this, an assessment of the environmental impacts of self-healing mixtures, compared to standard mixtures is needed to better understand the sustainability of the self-healing alternative.

As a result of the literature review, and inline with the research aim and objectives, the following question was established.

How does a combined self-healing asphalt mixture compare to a standard stone mastic asphalt mixture from a performance and sustainability perspective?

From this broader main question, the following sub-questions were derived:

1. What is the optimum composition of capsules for a combined (capsule-induction) self-healing system in SMA?
2. What are the performance differences compared to a reference SMA mixture?
3. How does the environmental impact of an optimal self-healing system compare to that of current asphalt mixtures?

In order to go about answering these questions, different approaches are needed. To answer sub-question 1, laboratory experimentation was carried out to determine the healing efficacy of the self-healing system. Mechanical performance evaluation was achieved via further laboratory testing to help answer sub-question 2. Life-cycle assessment methodology will aid in the discussion about the environmental aspects outlined in sub-question 3.

3

Mechanical Performance Evaluation

3.1. Mechanical assessment methodology

For the mechanical assessment, a range of methodologies will be used. Firstly an overview of the necessary materials and sample preparation will be given. This will be followed by mechanical property testing methods focused on strength, stiffness, water sensitivity, binder drainage and high temperature deformation.

3.1.1. Materials

According to the literature, the optimised capsule volume is yet to be determined for the self healing mechanism. Hence, some comparable asphaltic mixtures must be produced for testing. The capsule healing part of the combined system is preferred when the sample is aged. Therefore, four aged asphaltic mixtures with varying capsule content were proposed, alongside two reference samples (one aged, the other fresh) which will act as yardsticks to measure the change in properties. Cellulose fibres are added to improve binder retention during processing. The capsules and steel fibres are implemented at the expense of CRF in the mixture, while bitumen and cellulose fibre content remain constant. The exact compositions used in the samples for mechanical testing are as above in figure 3.1. The limestone aggregates, filler, CRF and 40/60 bitumen were all provided by contractors Roadstone.

The capsules used had an alginate/rejuvenator (A/R) ratio of 30/70 as per the work by Xu [5] which considered rejuvenator content and mechanical property optimisation. Capsule production consisted of adding sodium alginate powder to deionised water, before mechanically mixing in the oil rejuvenator to form a homogeneous mixture. Using pressure applied to a modified shower-head, the mixture was dripped into excess calcium chloride solution at a constant rate, to form uniform capsules accommodating the rejuvenator. The capsules were collected, then dried for 48 hours in an oven at 40^{o}C, in a process summarised in figure 3.2.

Mix Constituent		wt% Content in Mix				
		Capsule+Induction system(CIS)				Reference
		CIS1	CIS2	CIS3	CIS4	R
10 mm		50.2	50.2	50.2	50.2	50.2
6 mm		10	10	10	10	10
Filler		6	6	6	6	6
CRF		25.3	25.1	24.9	24.7	28
Self-healing materials	C	0.2	0.4	0.6	0.8	-
	SF	2.5	2.5	2.5	2.5	-
	Σ	2.7	2.9	3.1	3.3	0
	Bitumen	5.8	5.8	5.8	5.8	5.8

Figure 3.1: Asphalt compositions in wt% of mixture, where C represents capsules and SF represents steel fibres

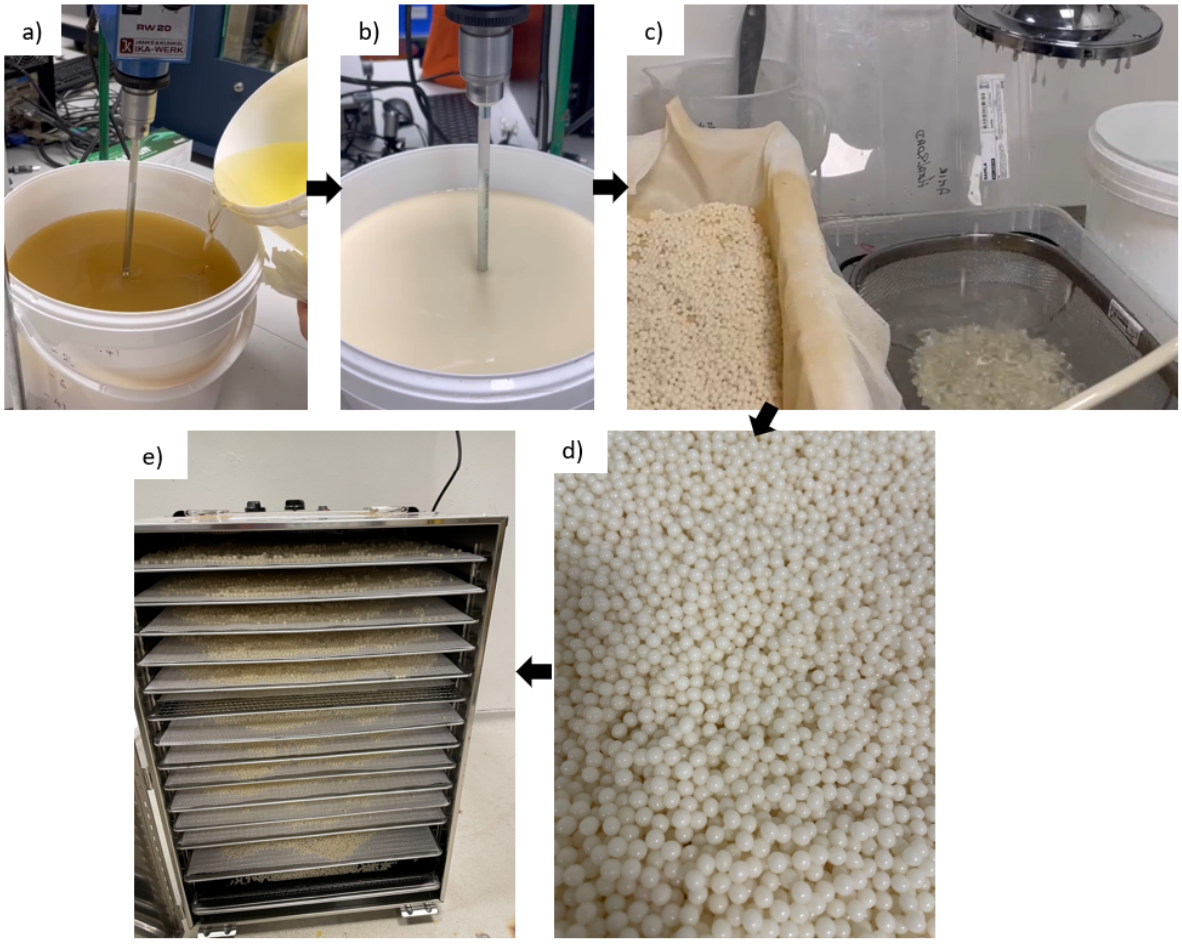

Figure 3.2: Summary of the capsule making process: a) Addition of oil to alginate solution, b) Mechanical mixing of the capsule solution, c) Capsule formation through droplets of alginate solution into calcium chloride solution, d) Wet capsules formed e) Wet capsules transferred to drying oven for drying for 24 hours at 40^{o}C

The dry capsules were measured and photographed using optical microscopy, giving an average diameter of 2.74mm. Overall, the capsules produced exhibited a good level of homogeneity in terms of composition with few inclusions or visible surface defects. Many capsules assumed a spherical shape with relatively few exceptions. A random selection of 10 capsules taken from the post-production phase can be seen in figure 3.3.

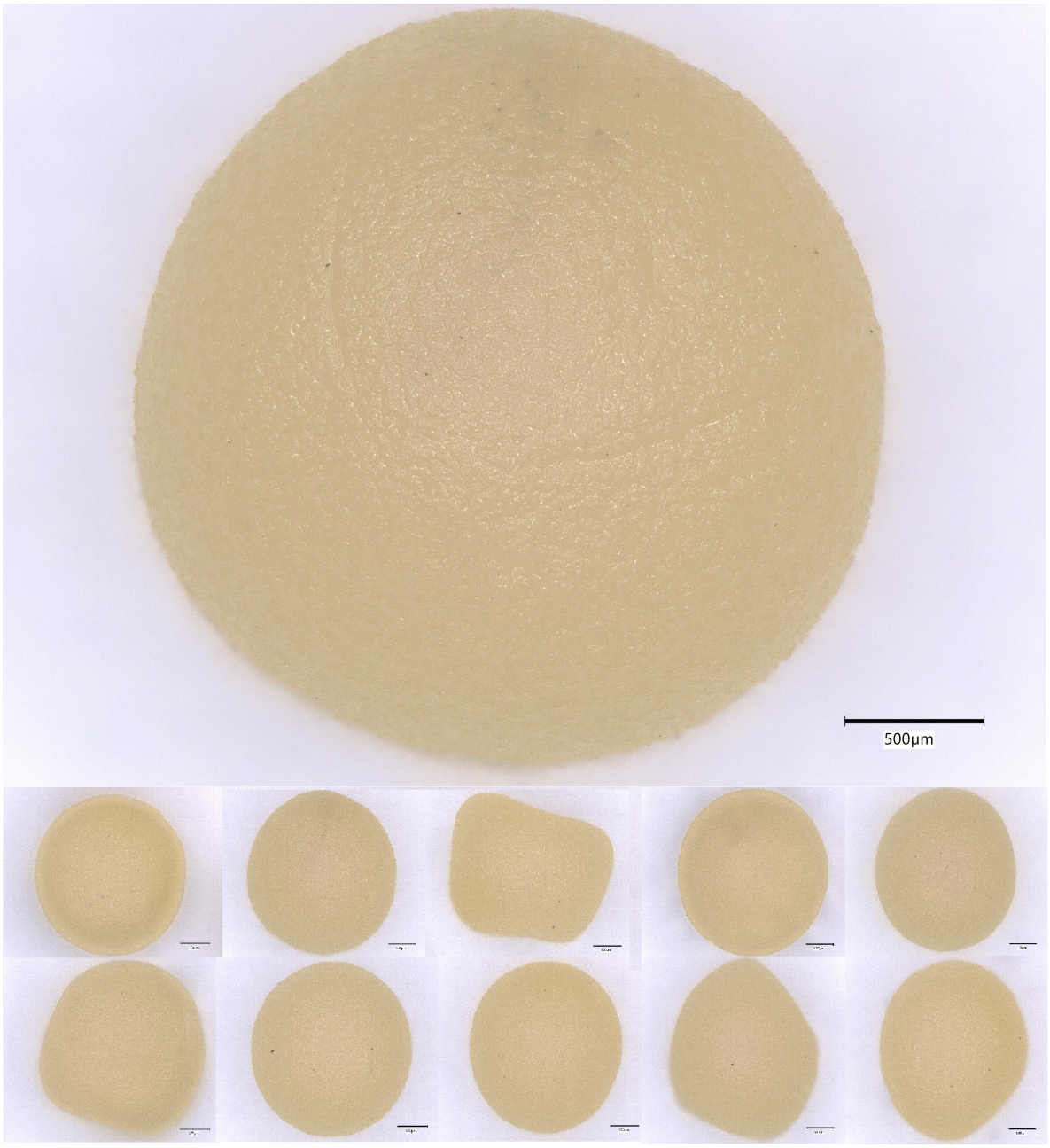

Figure 3.3: Microscopic images of the capsules produced, alongside 10 randomly selected capsules to show the variation in shape, captured using an optical microscope.

3.1.2. Sample preparation

The samples of asphalt for property testing were prepared in a **gyratory compactor** in conjunction with the standard NEN EN 12697-31 and the compositions outlined in section 3.3.1. The gyratory compactor produces cylinders with diameter 100mm +-2mm and a set height which are then further processed depending on the mechanical test conducted.

Laboratory ageing was carried out for the healing test samples to simulate the oxidation of the asphalt mastic which occurs over time when in active use conditions. The samples were subjected to temperatures of 135^{o}C for 4 hours in a short-term thermal ageing procedure to simulate the asphalt ageing during the mixing and production process. Subsequently, the sample underwent a long-term ageing process at 85^{o}C for 120hrs to simulate 5-10 years of field service. This ageing method is concurrent with the standard (AASHTO) R30.

Figure 3.4: 100mm x 50mm samples post compaction

3.1.3. ITT and ITS

In order to evaluate road performance, there are standard tests designed for fresh asphaltic mixtures which must meet certain criteria for road use. Firstly, **Indirect Tensile Tests** were conducted to further investigate the strength and stiffness properties of each test group. Once again samples of diameter 100mm and a height of 50mm

were used. The samples were tested with non-destructive indirect tensile stiffness test (ITS) following the European standard NEN-EN 12697-26 and the destructive indirect tensile strength test (ITT) following the standard NEN-EN 12697-23. The tests were conducted in a UTM with temperature control.

The test setup involved a pair of displacement transducers at the front and rear of the cylinders to measure horizontal deformation as a result of vertical loading. The sample was clamped to ensure that the displacement transducers do not experience any unwanted lateral movement during the test. The test setup is as shown in figure 3.5 and the equations below indicate how indirect tensile stiffness modulus and strength were calculated from the parameters measured.

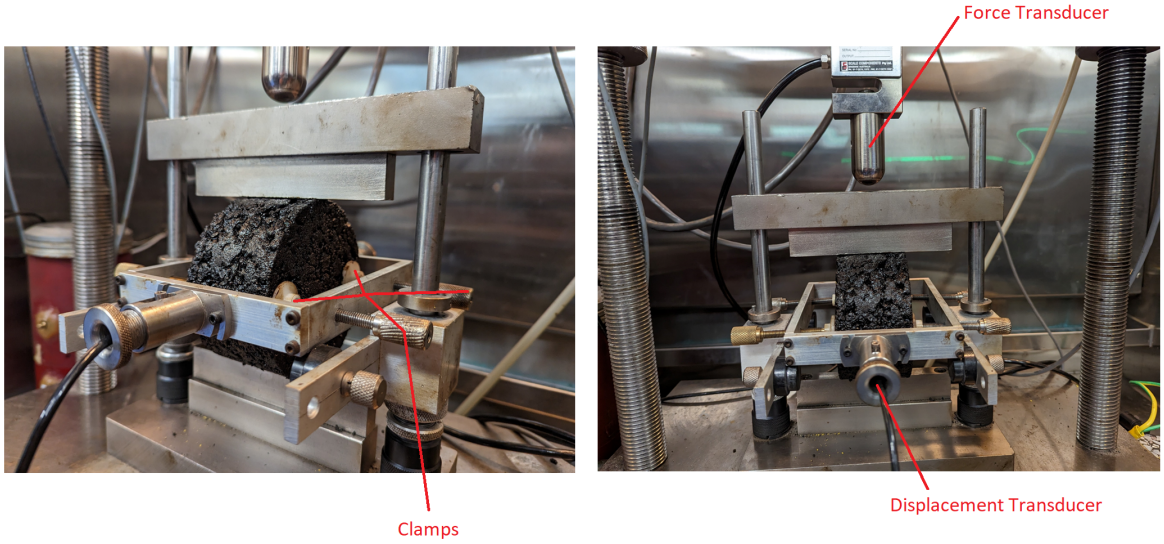

Figure 3.5: Test setup for Indirect tensile strength and stiffness

$$ITSM = \frac{F(v + 0.27)}{Zt}$$

Where:
$ITSM$ = Indirect tensile stiffness modulus (MPa);
F = Maximum vertical load (N);
v = Poissons ratio;
Z = the amplitude of the horizontal deformation during the load cycle (mm);
t = specimen thickness (mm).

$$ITS = \frac{2P}{\pi DH} \times 1000$$

Where:
ITS = Indirect tensile strength (kPa);
P = Peak load (N);
D = Sample diameter (mm);

H = Sample height (mm);

In this thesis, ITSM measurements were conducted at 3 different temperatures (15, 20 and 25^{o}C) each at 4 different loading frequencies (1Hz, 2Hz, 4Hz, and 8Hz). The Poisson's ratio was assumed to be 0.27 for these SMA mixtures. The indirect tensile strength tests were performed at 5^{o}C at a loading speed of 0.85mm/s with the same setup loaded by a MTS 50.

3.1.4. Water sensitivity

Water sensitivity of the asphalt mixture is a necessary prerequisite to understanding the adhesion between binder and aggregates. Water sensitivity can be effectively measured by conditioning the sample in water over a period of time, and obtaining the percentage difference in mechanical properties between the dry and conditioned samples. Using the standard NEN-EN 12697-12, water sensitivity based on the differences in indirect tensile strength of the samples can be carried out. A schematic of the conditioning of samples can be seen in figure 3.6. The samples were immersed in water and a vacuum was applied for 40 minutes, before being brought back to atmospheric pressure. The samples were then conditioned in a water bath at 40^{o}C for 72 hours before being towel dried and placed in a temperature chamber ready for the indirect tensile strength testing.

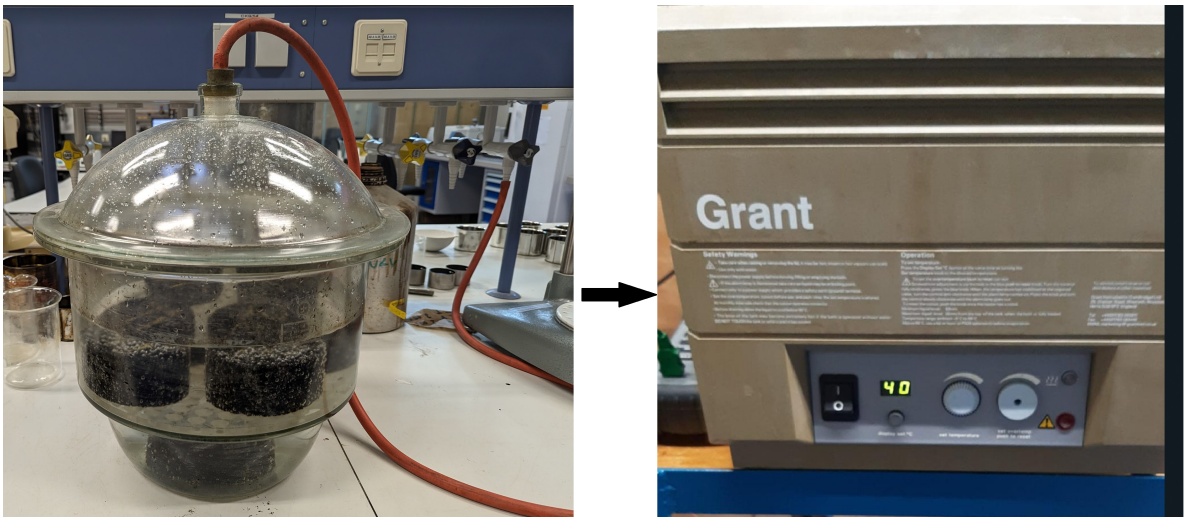

Figure 3.6: Sample conditioning for water sensitivity, left: vacuum chamber with immersed samples, right: water bath set to 40^{o}C.

The test setup to obtain ITS was identical to the dry samples as described previously. Water sensitivity can be calculated as follows:

$$ITSR = 100\% \times \frac{ITS_w}{ITS_d}$$

$$WS = 100 - ITSR$$

Where:
$ITSR$ = Indirect tensile strength ratio (%);
ITS_w = Indirect tensile strength of the wet, conditioned specimen (kPa);
ITS_d = Indirect tensile strength of the dry specimen (kPa).
WS = Water sensitivity (%).

3.1.5. Void content and density

The **void content** can be measured using references to the bulk density using the standard NEN-EN 12697-8. **Density** was measured via immersion of the sample in water at a known temperature, and the following equations were used to obtain ρ_b and subsequently the void content:

$$V_c = \frac{\rho_m - \rho_b}{\rho_m} \times 100$$

Where:
V_c = Void content (%);
ρ_m = Maximum density of the mixture (Mg/m^3);
ρ_b = Bulk density of the mixture (Mg/m^3);

$$\rho_w = 1.00025205 + \frac{7.59 \times t - 5.32 \times t^2}{10^6}$$

Where:
t = Temperature of the water (^oC);
ρ_w = Density of the water at test temperature t (Mg/m^3).

$$\rho_b = \frac{m_1}{m_1 - m_2} \times \rho_w$$

Where:
m_1 = Mass of dry specimen in grams (g);
m_2 = Mass of specimen in water in grams (g);

3.1.6. Binder drainage

Binder drainage plays a key role in understanding the rutting resistance and moisture damage susceptibility of asphalt pavements. A **Binder drainage test** (BD) according to the standard NEN-EN 12697-18 was used to understand whether the proposed self-healing mixtures comply sufficiently to limits for binder content within the mix. BD measures how much of the binder, and fine particles contained therein, is separated from the mixture after the mixing process. BD can be therefore defined as a percentage of the mass of drained material after being exposed to high temperatures

(mixing temperature +25^{o}C). The beaker method was followed in this instance. The mixtures were prepared without compaction and heated in a beaker at 180^oC for a period of 1 hour. Immediately after removal from the oven, the mixture was poured out of the beaker in a controlled manner and the relevant masses were recorded. Binder drainage was calculated as follows:

$$BD = 100 \times \frac{W_3 - W_1}{W_2 - W_1}$$

Where:
BD = Drained material (%);
W_1 = Mass of empty beaker (g);
W_2 = Mass of beaker + batch (g);
W_3 = Mass of beaker plus residue after upturning;

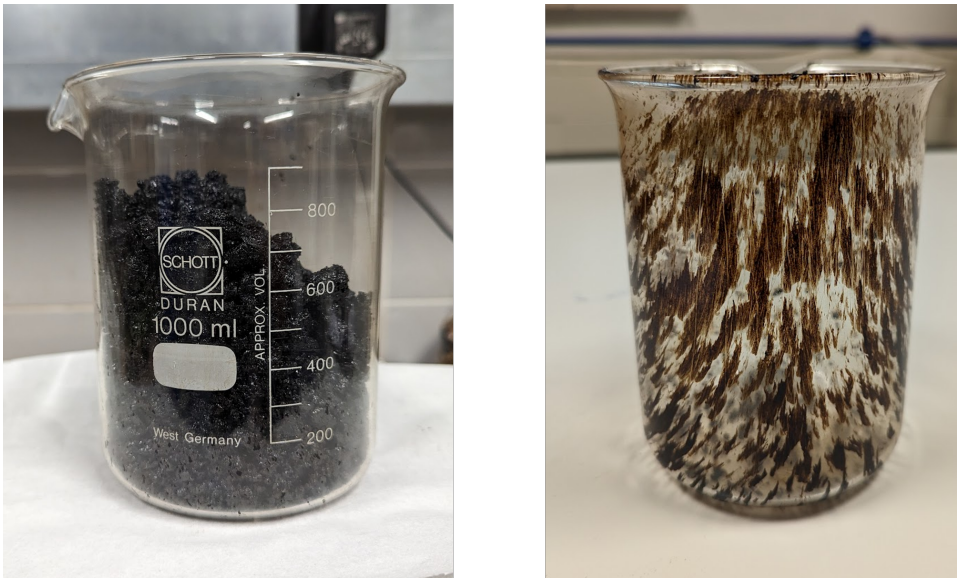

Figure 3.7: Binder drainage test before and after. Left shows prepared mixture in a beaker. Right shows binder residue when the beaker was removed from the oven and upturned.

3.1.7. Triaxial testing

A **Triaxial test** was undertaken to help understand the high temperature properties of each asphalt mixture by subjecting them to cyclic compression tests under confinement. The samples in this case were 100mm +/- 2mm in height and 100mm +/- 2mm in diameter. A taller sample height was decided to mitigate the effects of friction on the test results, and the samples were polished to ensure a flat surface. In each case, the samples were confined in an airtight flexible polymer sleeve with rubber seals at either end and subjected to a cyclic vertical load induced by a force transducer. In this case, 10000 loading cycles were used at 40^{o}C to determine the creep performance of each mixture by measuring sample deformation. The confinement pressure was set to 50kPa and the loading frequency was 1Hz. The test setup is depicted in figure 3.8.

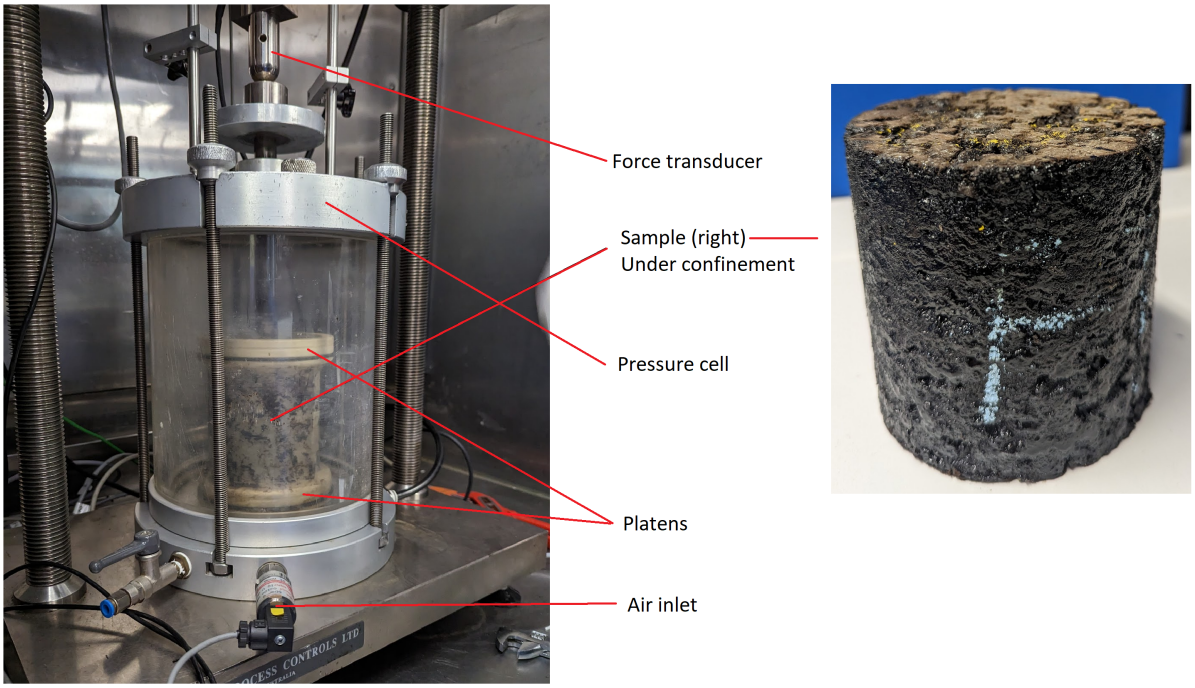

Figure 3.8: Triaxial test setup, using cylindrical samples of 100mm by 100mm.

As a measure of high temperature properties, the cumulative strain was calculated as a percentage of the initial test specimen as follows:

$$\epsilon_{10000} = \frac{|h_0 - h_{10000}|}{t_i}$$

Where:

ϵ_{10000} = the cumulative axial strain of the test specimen after 10000 loading cycles in percent (%) to the nearest 0.01%;
h_0 = the mean vertical position of the uper loading platen after preload of the test specimen (mm);
h_{10000} = the mean vertical position of the upper loading platen after n loading cycles (mm);
t_i = the initial thickness of the test specimen (mm).

3.2. Mechanical testing results

In this section, the results from the tests outlined in the previous section will be presented and discussed.

3.2.1. Void content and density results

Void content and density are material properties which are critical to understanding the road performance of asphaltic material. For the SMA mixtures tested in this project, a correlation between the capsule content and void content was observed. Figure 3.9 depicts the variation in void content with mixture composition.

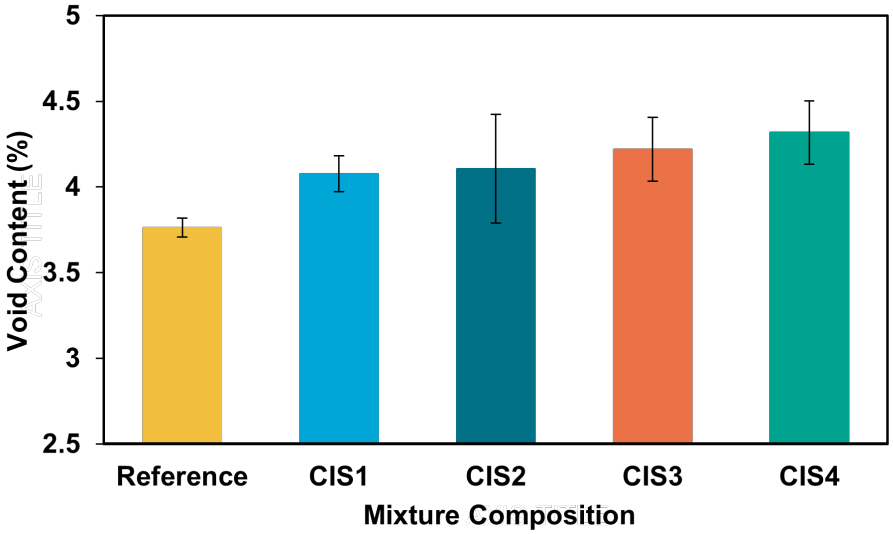

Figure 3.9: Void content of SMA samples from each testing groups

The reference sample exhibited the lowest void content which is attributed to the lack of capsules and steel fibres in the mixture. The first increase in void content from Reference to CIS1 is the largest, with an increase from 3.78% to 4.13%. This is due to the addition of the healing system containing steel fibres and capsules. Capsules replace CRF in the mixture, CRF is finer and denser than the capsules which inevitably leads to a lower density within the system. This observation is exacerbated by the increase in content of calcium alginate capsules. The capsules occupy space within the mixture, displacing the aggregate particles and binder. This displacement can disrupt the close packing of aggregates, resulting in a higher void content. As the capsule content increases, this effect is exacerbated, and the void content increases in a quasi-linear manner.

The increase in capsule content causing a decrease in density is shown in figure 3.10. A similar trend to that of void content can be observed with increasing capsule content. The first reduction (Reference to CIS1) being the largest from 2365kg/m^3 to 2300kg/m^3. This further solidifies the idea that the healing mechanism addition leads to an increased void content, and a lower overall density.

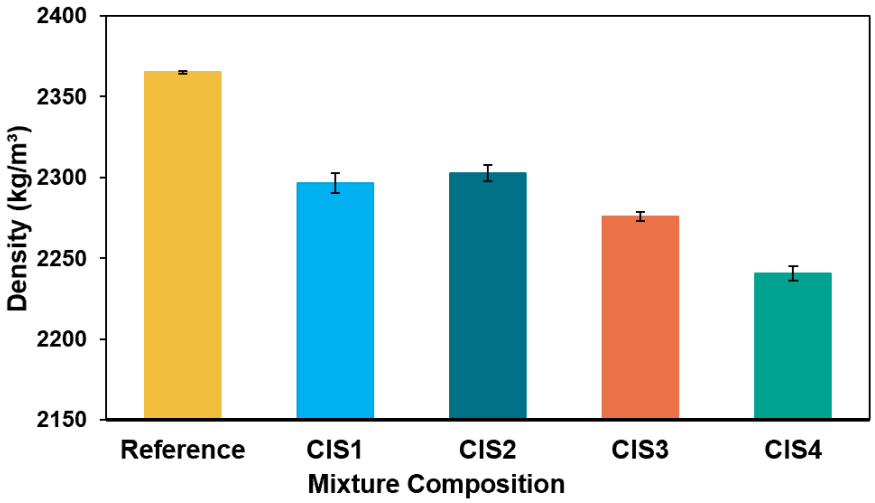

Figure 3.10: Density of SMA samples from each testing group

While the combined healing mechanism may affect the overall performance of the mixture in terms of healing and durability, the immediate impact of capsule content on void content and density can be attributed to the displacement of aggregate particles and binder, causing the introduction of additional voids within the mixture.

3.2.2. Binder drainage results

Binder drainage (BD) was tested to help understand the processing requirements of the different mixtures. High levels of BD are undesirable as it can result in lower binder contents in the final processed pavement, leading to reduced rutting resistance and increased moisture damage susceptibility. This can lead to greater uncertainty in predictions of mechanical properties and result in premature failure. The results of BD for each mixture are outlined in figure 3.11.

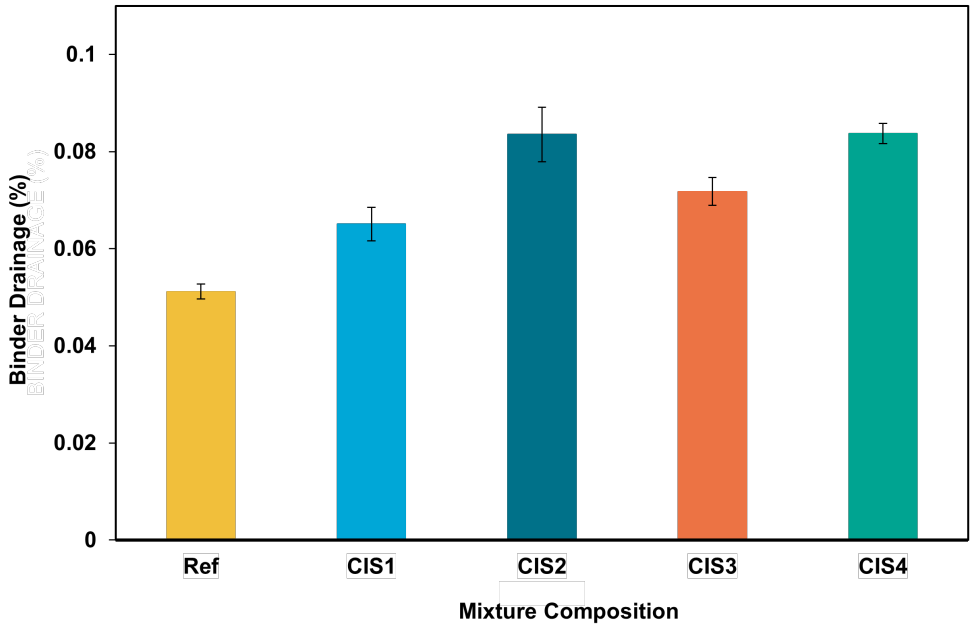

Figure 3.11: Binder drainage of each SMA mixture measured before compaction

The inclusion of drainage inhibitors in the form of cellulose fibres helped to keep binder drainage low in each mixture. The observed trend was a slight increase in binder drainage with increasing capsule content. One reason for this could be the softening of the binder. Residual oil on the surface of the capsules could provide rejuvenation and flexibility to the asphalt mastic causing softening. This effect can potentially increase flow and drainage of the binder through the mixture. Thus, the incremental increase in capsule content can cause a marginal increase in binder drainage in each instance.

It is thought that steel fibres have a positive effect on binder drainage, as shown by Liu et al [66]. This is unclear from these results, but the increase in BD is nearly linear from CIS1-4 with the exception of CIS2. Once again the reduction in fine particles due to the substitution of capsules for CRF causes a reduction in binder retention. This is due to the reduction in aggregate surface area for the binder to adhere to. This suggests that the capsule effect is more pronounced than that of the steel fibres on the eventual binder drainage. In any case, the binder drainage for all mixtures lies beneath the recommended level for SMA of 0.2% as outlined in *'Stone Matrix Asphalt: Theory and Practice'*, which suggests that mitigation of binder drainage for all mixtures tested was adequate [67].

3.2.3. Indirect tensile strength results

As shown by figure 3.12, each SMA mixture tested showed significant differences in indirect tensile strength. In general decreasing strength was observed with increase in capsule content. The effect of ageing appeared to be relatively insignificant, with an increase in strength by 3.82% post ageing. However, when comparing the fresh

reference with capsule containing mixtures, there was a drop in measured strength of 14% with CIS1, a 14.1% drop when comparing CIS2, a 24.9% drop for CIS3 and 24.8% drop for CIS4. Unlike porous asphalt, as found by Xu [5], the addition of a combined healing system particularly with high capsule content had a negative effect on strength. Moreover, the reinforcing effect of the steel fibres and capsules exhibited in porous asphalt does not appear to be present. The decrease in strength could be attributed to premature rejuvenator release causing binder softening, and the lower strength of the capsules compared to the aggregate. A combination of these factors would result in a lower peak load and subsequent strength.

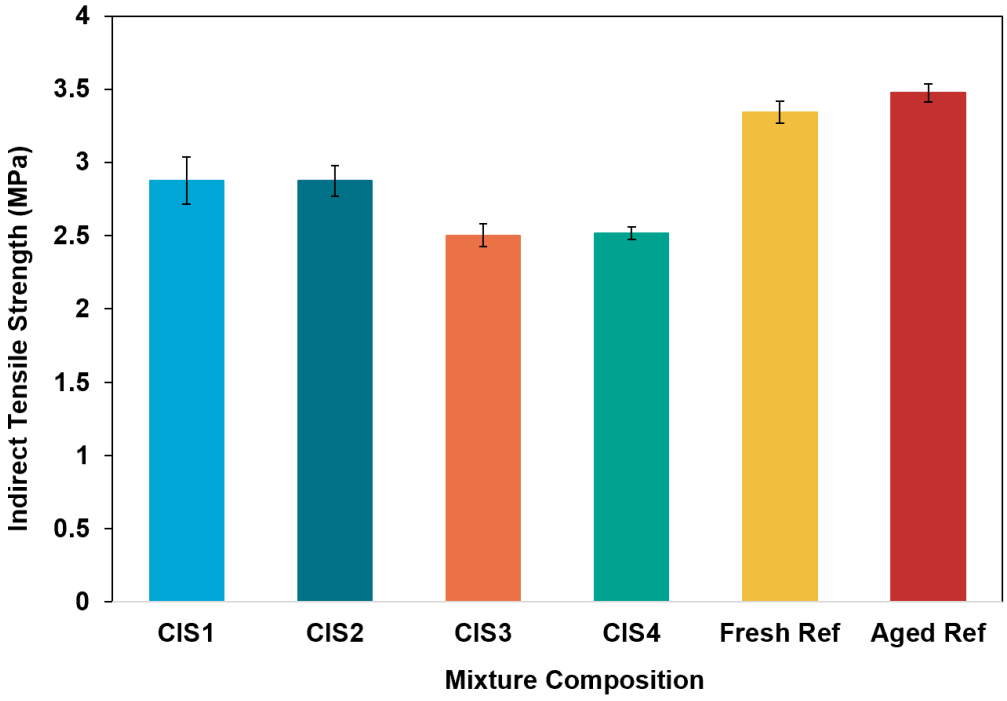

Figure 3.12: Indirect tensile strength of SMA samples from each testing group

3.2.4. Indirect tensile stiffness results

Indirect tensile stiffness tests were conducted at 15^o, 20^o and 25^{o}C and at loading frequencies 1Hz, 2Hz, 4Hz and 8Hz, respectively. The results of testing can be seen in figures 3.13, 3.14, and 3.15. Due to the viscoelastic nature of asphalt, higher loading frequencies resulted in higher stiffnesses due to reduced relaxation times. Hence, at higher frequencies the asphalt samples exhibited a more rigid response and higher stiffnesses. At lower frequencies, viscous behaviour is more prevalent and the elastic stiffness of the mixture is reduced. This held true for all mixtures, but was more pronounced at lower temperatures.

At each temperature, the aged reference mixture proved to be the stiffest. Lower capsule contents (CIS 1-3) showed comparable stiffness values to the fresh reference. CIS4 exhibited the lowest stiffness at each temperature. This trend suggests that an

increased capsule content reduces the stiffness of the mixture. At lower temperatures, there is a greater discrepancy in stiffness between the different mixtures, but frequency trends remained similar despite temperature variation.

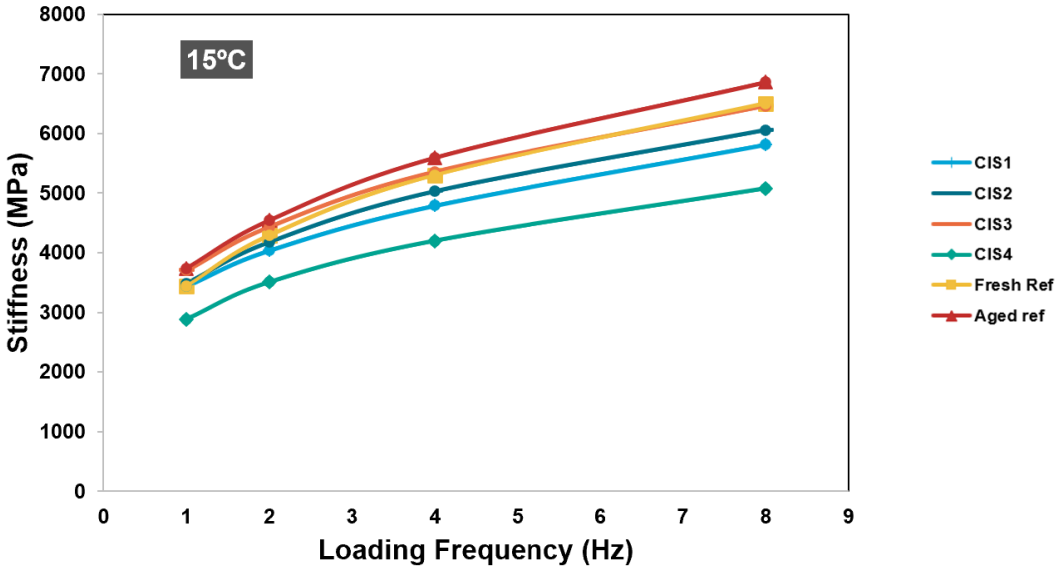

Figure 3.13: Indirect tensile stiffness of SMA samples from each testing group at 15^{o}C

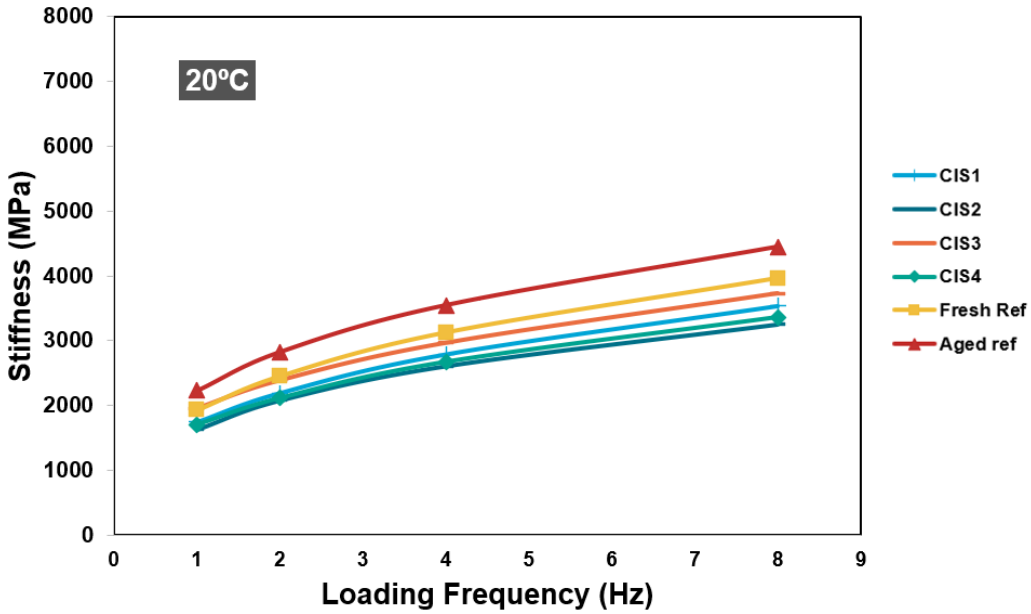

Figure 3.14: Indirect tensile stiffness of SMA samples from each testing group at 20^{o}C

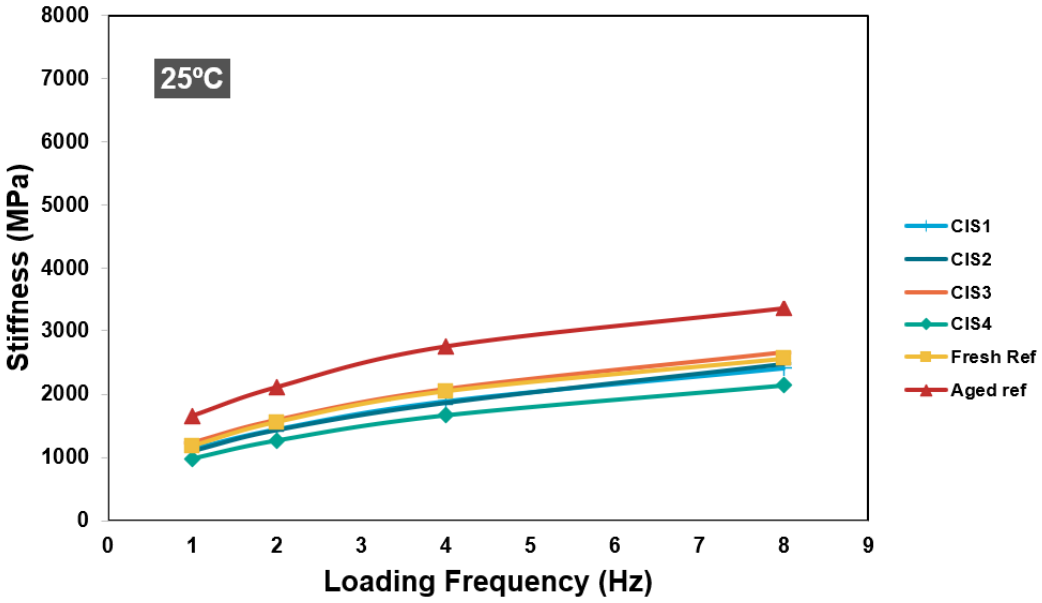

Figure 3.15: Indirect tensile stiffness of SMA samples from each testing group at 25^{o}C

3.2.5. Water sensitivity test results

The water sensitivities of each mixture tested are outlined in figure 3.16.

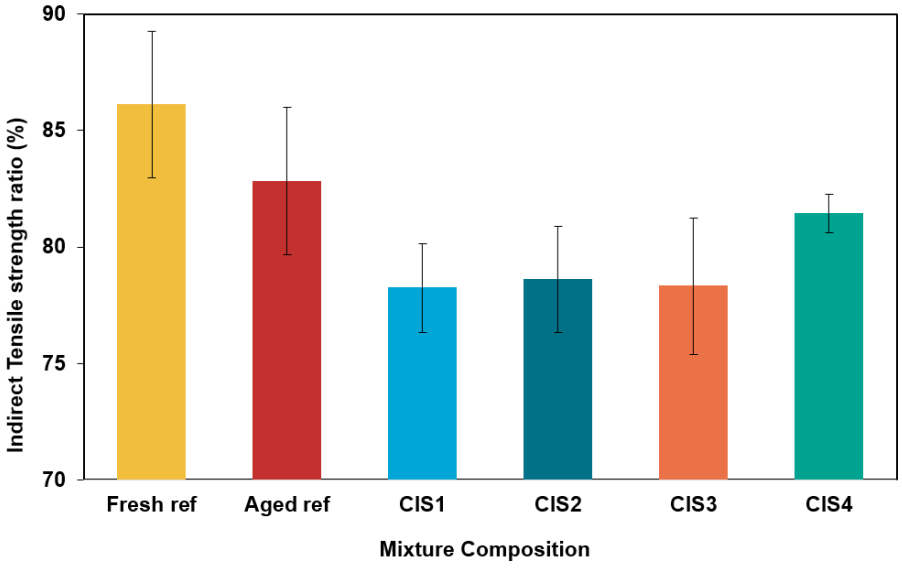

Figure 3.16: Water sensitivity of SMA samples from each testing group

It was observed that the reference samples exhibited lower water sensitivities than the self-healing samples. The fresh reference sample performed best, with a water sensitivity measured at 13.9%. The effect of ageing increased the water sensitivity to 17.2%, which can be attributed to the hardening of the binder and decreased binder-aggregate adhesion due to oxidation in the ageing process. The self healing

specimens exhibited a water sensitivity of between 18.6 and 21.7%, with a slight decrease with increasing capsule content. The greater void content of the self-healing mixtures allows for greater moisture ingression into the asphalt mastic, this may result in a greater degree of loss of binder adhesion with the aggregates, and subsequently lead to a drop in strength post conditioning.

In contrast, increasing capsule content slightly decreases the water sensitivity. One explanation for this observation may be that during conditioning, prolonged exposure to water and elevated temperatures may lead to a degree of capsule swelling, which has the potential to cause a rupture in the capsule structure as shown by Mendes et al [68]. As a result, some rejuvenator may have been released during the water sensitivity conditioning process. Consequently, the released rejuvenator may help to maintain the properties of the fresh binder in the presence of water, and reduces its susceptibility to moisture damage due to slightly improved binder adhesion, leading to a marginally greater retention in strength.

Overall, the addition of a combined healing mechanism increases the susceptibility to moisture damage, but higher capsule contents obtain slightly better results. Due to the many determining factors of water sensitivity, the exact mechanism is not clear and requires further research.

3.2.6. Triaxial test results

The triaxial test was used to gain a better understanding of the permanent deformation properties of the asphalt mixture at high temperatures. Figure 3.17 depicts the accumulated strain values of each mixture under the conditions specified.

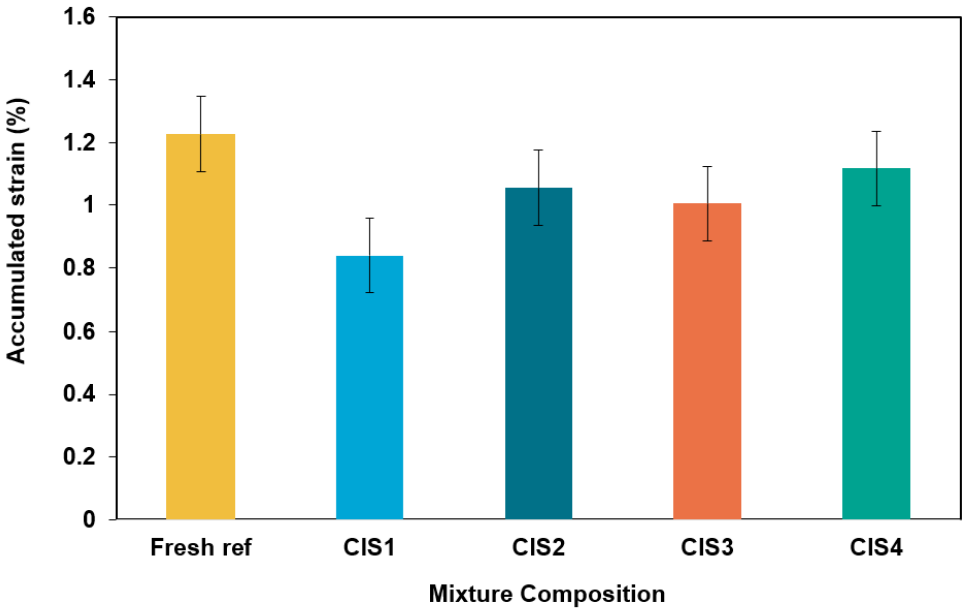

Figure 3.17: Triaxial test results showing accumulated strain after 10000 loading cycles at different mixture compositions.

A higher accumulated strain value signifies greater susceptibility to permanent de-

formation at elevated temperatures, indicating a lower resistance to rutting. Of the mixtures assessed, the inclusion of a healing system generally had a positive impact on rutting resistance, with lower accumulated strains observed than that of the reference SMA mixture. As capsule content increased however, the accumulated strain increased indicating that higher capsule content would have a detrimental effect on high temperature permanent deformation and rutting properties. This might be due to the higher void content as a result of capsule inclusion. This suggests that it is the inclusion of steel fibres which leads to a marked positive impact on the rutting resistance of the pavement. Of the self-healing mixtures, CIS1 exhibited the best rutting resistance properties.

3.2.7. Optical observations

Optical microscope images of a sample crossection of both the reference and self-healing mixtures are depicted in figure 3.18. Distribution of capsules and steel fibres was seen to be homogeneous throughout the binder in the self-healing samples analysed which suggests that mixing during sample preparation was successful. In the reference sample, fewer pores can be seen when compared with the healing sample (as indicated by the darker textured zones in the lower part of the figure) which is concurrent with the data from density and void content observed during mechanical testing.

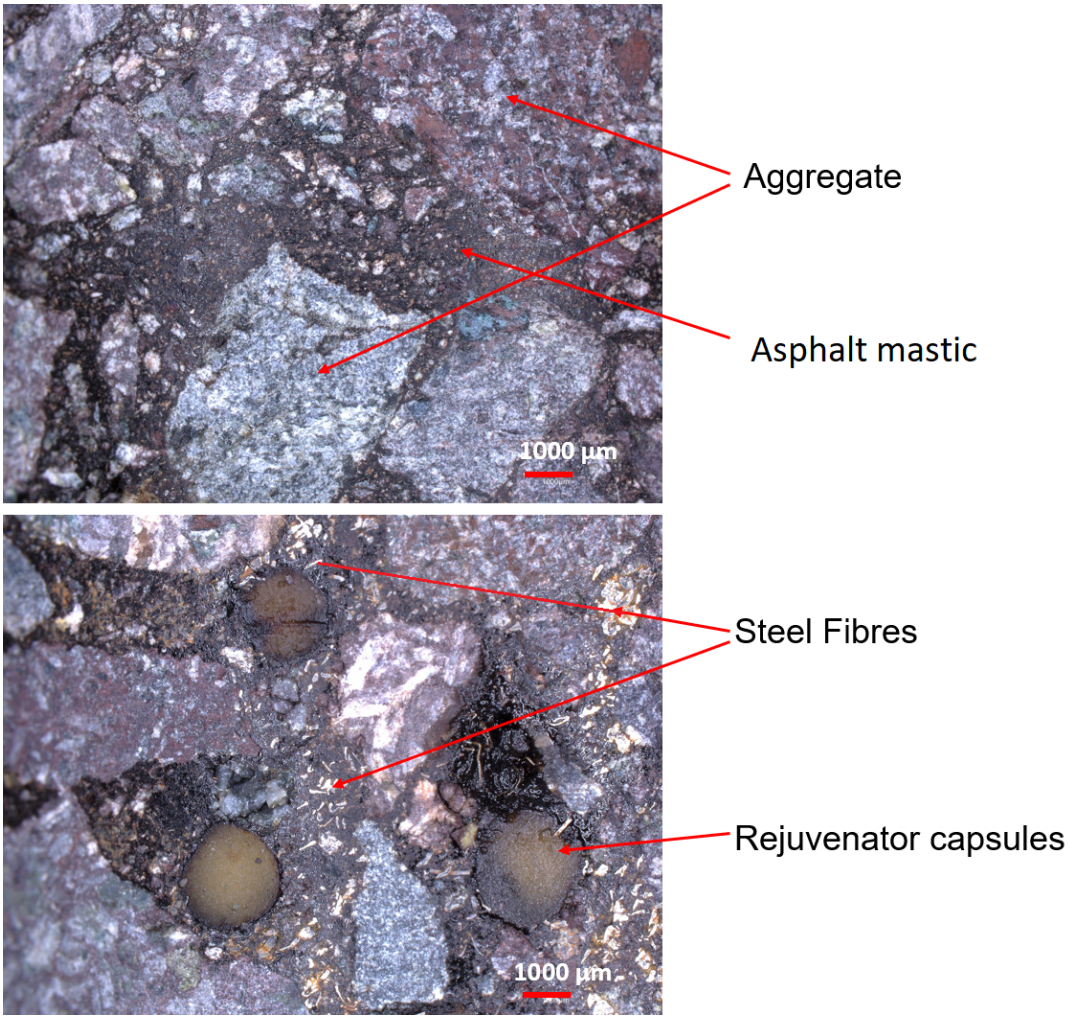

Figure 3.18: Microscopic images of the reference (top) vs self-healing (bottom) samples

While most capsules remained intact, there was some evidence for ruptured capsules which had been crushed in the compaction process during sample preparation. An example of this phenomenon can be seen in figure 3.19. This may have implications on the mechanical properties observed in this thesis, due to premature rejuvenator release. If released prematurely, the bitumen may be softened in the fresh mixture, leading to lower strength and stiffness values. This could also lead to reduced rejuvenation potential in aged mixture. It is unclear to what extent this has occurred within the mixture, but this may explain slight variations in mechanical properties between samples.

Figure 3.19: Microscopic image of a crushed capsule in the asphalt mastic, as is evident from the change in shape.

3.3. Concluding remarks

This chapter provided the methodology and results of the mechanical performance evaluation. In summary, the following conclusions were drawn.

- Indirect tensile strength of the self-healing samples generally decreased with increasing capsule content. Of the CIS mixtures, CIS1 showed the highest strength of 2.81MPa.
- Stiffness values of low capsule content (CIS1) showed comparable stiffness values to the reference samples suggesting similar low temperature stiffness properties.
- Increasing capsule content increased void content. Lowest void content of the self-healing samples was CIS1 with 4.31%.
- Self-healing samples showed superior rutting resistance to the reference samples as per the triaxial test results. Lower capsule content resulted in a lower overall deformation.
- Increasing capsule content increased binder drainage values, however all results remained within the recommended 0.2% limit.
- Due to the high density of the SMA mixture, crushing of capsules during compaction did occasionally occur. This may have caused premature rejuvenator release, and affected binder properties as a result.

4

Self-healing Performance Evaluation

4.1. Healing system evaluation methodology

In this section the methods used for assessing self-healing capacity of the asphalt samples is outlined. Firstly the semi-circular bending test method is outlined. Secondly, the determination of the healing procedure is undergone, including the induction heating optimisation of the samples.

4.1.1. Semi-circular bending test

In order to measure healing efficiency, samples must first be damaged. The damage mechanism chosen for this work was the **Semi-Circular Bending (SCB)** test. A universal testing machine (UTM-25) equipped with temperature chamber was used to perform the SCB tests according to the standard NEN-EN 12697-44. The semi-circular samples were produced by halving the cylinders produced by the gyratory compactor lengthwise, providing semicircular samples with a diameter of 100mm +/- 2mm. The supporting spans for the SCB samples resided 80mm apart, and a rectangular notch of depth 10mm +/- 0.2mm, and width 2mm +/- 0.1mm was used in each sample (see figure 4.1). The test was performed at temperature of 0^{o}C, and the loading condition used was 5mm/min.

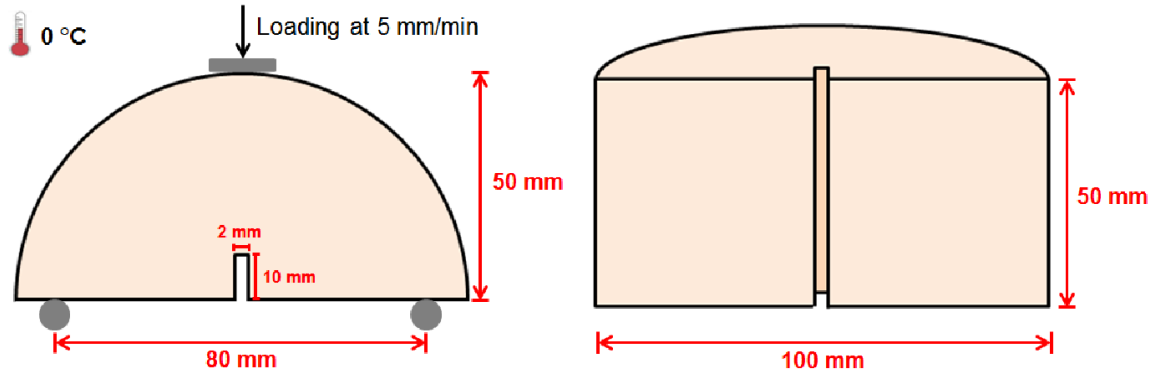

Figure 4.1: Sample dimensions of the SCB test specimens [5].

The goal of the SCB tests were to calculate the fracture toughness from the applied load and sample dimensions. Fracture toughness K_{1c} is given by:

$$K_{1c} = Y_{1c(0.8)} \frac{P_{max}}{Dt} \sqrt{\pi a}$$

$$Y_{1c(0.8)} = 4.782 - 1.219(\frac{a}{r}) + 0.063e^{7.045(\frac{a}{r})}$$

Where K_{1c} is the fracture toughness (N/mm$^{1.5}$);
$Y_{1c(0.8)}$ is the stress intensity factor;
P_{max} is the peak load (N);
D is the diameter of the specimen (mm);
t is the thickness of the specimen (mm);
a is the notch depth of the specimen (mm);
r is the radius of the specimen (mm).

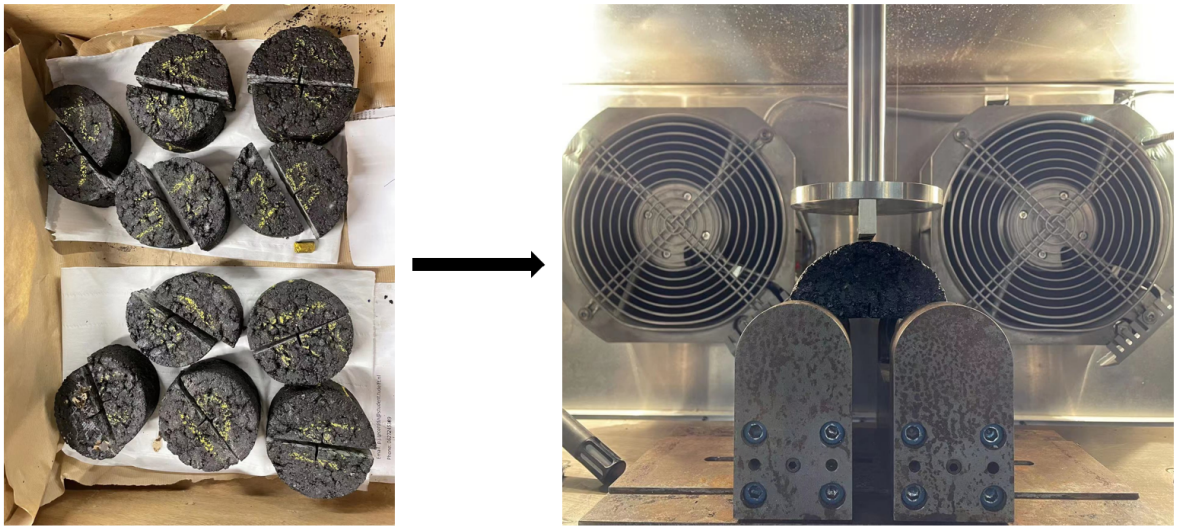

Figure 4.2: Left: SCB samples cut and notched ready for testing. Right: SCB sample in test chamber kept at 0^{o}C

4.1.2. Induction healing procedure

In order to assess healing capacity, several healing events of fractured samples must be carried out. The process of healing was kept constant across all the self-healing samples and was conducted using a combination of rest and **induction heating** over a 24 hour period. For the reference samples only the curing and rest period were applied.

Combined healing technology is dependent on temperature and/or rejuvenation of aged material. To ensure that the results are comparable and reasonable, a testing and healing procedure must be devised that is suitable to assess healing efficiency. As per the healing procedure design proposed in prior work by Xu [5], the importance of a rest period, and controlled environmental conditions cannot be understated. It was decided that a 24 hour cycle should be used as shown in figure 4.3.

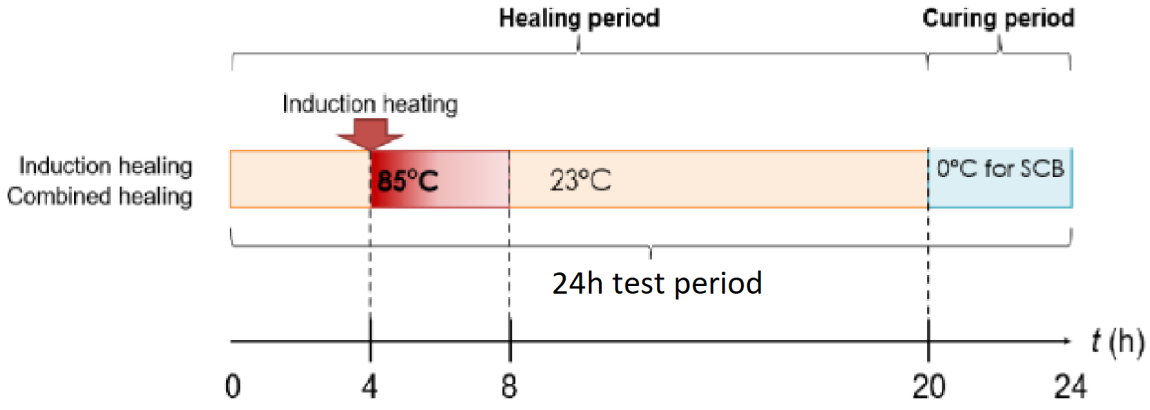

Figure 4.3: Self-healing process timeline.

Once the samples had been damaged in the SCB test, they were wrapped in tape to prevent permanent deformation resulting from loose material and bitumen flow caused by the induction heating. They were placed on a planar surface and allowed to warm to ambient temperature (23^{o}C), and subsequently subjected to induction heating via induction machine 4 hours after damage. The samples were then allowed to rest, until the curing period, in which the samples are cooled to ensure they are at 0^{o}C for the following SCB test.

The induction procedure must also be controlled to ensure validity of results, given the high temperature dependence of mechanical properties and healing of asphalt mixtures. The induction machine used has a power capacity of 50kW at a frequency of 70kHz and the samples were kept at a distance of 5mm from the induction coil during heating as depicted in figure 4.4.

Figure 4.4: An SCB sample under induction coil from a) front view and b) top view.

Average temperature measurements were taken at different points of the sample surface to show the temperature gradients. This was done in order ensure optimisation of the healing process could be achieved. Figures 4.5 shows the measurement lines used and 4.6 depicts the temperature gradients within the sample. By the end of the induction cycle, the temperature of the sample surface was uniform to within 5^{o}C

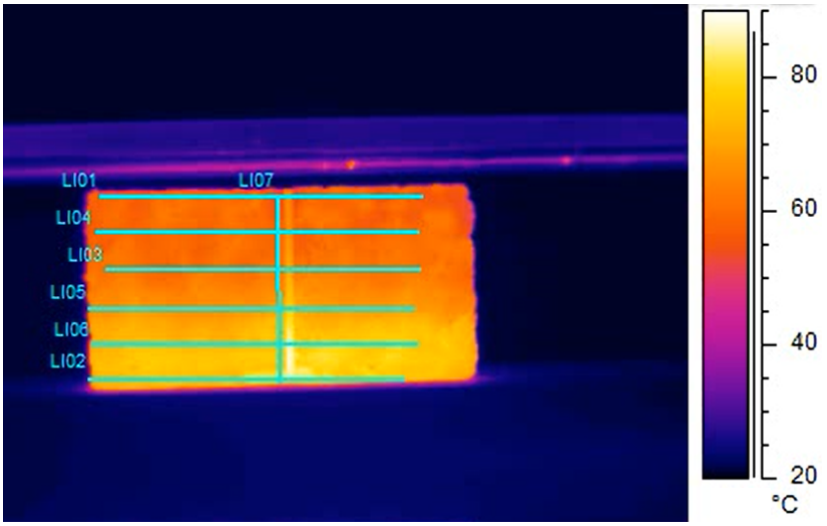

Figure 4.5: Thermal image of a self-healing sample with lines at which the temperature gradient was measured. Thermal image taken after 120 seconds of the induction process.

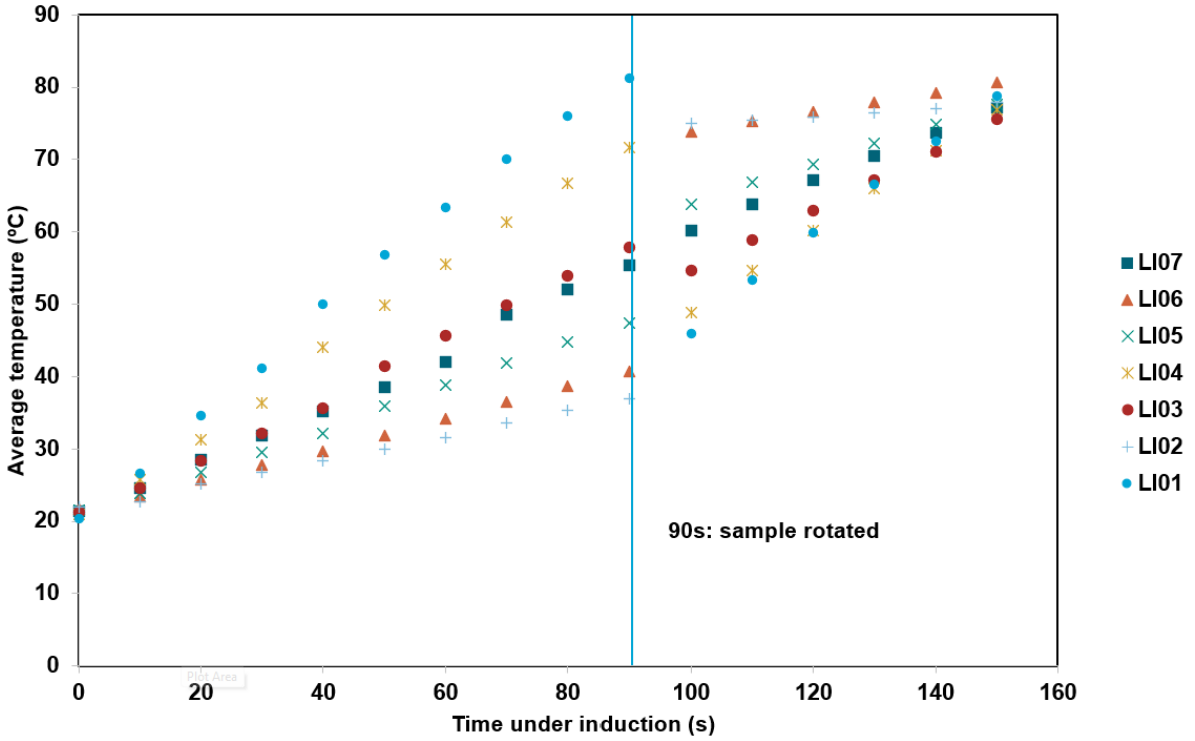

Figure 4.6: Average temperature values of each line over the induction healing cycle.

An infrared camera monitored temperature to ensure optimised and uniform heating of the specimens such that they didn't exceed the optimum healing temperature of 85^{o}C. Due to the temperature gradient arising from the induction heating on one side, each sample had to be turned 180^{o} to ensure homogeneous heating. The process was as follows and is depicted in figure 4.7:

1. Step 1: An alternating current in the coil induces a magnetic field. Resulting eddy currents in the steel fibres within the specimen heat up, with the ones closest to

the coil heating up fastest due to higher field intensity. It takes 90 seconds for the sample surface to reach 85^{o}C.

2. Step 2: The sample turned over and the process of induction heating is repeated on the other side until the 85^{o}C is reached on the other surface and quasi-uniform heating of the entire sample is achieved. The second step takes 60 seconds. In so doing, this forgoes the issue of overheating and insufficient heating within the sample.

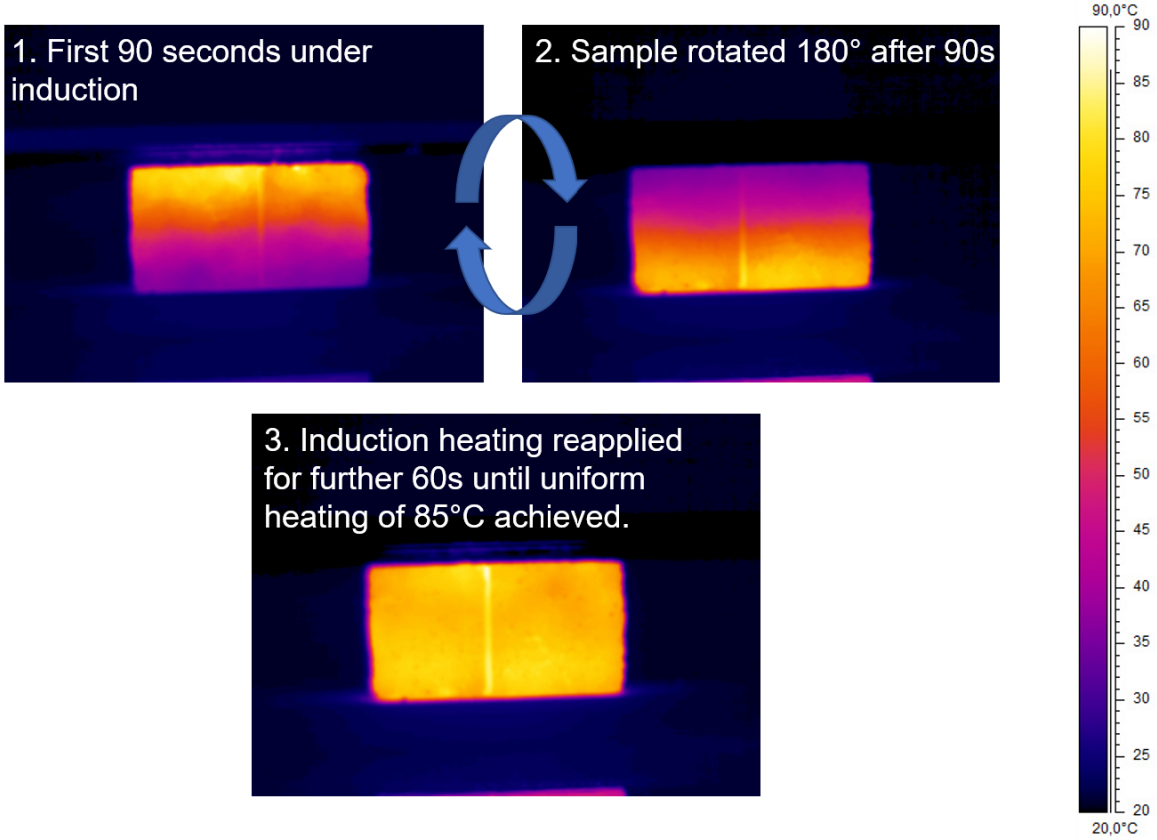

Figure 4.7: Thermal images taken during the induction heating process showing the temperature distribution in samples at different stages of the 2.30 minute process.

The healing index of each mixture can be calculated from measurements of fracture toughness at healing event i, $K_{1c}(i)$, vs the original fracture toughness of the mixture K_{1c}.

$$HI = \frac{K_{1c}(i)}{K_{1c}} \times 100\%$$

The process was repeated multiple times, to assess how each mixture composition fared under repeated SCB loading cycles.

4.2. Healing evaluation results

The SCB tests were used to simulate the crack propagation through the SMA samples. The peak load and fracture toughness were used to ascertain the fracture resistance of the asphalt samples after each induction healing event.

Figure 4.8 shows the results of fracture toughness measured after each SCB and healing cycle. Initial fracture toughness was highest for the fresh reference and lowest for the aged reference with each combined system falling in between these values. The presence of the combined healing system acts as a barrier to crack propagation as shown by the slight improvement the initial fracture resistance with increasing capsule content. After the first healing cycle, the CIS samples were able to regain between 37-43% of their initial fracture toughness, up to around 15N/mm$^{1.5}$. By contrast, the reference samples experienced a serious decrease in fracture toughness to less than 10% of the initial toughness after the first cycle.

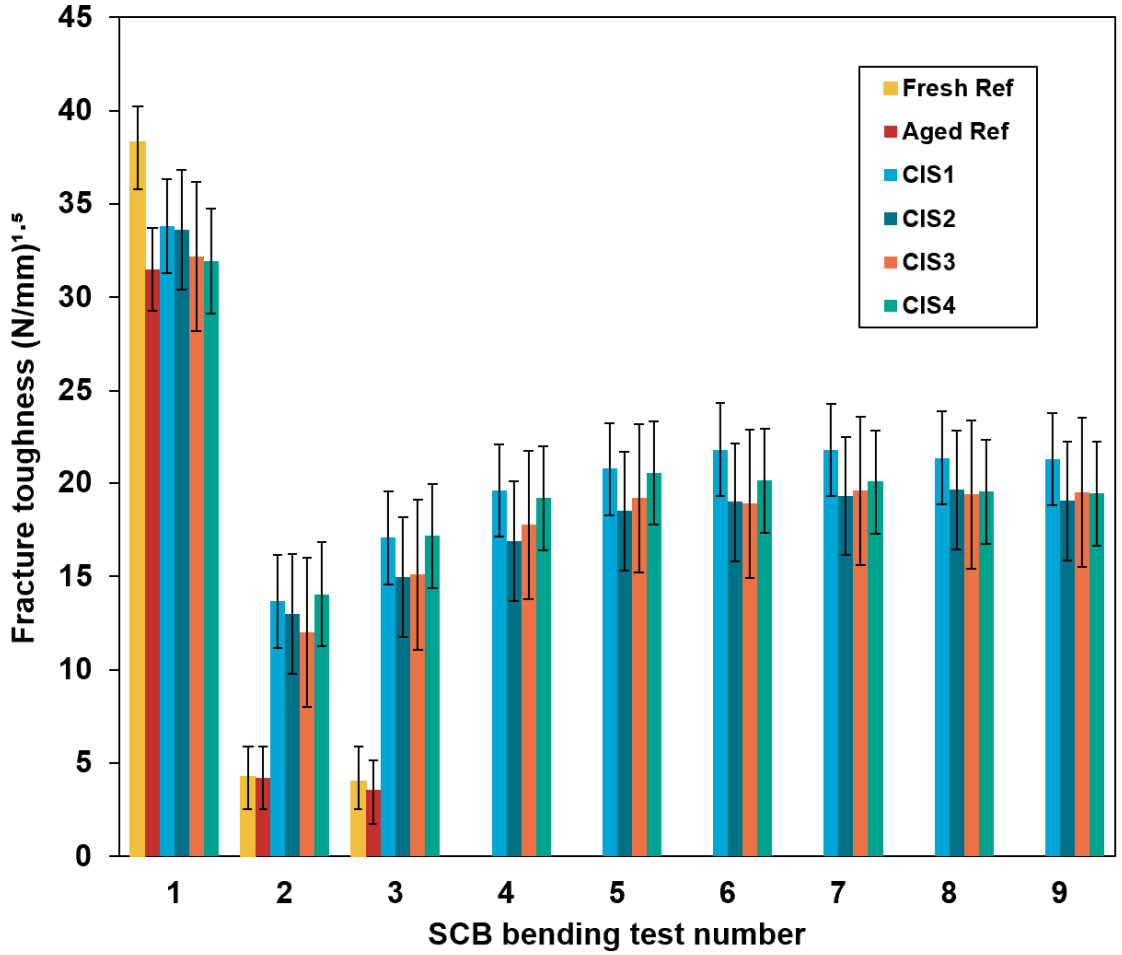

Figure 4.8: Absolute fracture toughness of every testing group after each healing event

In the second cycle, the reference samples experienced a further slight decrease in fracture toughness before failing completely by the third cycle. The CIS samples experienced an opposing trend however, increasing fracture toughness with each heal-

ing event until the sixth repetition. This may be because once the capsules in the CIS samples were ruptured during testing, they released rejuvenator. Following rejuvenator release, the oil rejuvenator could diffuse into the asphalt matrix in the time between tests. The diffusion process became evident after 2-3 days, as is shown by the increase in healing efficacy after 3 cycles. Moreover, the rate of diffusion would increase upon heating by induction. In each case, the first 3-4 rounds of healing events yielded an increase in healing efficiency before a plateau between SCB test number 6 and 7. Thereafter, a slight decrease in absolute fracture toughness was observed, and a similar trend in overall healing efficacy as demonstrated in figure 4.9.

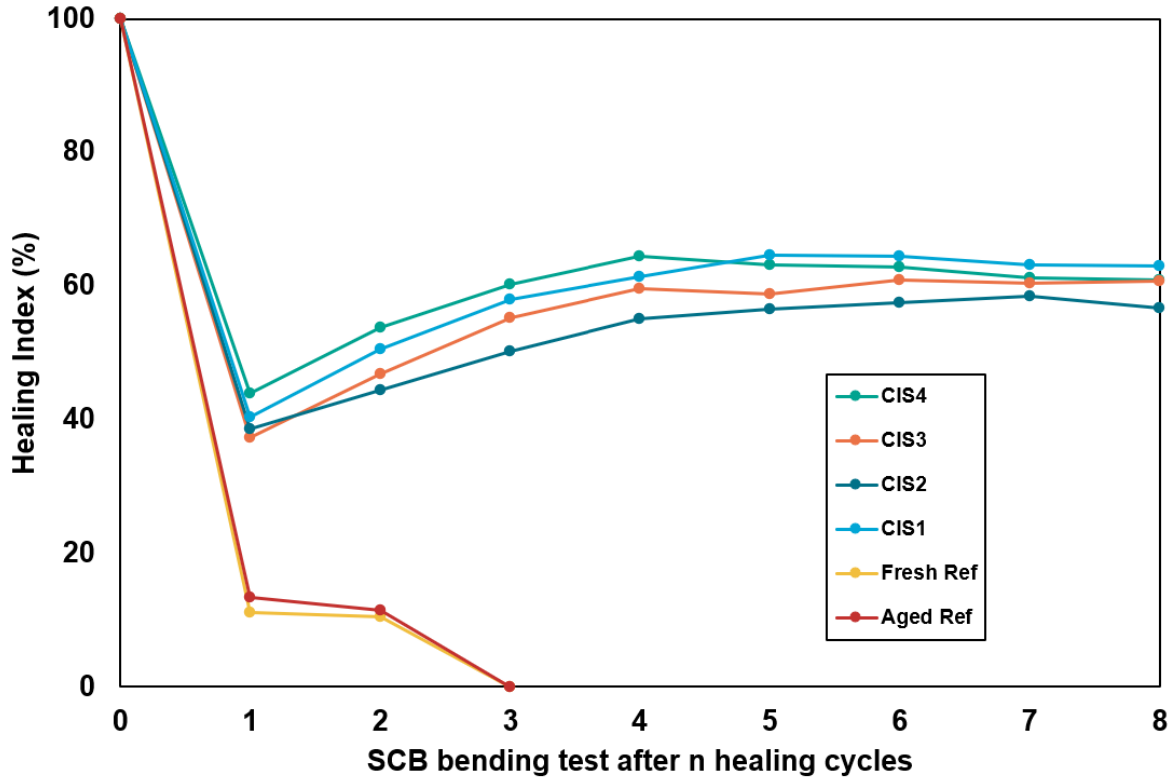

Figure 4.9: Healing efficacy of each SMA mixture type relative to initial fracture toughness

All CIS systems showed substantial retention in fracture toughness throughout the assessment. The system with the greatest healing efficiency after 8 cycles was CIS1 with a healing efficiency of 62.9%, followed by CIS4 with 60.9% and CIS3 with 60.7%. The lowest healing efficiency was CIS2 with 56.7%. It is thought that the capsules provide localised rejuvenation to the aged SMA mixture, which benefits the healing obtained via induction, though the correlation between increasing capsule content and self healing efficiency is inconclusive.

4.3. Concluding remarks and optimal mixture determination

This chapter provided the methodology and results of the healing performance evaluation. In summary, the following conclusions were drawn.

- Reference samples showed a maximum of 10% retention in fracture toughness via autogenous healing.
- CIS1 showed highest healing efficiency of the healing samples, with an overall healing efficiency of 62.9% after 8 healing cycles.

Based on the conclusions of the mechanical and healing assessments in sections 3.3 and 4.3, it is necessary to determine the optimal self-healing mixture to assess from a sustainability perspective.

The inclusion of a combined healing system generally lead to a decrease in strength of the fresh mixture, suggesting that the inclusion of capsules and fibres may lead to a slightly weaker asphalt mastic. However, each dual healing system was able to retain at least 57% of its fracture toughness after 8 healing cycles, meaning that delayed onset of failure can be achieved with regular healing events to great effect. Given the conclusions made in both sections, **CIS1** was taken forward to the sustainability assessment as the optimum combined self-healing mixture.

5

Sustainability Assessment

5.1. LCA methodology

The second part of this thesis will discuss the environmental implications of the optimised self-healing system compared to the reference mix used in pavement applications today. It aims to answer the 3rd research question: How does the environmental impact of an optimal self-healing system compare to that of current asphalt mixtures? This was achieved via a comparative life cycle assessment (LCA) in accordance with the standard ISO 14040 and ISO 14044.

5.1.1. Goal and scope definition

The main goal of the LCA analysis is to evaluate the differences in environmental impacts between a traditional asphalt mixture, and the optimised self-healing mixture in an application as the top layer of a road surface. The assessment is based on data from the mechanical assessment aspects of this thesis and is supplemented by the available literature and relevant databases. The LCA takes into account the production phases of both asphalt mixtures (cradle to gate), and takes into account the use phase and maintenance procedures until end of life (gate to gate). The considered lifecycle phases covered in this LCA are shown in figure 5.1

A timeframe of 40 years was used as a benchmark to compare the reference and self-healing mix. This was selected based on literature and field data concerning conventional SMA mixtures, and previous estimates for the lifecycle of self-healing layers, coupled with data from the mechanical testing in this thesis.

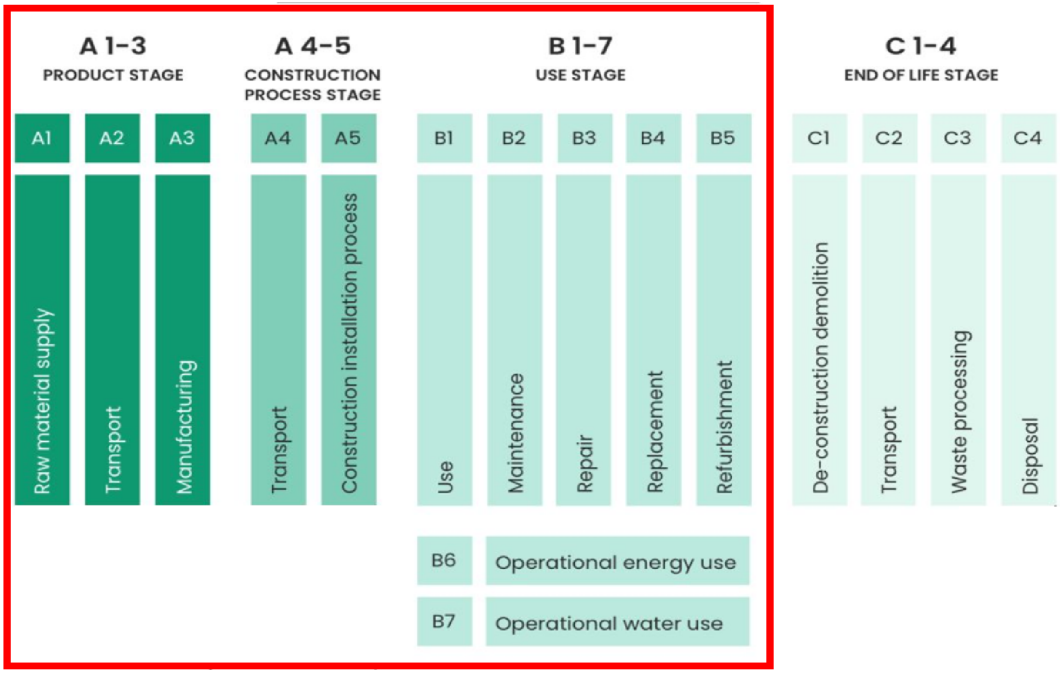

Figure 5.1: Overview of the LCA stages for consideration in the construction sector as per ISO14040 (2006) [69]

5.1.2. Functional unit and system boundaries

The system boundaries were obtained based on literature, and previous LCA data from various pavement types. This LCA only considers the top layer of asphalt, disregarding the underlayer material and maintenance requirements. It does not consider any processes beyond the end of pavement lifetime, and does not consider the reuse of reclaimed asphalt pavement.

The average lifetime of SMA pavements as researched by the Department of Transport in the US, is hypothesised to occur after 16-25 years of service, depending on the traffic load and external conditions the road surface is subjected to [70]. This is based on a 'critical condition index' where deterioration of the pavement has occurred to a point where the safety and mechanical properties are compromised. Therefore, the average of 20 years was decided, as a basis for this LCA, at which the removal of the top layer must occur before relaying with fresh material. A summary of the system boundary for the reference mixture is outlined in figure 5.2.

Table 5.1: Composition of Self-Healing mix vs reference mix in terms of raw materials.

Raw materials	Reference (wt%)	CIS1 (wt%)
Aggregate	94.2	91.5
Bitumen	5.8	5.8
Capsules	-	0.2
Steel Fibres	-	2.5

The functional unit used in this LCA is per 1m^2 of paved asphalt mixture, of 50mm thickness. An equal traffic volume is assumed for both types. The wider effects of road closures for maintenance and associated environmental burdens are not considered in this analysis. The most prolific of the self-healing mixtures according to the results obtained from mechanical testing was CIS1, with a capsule content of 0.2wt%. As such, the mixes analysed in the comparative LCA were the reference mix and CIS1 with the following compositions outlined in table 5.1.

In the reference system, the raw materials consist of limestone aggregate, and bitumen. Over the 40 year lifecycle, the following processes are required:

1. Raw material production and transport to site
2. Construction of pavement at t = 0 years
3. Maintenance Procedure at t = 10 years
4. Pavement reconstruction at t = 20 years due to forecast ageing and pavement degradation
5. Maintenance procedure at t = 30 years
6. Pavement reaches end of life cycle at t = 40 years

The raw materials required for the self-healing mixture are somewhat different, with the addition of steel fibres and rejuvenative capsules constituting a total of 2.7 weight percent. Moreover, the maintenance procedure of the self-healing mixture differ inherently. Both of these differences must be accounted for in the LCA. Results from the SCB testing indicate that the healing of an aged mixture can recoup up to 60% of its strength after 8 healing events. For this LCA, it is assumed that similar results can be obtained for 7 healing events over a lifespan of 40 years, with one healing event every 5 years. This was based on similar constraints used by TNO for an LCA of induction healed porous asphalt [71]. Given that the lifetime of SMA is around 40% longer on average [72] [73], it is reasonable to assume that a self-healing procedure for maintenance would need to be 40% less frequent than in a porous asphalt case.

1. Raw material production and transport to site
2. Construction of pavement at t = 0 years
3. Healing event at t = 5, 10, 15, 20, 25, 30 and 35 years
4. Pavement reaches end of life cycle at t = 40 years

A breakdown of the system boundaries for the self-healing system can be seen in figure 5.3.

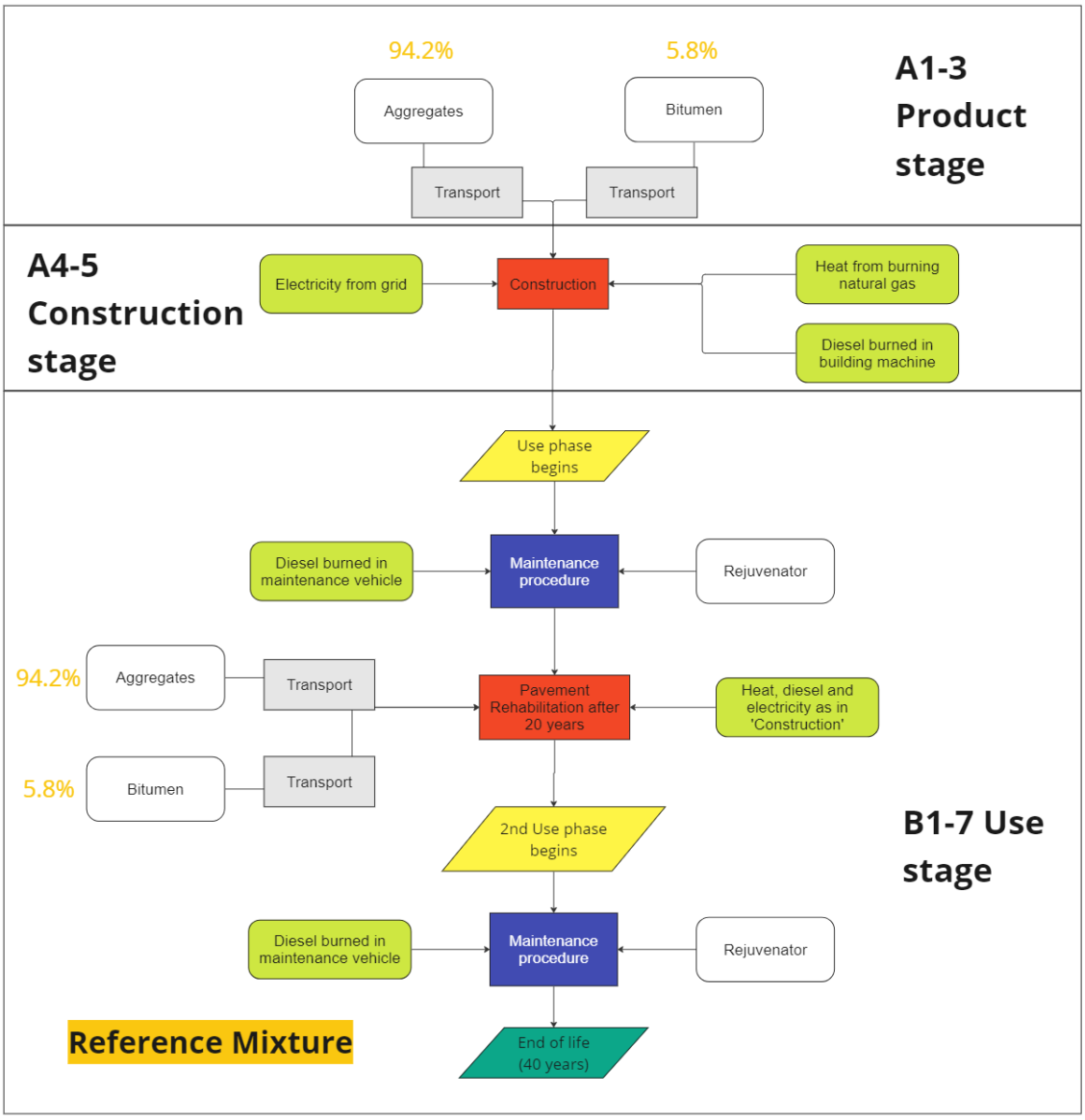

Figure 5.2: System considerations for the reference system including the life cycle stages within the scope of this LCA

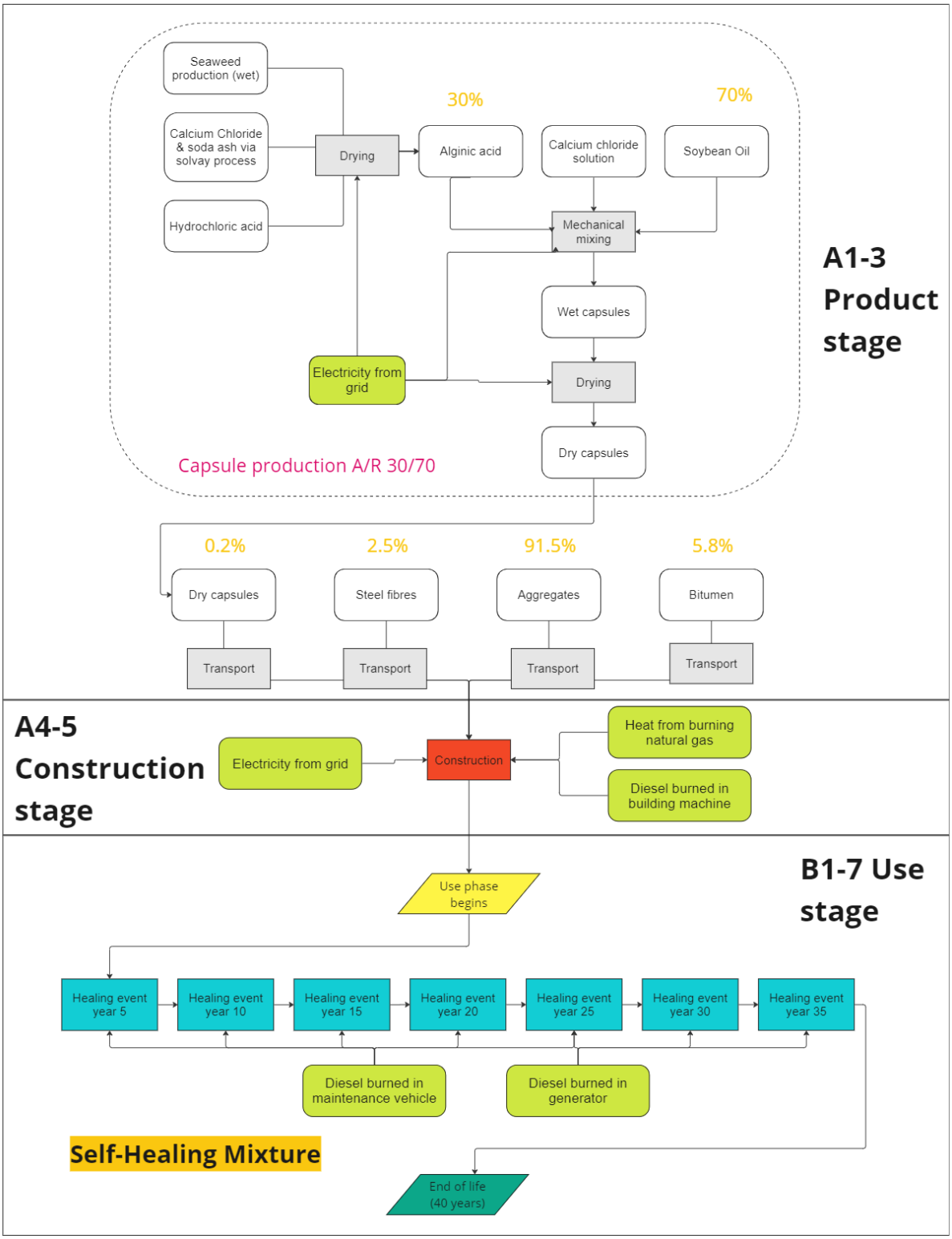

Figure 5.3: System considerations for the self-healing system

Methods and tools for LCI and LCIA

The environmental inventory data was obtained from relevant literature and databases ecoinvent 3.9 and agribalyse 3.0. The data was collated based on European geog-

raphy and to be as representative of current technology and time frames as possible. The environmental impact assessments were were performed using OpenLCA 1.11 software and based upon the indicators of the revised European norm NEN:EN 15804+A2 (2019) to optimise transparency and relevancy. The raw output data from OpenLCA was processed using Microsoft Excel.

5.1.3. Further assumptions

LCA studies aim to assess the environmental impacts of products and/or systems holistically, considering a wide range of factors. However, to ensure the assessment can be achieved within a suitable timeframe for this thesis project, simplifications and assumptions must be made to aggregate data, model processes, or estimate impacts. The following subsection outlines the remaining assumptions made for this assessment.

Raw materials

For simplicity, it was assumed that LCI data for the aggregates, filler and fine crushed rock (CRF) falls under that for 'market for limestone, crushed, washed' in the ecoinvent database. Likewise for bitumen, LCI data was taken from the ecoinvent database 'production bitumen adhesive, cold, at plant'. Due to the lack of LCI data surrounding alginate capsules, a production route was hypothesised based on a combination of laboratory work and literature. To this aim, the transport of raw materials for capsule production are not considered and the electricity required for drying and mechanical mixing are assumed to come from the grid. Therefore, the only contributors to the environmental burden of the capsules are raw materials production and electricity required during processing which are outlined in table 5.2.

Table 5.2: Capsule raw materials required for the self-healing mixture

Capsule raw materials required per m^2		
Material	**Amount (kg)**	**Assumption and/or database used**
Brown seaweed	4.82	Optimised production of brown seaweed (agibalyse 3.0)
$CaCl_2$	0.60	Calcium chloride, Solvay process (ecoinvent 3.9)
Soda Ash	0.24	Sodium Carbonate, Solvay process (ecoinvent 3.9)
Hydrochloric acid	0.08	30% solution concentration (ecoinvent 3.9)
Soybean oil	0.51	see table 5.3 (x)
Deionised water	0.83	deionised water, at user (ecoinvent 3.9)

Process	**Amount**	**Assumption**
Drying and mixing	31.13 MJ	Electricity from grid medium voltage (ecoinvent 3.9)

The densities of the two mixtures are assumed to be equal to the average as found in the mechanical assessment: (ρ_{ref} = 2350kg/m^3, ρ_{CIS1} = 2300kg/m^3). Cellulose fibres within each mixture are not considered due to their small contribution in wt%,

Table 5.3: Summary table of the required raw materials needed for the construction and maintenance procedures in each case, including relative frequency.

REFERENCE				
Material	**Amount (kg)**	**Transport* (t.km)**	**Assumption**	**Frequency**
Aggregate	111.39	5.5695	(v)	2
Bitumen	6.87	0.3436	(w)	2
Rejuvenator**	0.21	0.01055	(x)	2

SELF-HEALING				
Material	**Amount (kg)**	**Transport (t.km)**	**Assumption**	**Frequency**
Aggregate	103.63	5.1815	(v)	1
Bitumen	6.61	0.3305	(w)	1
Steel Fibres	2.84	0.142	(y)	1
Capsules	0.23	0.0114	(z)	1

Assumptions
(v) ecoinvent 3.9 - market for limestone, crushed, washed
(w) ecoinvent 3.9 - bitumen adhesive compound, production, cold
*Transport on land via lorry of 16-32 metric tonnes, emission band EURO6 (ecoinvent 3.9)
(x) ecoinvent 3.9 - market for soybean oil, crude
**used in maintenance procedure
(y) steel production, electric, low alloy, production mix. Fibres formed by milling, at an energy of 0.77MJ/kgproduced by electricity from the grid[74]
(z) As outlined in table 5.2. data taken from ecoinvent and agribalyse databases

and are hence considered as part of the aggregate. Table 5.3 details the amounts of raw materials required for the construction and maintenance of both mixtures per m^2 of mixture.

Construction

In the construction phase of both mixtures, the environmental burdens were assumed to be due to the combustion-related emissions from construction machinery usage. This is primarily from diesel usage of a steady state building machine (power >74.57kW) and natural gas burned in heating up the mixture pre-spreading, rolling and compaction. Moreover, the construction processes were assumed to be identical for each mixture. Transport of constituent materials to the site is considered, and is assumed to be 50km in each case and achieved inland via 32t lorry of EURO6 emission category as per the recommendation of Bepalingsmethode Milieuprestatie Bouwwerken 2022 [75]. The lorries are considered to carry 25% less cargo on the return journeys.

Reconstruction of the reference pavement after 20 years, is assumed to be two large vehicle passes, one for removal of the toplayer, and one for reapplication with

fresh raw materials. The transport of removed asphalt away from the site (again 50km) is considered, but further processing and environmental implications for the reuse or disposal of this asphalt are not.

Maintenance (Reference)

Maintenance of the reference mixture is required to slow the deterioration of the pavement surface. The degree to which this can be achieved depends on timing and frequency of the maintenance activities. Understanding the effects of timing on maintenance and rehabilitation action is challenging due to its highly variable nature [76]. For this LCA, it is assumed that routine maintenance (filling of cracks and potholes) and periodic maintenance (application of a seal/rejuvenator) will have occurred across the whole pavement, on minimum one occasion, every 10 years. This is in line with periodical maintenance intervention guidelines for asphalt concrete outlined in reports such as the current state of the art presented General Directorate of Techniques Road Infrastructure Department in Japan for 2018 which uses similar SMA mixtures [77].

As such, environmental outputs for the maintenance procedure of the reference SMA mixture is assumed to be the sum of: 1 large slow-moving vehicle pass plus the production of a layer of rejuvenator. Other added material to fill cracks and potholes is considered negligible relative to the scale of the pavement infrastructure.

Maintenance (Self Healing)

Maintenance of the self-healing mixture would take place using an induction coil with a power equivalent to the mean of the two coils used in an LCA by TNO, namely the 'SGS INTRON coil' and the 'Huttinger spoel' [71]. It is assumed that the induction coil uses a diesel generator of 30% efficiency as its source of electricity. Each healing event was assumed to be 1 vehicle pass of a slow moving large vehicle and healing efficiency equivalent to the results found in laboratory testing. Therefore, the environmental outputs for this maintenance procedure equate to the sum of these activities and consider only the burning of diesel in the generator, and in the maintenance vehicle, per m^2 of pavement. Table 5.4 outlines the required processes and flows needed to construct and maintain the pavement for each mixture per functional unit. The frequency of each process is also included, to help understand the differences between both systems.

5.1.4. Methods for interpretation

The LCA results for different impact categories have different units. In this format, it is not possible to make a valuable comparison of initial results nor understand the relative magnitude of the impacts. In order to overcome this barrier, eco-cost indicators (ECI) values were used to normalise the results, and gain a better understanding of total environmental impact. The conversion of the EN15804+A2 impact categories into monetary values are outlined in table 5.5.

Notes for table 5.5:
(a) Different midpoint system for Abiotic depletion, metals and minerals
(b) Different midpoint system for Abiotic depletion, fossil.

Table 5.4: Summary table of the required processes and flows needed for the construction and maintenance procedures in each case.

REFERENCE				
Process	**Amount**	**Unit**	**Assumption**	**Frequency**
Heat from natural gas	31.13	MJ	(a)	2
Electricity	0.64	kWh	(b)	2
Diesel burned, construction	3.328	MJ	(c)	2
Diesel burned, maintenance	1.77	MJ	(d)	2

SELF-HEALING				
Process	**Amount**	**Unit**	**Assumption**	**Frequency**
Heat from natural gas	31.13	MJ	(a)	1
Electricity	0.64	kWh	(b)	1
Diesel burned, construction	3.328	MJ	(c)	1
Diesel burned, maintenance vehicle	1.77	MJ	(d)	7
Diesel burned, induction machine	13.9	MJ	(e)	7

Assumptions
(a) Propane - 0.265MJ/kg needed to reach temperature of mixing and compaction [71]
(b) Electricity of medium voltage, from grid
(c) Includes diesel burned in building machine, rolling and compaction
(d) Diesel burned in maintenance vehicle, per vehicle pass, consumption estimated to be 38L/km [71]
(e) Diesel burned in electric generating set, of 30% efficiency

Table 5.5: Eco cost as per the EN15804+A2 impact categories.

Impact category	Quantity and unit	Associated cost
Climate change	1 kg CO2 eq	0.12 €
Ozone Depletion	1 kg CFC 11 eq	0.00 €
Acidification	1 mol H+ eq	7.08 €
Eutrophication freshwater	1 kg P eq	15.32 €
Eutrophication marine	1 kg N eq	22.12 €
Eutrophication terrestrial	1 mol N eq	1.58 €
Photochemical ozone creation	1 kg NMVOS	5.67 €
ADP, metals and minerals	1 kg Sb	**note (a)**
ADP, fossil fuels	1 MJ	**note (b)**
Water use	1 m^3 dep.	**note (c)**
Particulate Matter emissions (PM 2.5)	disease inc. (cases)	147,000 €
Ionizing radiation, human health	1 kBq U235 eq	**note (d)**
Eco-toxicity	1 CTUe	3.63E-03 €
Human toxicity cancer	1 CTUh	920,000 €
Human toxicity non-cancer	1 CTUh	216,000 €
Land Use	Pt (Production per time)	**note (e)**

(c) Different midpoint system: Baseline Water Stress
(d) as an energy carrier, it is considered separately
(e) Land-use and biodiversity considered separately due to geographical sensitivity
These factors will be considered in the discussion of results.

Using these values, it is possible to obtain an environmental cost for both the reference and self-healing mixtures as follows:

$$LCA_{impact}(€) = \Sigma LCA_x \times ECI_x$$

Where:
LCA_x = Environmental impact (in reference units) of the midpoint x;
ECI_x = Environmental cost indicator of midpoint x expressed in euros per reference unit.

5.2. LCA results

This section will present the results of the LCA analysis, including the relative impacts and a comparison of eco-costs between the two mixtures where relevant. Following

that, the results of the eco-cost analysis will be discussed and future prospects will be considered. LCA impacts were calculated using Open LCA 1.9 (2023) software, which has characterisation capabilities for the new norm NEN-EN 15804+A2. Each category was calculated using the following equation:

$$LCA_{impact}(eq.unit) = LCA_{A1-3} + LCA_{A4-5} + LCA_{B1-7}$$

Where:
LCA_{A1-3} = Environmental impact of production phase including raw material production and transport;
LCA_{A4-5} = Environmental impact of construction phase phase including construction activities;
LCA_{B1-7} = Environmental impact of use phase including maintenance and rehabilitation activities.

Figure 5.4 shows the impacts of the self-healing mixture compared to the reference mixture pre-normalisation. Discrepancies can be observed between the impact categories, with some showing a higher impact for the reference such as Ecotoxicity, Land use, and Ozone depletion/formation. Other impact categories are higher for the self-healing sample. Particularly eutrophication related impacts (Eu), but also Human toxicity (HT), Acidification (AC) and a slight increase in climate change (CC) related impacts. While this is somewhat indicative of the environmental impacts, it does not account for impact magnitudes or shed light on which part of the lifecycle provides the largest contribution to each impact. Firstly, it is important to understand which activities contribute most to each impact category.

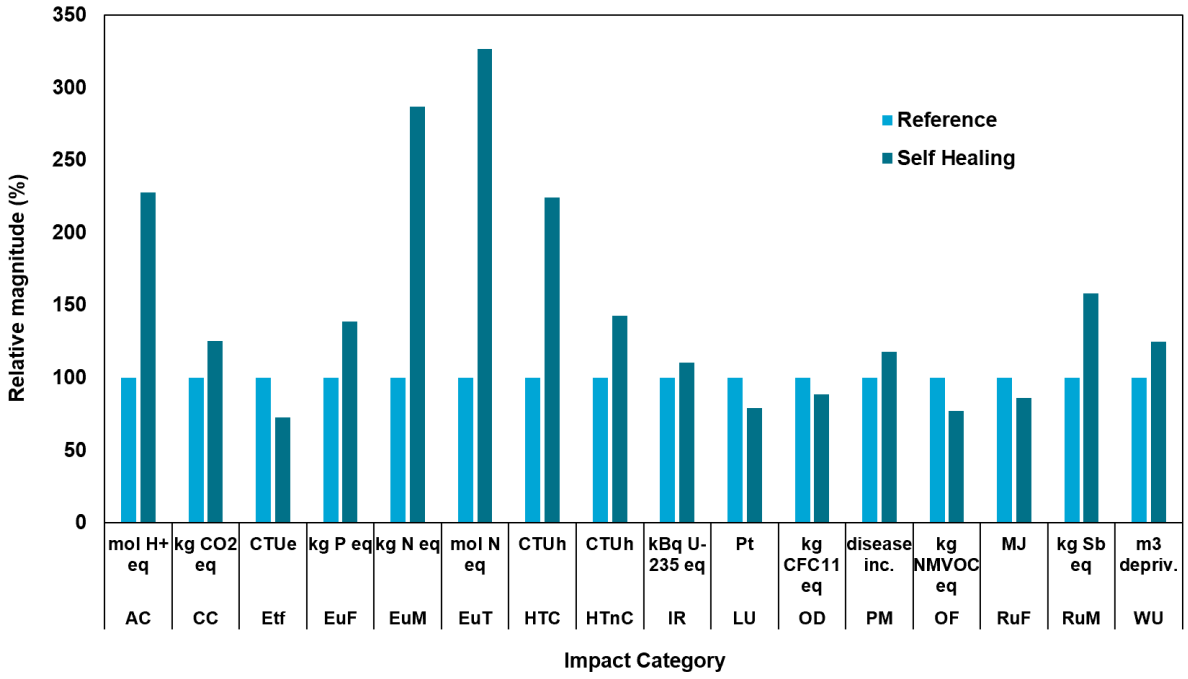

Figure 5.4: Relative LCIA impacts

Figure 5.5 shows how each of the relevant life cycle phases contribute to the re-

spective impact categories in the reference mixture. Notably, a large portion of many impact categories comes from the bitumen contribution, with bitumen accounting for 40% or more of the total impact in 10 of the 16 listed ICs. The other phases such as aggregate production, transport, construction and maintenance contribute towards smaller portions of each impact category. Exceptions to this trend include Ecotoxicity (EcT) of which 62.4% constitutes impacts related to aggregate production. Land use (LU) also is proportionally high due to the need for land to grow soy crops to be used for soybean oil rejuvenator.

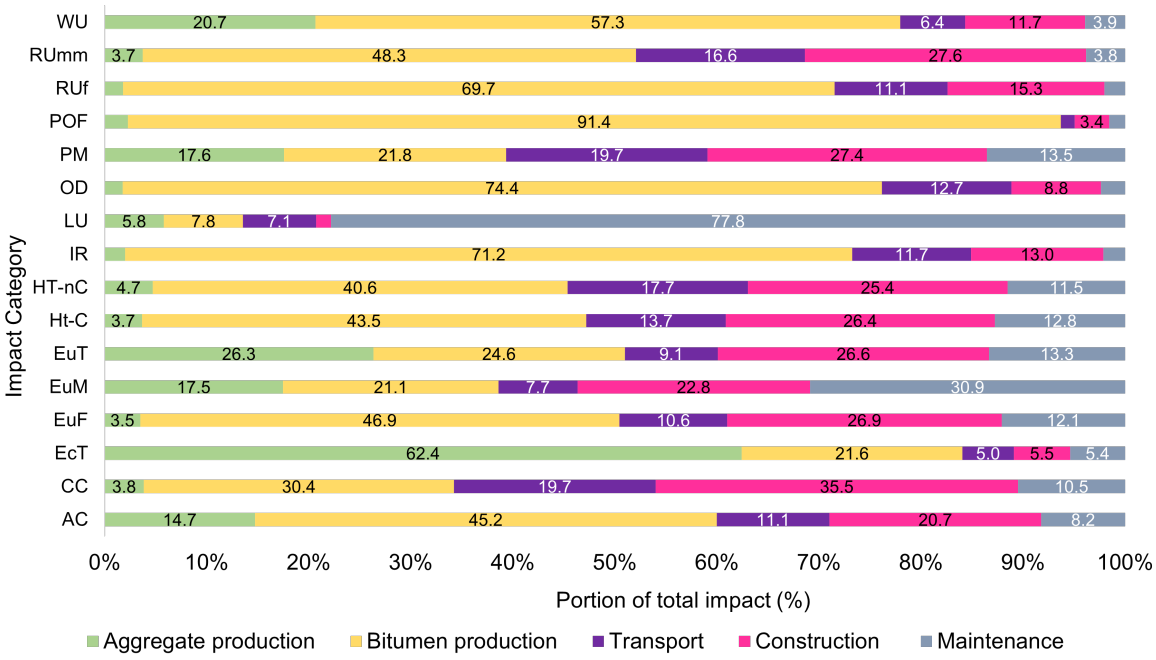

Figure 5.5: LCIA findings of the reference mix, showing the contribution of each important lifecycle phase to each impact category.

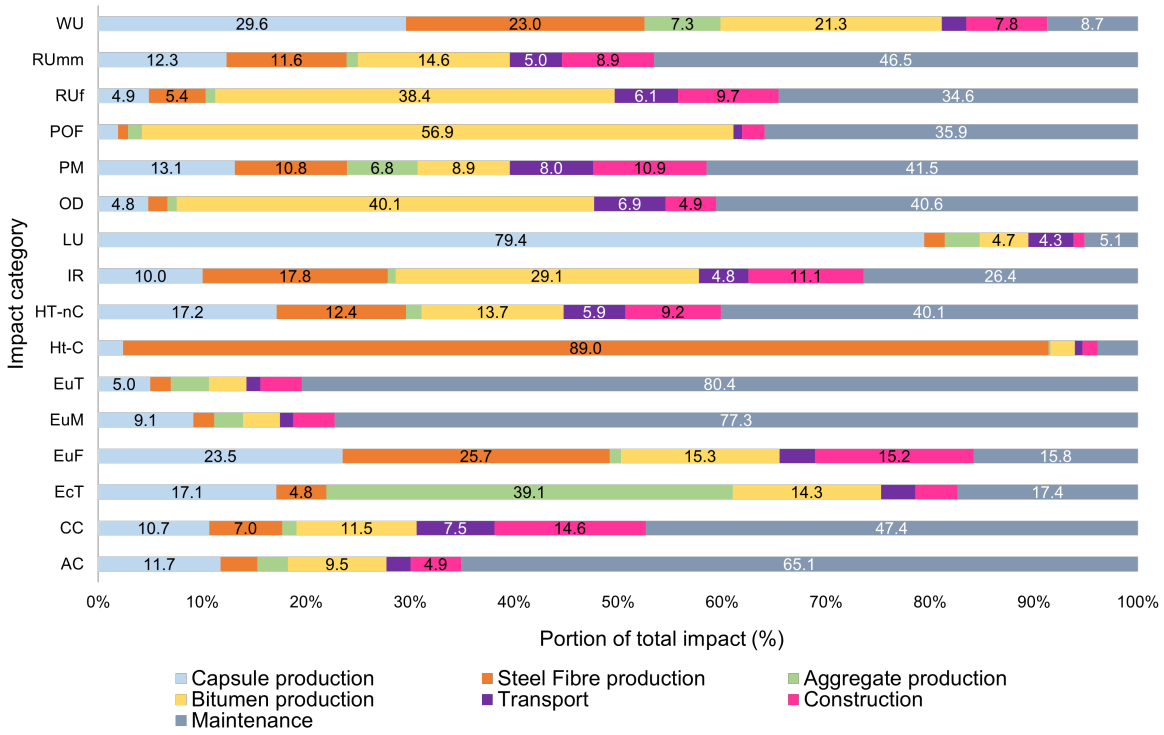

Figure 5.6: LCIA findings of the self-healing mix, showing the contribution of each important lifecycle phase to each impact category.

Figure 5.6 shows the equivalent in the self healing mixture. Here it can be seen that the maintenance contributes to a large portion of the impacts with a 40+% contribution in 8 impact categories. Maintenance activities for the self-healing mixture as described in the previous section are fossil fuel dependent. As expected, impact categories such as acidification and climate change are largely impacted by the burning of fossil fuels, and are prevalent in the use of a diesel generator during maintenance.

Other notable relative contributions come from LU at 79.4% for capsule production. Once again this is largely due to the land required to grow soy for soybean oil. The inclusion of steel fibres contributes 89% of the overall Ht-C. Construction and transport contributions are significantly reduced compared to the reference mix in all categories due to the lack of need for rehabilitation activities. Bitumen production related contributions also decrease substantially for the same reasons.

In order to more accurately compare the environmental impacts it is necessary to normalise the weighting of the impact categories. This can be done by using an eco-cost-indicator (ECI) as described in chapter 5. The eco-cost indicators do not consider impact categories of LU, WU, IR, Rmm and RU as they use different midpoint indicators when determining environmental impact so will be discussed separately. Figure 5.7 shows the contribution of each ECI impact category to the overall environmental cost of the reference mixture. The most important costs come from ozone formation, ecotoxicity and climate change, within these, raw material production plays a major role. Eutrophication and acidification contribute to costs somewhat, but neither terrestrial nor marine eutrophication contribute more than €0.70. Human toxicity costs are small to almost negligible in the reference case.

In figure 5.8 the contribution of each relevant impact category to the overall envi-

ronmental cost of the self-healing mixture is illustrated. It once again highlights the importance of ozone formation, ecotoxicity and climate change as impact categories in this case study, though here maintenance activities contribute a far greater portion than in the reference case. Eutrophication and acidification forms a significantly larger portion of the environmental cost in the self-healing mixture compared to the reference, mostly due to maintenance activities once again. Human toxicity costs remain very low, only slightly increased by the inclusion of steel fibres.

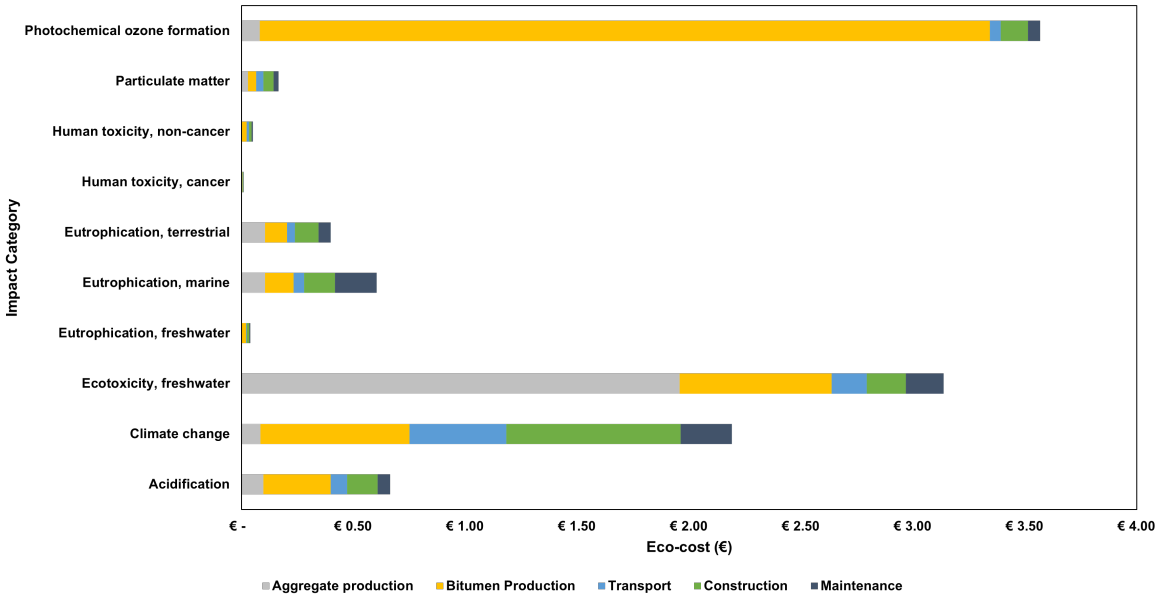

Figure 5.7: Ecocost per m^2 of reference pavement, per impact category per activity

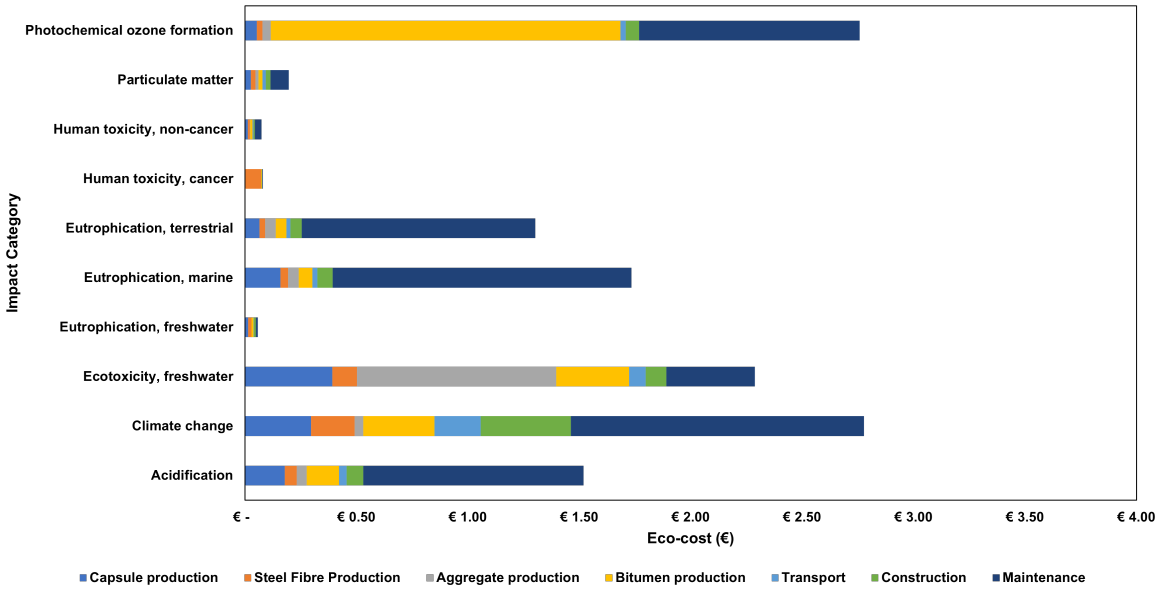

Figure 5.8: Ecocost per m^2 of self-healing pavement, per impact category per activity

Overall comparative eco-cost is outlined in figure 5.9. The environmental cost bur-

den for the reference system totals €10.82. Of the total environmental cost, the product phase including raw material production (A1-3) contributes 70.8%, construction and transport (A4-5) contributes 21.8% and use phase (B1-7) contributes 7.2%.

Similarly, the total environmental cost burden for the self-healing system is €12.78. Of this environmental cost, the product phase A1-3 contributes 42.3%, A4-5 contributes 9.3% and the use phase (B1-7) contributes 48.5%.

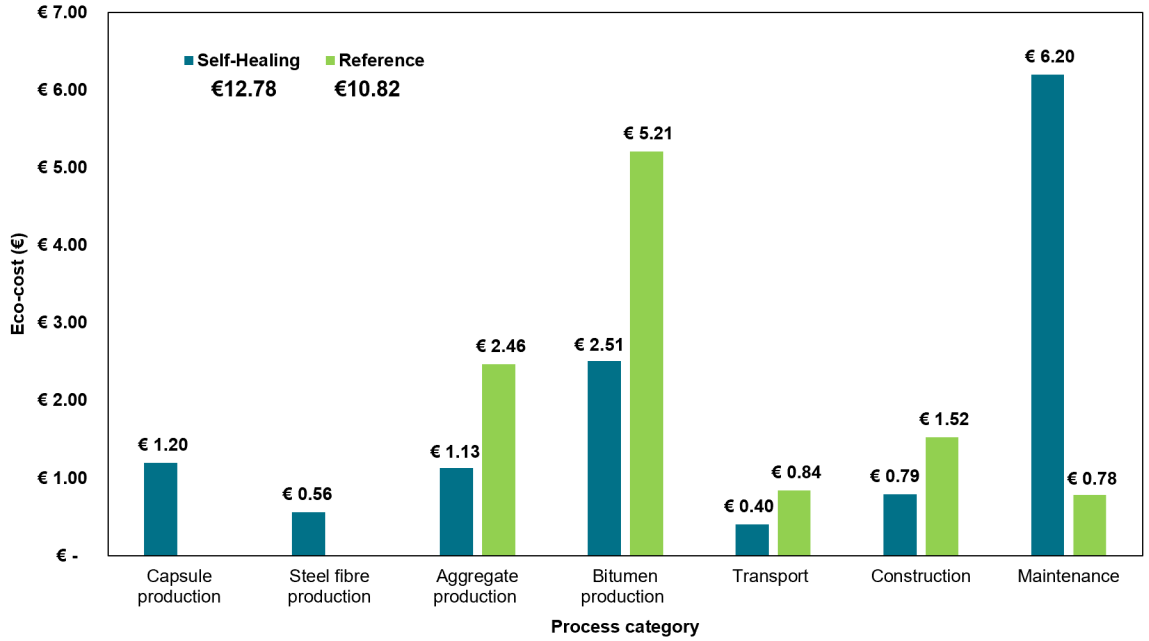

Figure 5.9: Total comparative Eco-cost per m^2 of pavement mix, per lifecycle activity

5.3. Interpretation and discussion

Based on the data solely considering eco-cost impacts of the two mixtures, it would seem that the self-healing mix incurs a greater environmental burden. However, there are more variables requiring consideration for the analysis. Figure 5.10 considers the remaining impact categories that were unsuitable for the eco-cost calculation due to their use of different midpoint indicators (see table 5.5). Most significantly, the land use required for the reference mix is greater than that of the self-healing. This is due to the need for greater amounts of raw materials and rejuvenator, which increases the overall amount of land required for growing/quarrying/drilling of these constituents. The impact of land use is also geographically sensitive and its occupation is costed in €/m^2 for other impact assessment methods. In Europe, these values can range between 1 - 4.5€/m^2 depending on factors such as soil fertility, biodiversity and other location dependent characteristics [78]. While the unit m^2 is not equivalent to the one used for the impact assessment in this thesis, one can hypothesise that the 21% reduction in land use for the self-healing case could make up the difference in associated environmental cost as per the ECI impact categories.

Impact Category	Unit	Ref	SH
Land use	Pt	448.27	355.12
Water use	m³ dep.	3.85	4.81
RU fossil	MJ	468.61	404.11
RU metals	kg Sb eq	7.30E-05	0.00012
Ionising Radiation	kBq U235 eq	2.05	2.26

Figure 5.10: Other aspects for consideration that fall outside of the ECI, comparison of reference (Ref) and self-healing (SH).

Moreover, abiotic depletion as a result of fossil fuel use is higher in the reference mixture. This is largely due to the need for more bitumen over the life-cycle, which helps to offset the greater amount of diesel burned during maintenance procedures in the self-healing case. This is important given the finite nature of fossil resources. Extraction of crude oil, hard coal, and natural gas bears external societal costs because the stock reduction of these materials will accost present and future generations [79]. This cost is not possible to quantify in an ECI like other impact categories, due to its geographic variability and future dependent nature. However, a 14% reduction in abiotic depletion of fossil fuels is a very desirable outcome for the self-healing mixture. It reduces the need for extraction, processing and distribution of fossil fuels which reduces the associated long-term environmental burdens and geopolitical dependency on resources.

Water use is another impact that requires consideration. Once again it is highly geographically sensitive, with eco-costs in Europe varying from 0.04 to 0.5€/m^3 based on water scarcity metrics [78]. The reference mixture has a water consumption of 0.96m^3 less than that of the Self-healing mixture. This difference will mean a maximum of a 0.49€ difference in environmental cost per m^2 pavement which is unlikely to surpass the cost benefits of the self-healing system with respect to land use and abiotic depletion of fossil fuels over the long term. However, this is difficult to say with certainty given the unit discrepancy.

Resource use of metals and minerals is very low for both mixtures. With the eco-cost for 1kg of Antimony equivalent being 7.93€/kg, the associated eco-costs are below 0.01€ and therefore do not require consideration in this analysis. Similarly, ionising radiation impacts differ by just 0.21kBq in activity which was deemed sufficiently small to be discounted from consideration in this analysis.

The eco-cost comparison shows that maintenance is the most burdensome of the lifecycle activities in the case of the self-healing system. The critical activity in this case being the use of a diesel generator to produce the electricity for induction. Based on the LCA calculations, a 32% improvement in the efficiency of the induction machine would be sufficient to equalise the eco-costs assuming all other production, material properties and external factors were to remain the same. It would also result in a sig-

nificant reduction in the acidification, climate change, eutrophication and resource use (fossil) impact categories. In order to achieve this there are two main considerations.

1. The use of alternative sources to generate electricity for induction, such as solar energy, or improve the efficiency of the induction machine.
2. The improvement of material properties to reduce the maintenance frequency.

With regard to the first solution, the use of solar power would come with its own set of environmental challenges, but would greatly reduce greenhouse gas emissions and negate many of the direct environmental consequences resulting from burning fossil fuels. Technological advancement will likely result in improved efficiency of diesel-generator induction machines, reducing diesel consumption for an improved return on useful energy output. Improvements in efficiency could also be brought about by bettering the material performance. Should the pavement exhibit properties superior to those assumed and observed in a laboratory setting, such as better healing efficiency or greater rutting resistance than predicted, maintenance frequency would decrease and the associated environmental burden would diminish. A combination of the two scenarios is also possible. Nevertheless, extensive field work is necessary to ascertain whether the assumptions in this LCA are valid, and whether such benefits, or better, can be achieved in-situ.

It should be mentioned that there are factors outside the boundaries of this LCA which also have a bearing on the environmental costs. For example, the costs of road closure during the maintenance and rehabilitiation phases of the reference mix are not considered. Extra emissions as a result of traffic diversions and increased vehicle loads on other roads may last several days/weeks per maintenance event on any given stretch of road. These may lead to extra environmental costs which would be avoided when using the self-healing scenario, where maintenance can be done with only partial road closure, over reduced timescales compared to the reference rehabilitation activities. Furthermore, LCA data for capsule production was based largely on laboratory processes. If capsule production can be suitably scaled up, processing requirements per kg would decrease due to batch processing and more efficient energy use during production, further reducing the environmental footprint of the self-healing system. Finally, end-of-life reclamation value is not considered in this LCA, in theory it would be possible to reclaim the steel fibres at the end of the lifecycle to help minimise the steel-related environmental impacts experienced by the self-healing system.

This LCA is valid for asphaltic mixtures used in the top layer of pavement structures, though in principle it is also relevant for joints. While the failure mechanisms are not identical, it is predicted that a dual self-healing system can have a significant positive impact on joint lifespan. Given the similarities in mixture compositions used, and the failure mechanisms being dominated by crack formation, the relative lifetime extension is hypothesised to be similar to the pavement top-layer if periodic healing is applied.

In summary, the known eco-costs of the self-healing system outweigh those of the reference system based on the LCA research outlined in this thesis. However, considering impacts that do not feature in the ECI, the self-healing mixture performs better overall. Improvements in efficiency of present induction machines are crucial to improving the environmental viability of self-healing pavements. More field work must be done to ascertain whether the assumptions made in this LCA are valid in practice.

6

Conclusions and Recommendations

6.1. Conclusions

This thesis investigates the viability of a combined capsule/induction SMA mixture regarding its mechanical properties and sustainability. To this aim, mechanical testing and healing assessment was undertaken to find the optimum mixture composition, which was taken forward for sustainability assessment via LCA. The LCA evaluated the environmental impacts per functional unit of the optimum self-healing system against that of the reference system. The results of the impact assessment were attributed to different activities within the life cycle. They were then discussed to understand which activities provided the greatest environmental burden. Finally, future prospects for improving sustainabilty and limitations of the study are discussed. Summarised below are the answers to each of the previously defined research questions as per the findings in this thesis.

Research sub-question 1: What is the optimum composition of capsules for a combined (capsule-induction) self-healing system in SMA?

After extensive laboratory testing, subsequent analysis of results show that an increase in capsule content is deleterious towards the mechanical properties of the fresh mixture, without exhibiting a marked increase in healing capacity. Healing efficacy for each CIS system was between 57-63%, with CIS1 indicating showing the best retention in fracture toughness. Increasing the capsule content reduced the density, increased void content and showed lower stiffness and strength overall. Due to superior results amongst the self-healing mixtures in stiffness, strength, binder drainage, and rutting resistance, the optimum capsule content was deemed to be 0.2wt%. This mix design is able to achieve the most durable healing performance, and still achieve the highest overall healing efficiency after 8 healing cycles.

Research sub-question 2: What are the performance differences compared to a reference SMA mixture?

As expected, the self-healing capabilities of the reference were far reduced, indicating that the autogenous healing of the asphalt mixture is much lower than when extrinsic healing methods are applied. However, when considering strength of the fresh reference, samples proved between 14-25% stronger than the self-healing counterparts at low temperatures. Lower binder drainage and better moisture resistance were also observed in the reference mix. It is thought that increased void content contribute to the worse performance post water conditioning. Differences in binder drainage were small and remained within the recommended 0.2% limit in each case. The composition of the SMA mixture is thought to be the main factor in determining mixture strength. Higher capsule content is generally detrimental to strength due to their lower strength compared to the aggregate. At higher temperatures, the combined self-healing mixtures performed better than the reference based on the triaxial test results. Higher resistance to permanent deformation of up to 24% was observed, indicating superior rutting resistance. This was attributed to the inclusion of steel fibres due to their ability to distribute strain throughout the mixture, however, increasing capsule content had a somewhat negative effect on rutting resistance.

Research sub-question 3: How does the environmental impact of an optimal self-healing system compare to that of current SMA mixtures?

While the known eco-costs of the self-healing system are about 15% higher than that of the reference, other geographically sensitive factors such as Land use and resource use (fossil) are substantially improved by 21% and 14% respectively in the self-healing case. The largest burden in the reference case is from production of raw materials, and bitumen in particular. The greatest environmental burden for the self healing case comes from the diesel burned for the induction machine which may be possible to mitigate with future developments. It was determined that a 32% improvement in efficiency of the induction machine would equalise the known eco-costs of the self-healing mixture to that of the reference.

6.2. Recommendations

The addition of a combined capsule-induction healing system has proven to be very effective for increasing the lifespan of SMA in a laboratory setting. However, this thesis does not show real-world results. It is therefore recommended that field work is carried out to assess the insitu properties of such a system in a pavement or joint application. This will aid future research efforts and will lead to a more practical understanding of system properties under different environmental and traffic load conditions. Given the more rapid failure nature of asphalt joints compared to the pavement surface, it is logical that this is where the technology should first be implemented. Maximum benefits can be achieved and tangible results can be obtained more quickly.

Further modelling and laboratory work including the comparison to a separate single capsule system and induction system is needed to understand the interaction of the healing system with the asphalt mastic. Gaining a deeper understanding of how the dual healing system affects parameters like binder adhesion, diffusion of rejuvenator, and viscoelastic properties are necessary to be able to further optimise laboratory and

fieldwork approaches. Moreover, investigation into the crushed capsule phenomenon in a trial section is necessary to understand how to mitigate this phenomenon. This will shed light on the optimum processing conditions that could further optimise properties, and reduce the likelihood of premature rejuvenator release.

Given that the induction machine provides the greatest environmental burden to the self-healing system lifecycle, improvements in efficiency or use of renewable energy sources should be the primary focus. The use of alternative power sources such as solar energy should be investigated as a potential replacement and may be included in future analyses. Should the eco-burdens of the healing method be reduced by 32%, the known environmental costs would be equalised, and a substantial benefit would be seen from the improvement in other factors such as fossil resource use. To supplement this, it is necessary to complete a LCC (Life-cycle costing) assessment to ascertain the economic benefits that would follow post implementation of a self-healing system.

Self-healing technology is still novel, meaning that processes for mass production of capsules are not yet widespread. More efficient capsule production processes will further reduce environmental impacts. This will not only improve environmental viability, but will help to drive economic costs down. To this aim, an industrially suitable production method should be devised. Once this has been achieved, it is necessary for future research to update LCA findings to account for this technological breakthrough.

Damage monitoring and detection is needed to gain a more holistic picture surrounding maintenance frequency. For insitu applications it is particularly important to understand and predict failure mechanisms, as well as identify weak points. Implementing a suitable detection and monitoring strategy would provide valuable data to aid assumptions in future sustainability assessments, and assist in self-healing pavement design.

Finally, to ensure cohesion and transparency of future comparisons and LCA findings, current policies for documentation and assessment must shift towards uniformity. Currently, there are many methods used for the comparison of impact categories, which often do not have equivalent units. It also makes it challenging to define cost indicators for different pollutants/emissions and to compare studies with one another in a meaningful and productive manner. The changing of the European norm EN-15804+A2 remains a recent development and is not yet widely used to calculate impacts. Therefore, it is necessary to either develop a comparison tool that can compare the outcomes of LCA studies using different methodologies, or ensure that all studies follow the same impact assessment methods to ensure the validity and transparency of future work.

References

[1] G. Malkoc. *The Importance of Road Maintenance*. 2015. URL: https://www.worldhighways.com/wh8/wh9/wh10/feature/importance-road-maintenance.

[2] S. Bhandari, X. Luo, and F. Wang. "Understanding the effects of structural factors and traffic loading on flexible pavement performance". In: *International Journal of Transportation Science and Technology* 12.1 (2023), pp. 258–272. ISSN: 2046-0430. DOI: https://doi.org/10.1016/j.ijtst.2022.02.004. URL: https://www.sciencedirect.com/science/article/pii/S2046043022000211.

[3] L. Vita and M. C. Marolda. "Road Infrastructure - the backbone of the transport system". In: *EU Directorate General for Research and Sustainable Surface Transport* (2008). EU, Brussels, Belgium.

[4] A. K. Apeagyei, J. R. A. Grenfell, and G. D. Airey. "Moisture-induced strength degradation of aggregate-asphalt mastic bonds". In: *Road Materials and Pavement Design* 15.1 (2014). https://doi.org/10.1080/14680629.2014.927951, pp. 239–262.

[5] S. Xu. *Self-healing Porous Asphalt: A Combination of Encapsulated Rejuvenator and Induction Heating*. Dissertation. Delft, Netherlands: TU Delft, 2020.

[6] L. Mo et al. "Review on asphalt plug joints: Performance, materials, testing and installation". In: *Construction and Building Materials* 45 (2013), pp. 106–114. ISSN: 0950-0618. DOI: https://doi.org/10.1016/j.conbuildmat.2013.03.089. URL: https://www.sciencedirect.com/science/article/pii/S0950061813002997.

[7] N. Ghafoori and M Sharbaf. "Bridge deck asphalt plug joints: Problems and solutions". In: *Bituminous Mixtures and Pavements VI* (June 2015), p. 135. DOI: 10.1201/b18538-22.

[8] I. M. Reid and D. Coutellier. "Effects of Joint Geometry on Response of Asphaltic Plug Joints". In: *Journal of Transportation Engineering* 124 (July 1998). DOI: 10.1061/(ASCE)0733-947X(1998)124:4(311).

[9] J. R. Meijer et al. "Global patterns of current and future road infrastructure". In: *Environmental Research Letters* 13.6 (2018), p. 064006. ISSN: 1748-9326. DOI: 10.1088/1748-9326/aabd42. URL: https://dx.doi.org/10.1088/1748-9326/aabd42.

[10] ASTM. *Standard Specification for Asphaltic Plug Joints for Bridges*. July 2020. URL: https://www.astm.org/d6297-20.html.

[11] EOTA. "Flexible Asphaltic Plug Expansion Joints for Road Bridges, European Assessment Document". In: *European Organisation for Technical Assessment* (Aug. 2019).

[12] B. Bramel. *Asphalt Plug Joints: Characterisations and Specifications*. Apr. 1999. URL: https://trid.trb.org/view/509264.

[13] BJA. “Standard for Asphaltic Plug Joints”. In: *Bridge Joint Association* (May 2003).

[14] W. S. Mogawer and A. J. Austerman. “Evaluation of Asphaltic Expansion Joints”. In: 2004.

[15] Bin Liu et al. “Condition-based maintenance for systems with aging and cumulative damage based on proportional hazards model”. In: *Reliability Engineering & System Safety* 168 (Dec. 2017), pp. 200–209. DOI: 10.1016/j.ress.2017.04.010. URL: http://dx.doi.org/10.1016/j.ress.2017.04.010.

[16] T. Yu, C. Li, and S. Wu. “Performance of Polymer Modified Asphalt Bridge Expansion Joints in Low-Temperature Regions”. In: *Journal of Performance of Constructed Facilities - J PERFORM CONSTR FACIL* 23 (Aug. 2009). DOI: 10.1061/(ASCE)0887-3828(2009)23:4(227).

[17] Luh-Maan Chang and Yao-Jong Lee. “Evaluation of Performance of Bridge Deck Expansion Joints”. In: *Journal of Performance of Constructed Facilities* 16.1 (2002), pp. 3–9. DOI: 10.1061/(ASCE)0887-3828(2002)16:1(3).

[18] B. Neal. *Pavement Defects and Failures*. May 2022. URL: https://www.pavemanpro.com/article/identifying_asphalt_pavement_defects/.

[19] A. Abouelsaad and G. White. “Review of Asphalt Mixture Ravelling Mechanisms, Causes and Testing”. In: *International Journal of Pavement Research and Technology* 15.6 (2022), pp. 1448–1462. ISSN: 1996-6814. DOI: 10.1007/s42947-021-00100-7.

[20] S. Liu et al. “Preparation, microstructure and rheological properties of asphalt sealants for bridge expansion joints”. In: *Construction and Building Materials* 105 (Feb. 2016), pp. 1–13. DOI: 10.1016/j.conbuildmat.2015.12.017. URL: http://dx.doi.org/10.1016/j.conbuildmat.2015.12.017.

[21] M. Partl, S. Hean, and L. D. Poulikakos. “ASPHALTIC PLUG JOINT CHARACTERIZATION AND PERFORMANCE EVALUATION”. In: 2002.

[22] D. Perraton et al. “Rutting of bituminous mixtures: wheel tracking tests campaign analysis”. In: *Materials and Structures* 44.5 (2011), pp. 969–986. ISSN: 1359-5997. DOI: 10.1617/s11527-010-9680-y.

[23] M. Miljkovic and M. Radenberg. “Rutting mechanisms and advanced laboratory testing of asphalt mixtures resistance against permanent deformation”. In: *Facta universitatis - series: Architecture and Civil Engineering* 9.3 (2011), pp. 407–417. ISSN: 0354-4605. DOI: 10.2298/fuace1103407m.

[24] R. Ungureanu, M. Toma, and M. Dicu. “Effect of bitumen type and polymer on physico-mechanical properties of asphalt pavement”. In: *IOP Conference Series: Earth and Environmental Science* 664 (May 2021), p. 012104. DOI: 10.1088/1755-1315/664/1/012104.

[25] M. Guo et al. “Investigating the interaction between asphalt binder and fresh and simulated RAP aggregate”. In: *Materials & Design* 105 (2016), pp. 25–33. ISSN: 0264-1275. DOI: 10.1016/j.matdes.2016.04.102. URL: https://dx.doi.org/10.1016/j.matdes.2016.04.102.

[26] F.L. Roberts et al. *Hot mix asphalt materials, mixture design, and construction*. Transportation Research Board, 1996.

[27] A. Zaltuom. “A Review Study of The Effect of Air Voids on Asphalt Pavement Life”. In: Nov. 2018, pp. 618–625. DOI: 10.21467/proceedings.4.29.

[28] V. Bulatovic, V. Rek, and K. Marković. “Effect of polymer modifiers on the properties of bitumen”. In: *Journal of Elastomers and Plastics* (Jan. 2013). DOI: 10.1177/0095244312469964.

[29] M. Bilema et al. “Moisture Sensitivity of Crumb Rubber Modified Modifier Warm Mix Asphalt Additive for Two Different Compaction Temperatures”. In: *IOP Conference Series: Earth and Environmental Science* 140 (Apr. 2018), p. 012072. DOI: 10.1088/1755-1315/140/1/012072.

[30] Y. Gong et al. “Investigation of the High-Temperature and Rheological Properties for Asphalt Sealant Modified by SBS and Rubber Crumb”. In: *Polymers* 14.13 (2022), p. 2558. ISSN: 2073-4360. DOI: 10.3390/polym14132558.

[31] F. Chi and Z. Liu. “Title of the Paper”. In: *IOP Conference Series: Materials Science and Engineering*. Vol. 207. 2017, p. 012100. DOI: 10.1088/1757-899X/207/1/012100.

[32] S. R. Harnaeni et al. “The effect of temperature changes on mechanistic performance of hotmix asphalt as wearing course with different gradation types”. In: *AIP Conference Proceedings* (2018). DOI: 10.1063/1.5042946. URL: http://dx.doi.org/10.1063/1.5042946.

[33] H. A. Omar et al. “Effects of moisture damage on asphalt mixtures”. In: *Journal of Traffic and Transportation Engineering (English Edition)* 7.5 (Oct. 2020), pp. 600–628. DOI: 10.1016/j.jtte.2020.07.001. URL: http://dx.doi.org/10.1016/j.jtte.2020.07.001.

[34] R. Moraes, R. Velasquez, and H. Bahia. “MEASURING EFFECT OF MOISTURE ON ASPHALT-AGGREGATE BOND WITH THE BITUMEN BOND STRENGTH TEST”. In: *Transportation Research Board Annual Meeting, Washington* 140 (Nov. 2010).

[35] H. Yu et al. “Impact of Ultraviolet Radiation on the Aging Properties of SBS-Modified Asphalt Binders”. In: *Polymers* 11.7 (2019), p. 1111. ISSN: 2073-4360. DOI: 10.3390/polym11071111. URL: https://dx.doi.org/10.3390/polym11071111.

[36] F.C. Thyrion. “Asphalt Oxidation”. In: *Asphaltenes and Asphalts, 2*. Ed. by T. F. Yen and G. V. Chilingarian. Vol. 40. Developments in Petroleum Science. Elsevier, 2000, pp. 445–474. DOI: https://doi.org/10.1016/S0376-7361(09)70287-0. URL: https://www.sciencedirect.com/science/article/pii/S0376736109702870.

[37] S. Van Der Zwaag. “An Introduction to Material Design Principles: Damage Prevention versus Damage Management”. In: *Solar Cells and Modules*. Solar Cells and Modules, 2007, pp. 1–18. DOI: 10.1007/978-1-4020-6250-6_1.

[38] M. D. Hager et al. “Self-Healing Materials”. In: *Advanced Materials* 22.47 (2010), pp. 5424–5430. ISSN: 0935-9648. DOI: 10.1002/adma.201003036.

[39] J. Qiu et al. “Evaluating Self Healing Capability of Bituminous Mastics”. In: *Experimental Mechanics* 52.8 (2012), pp. 1163–1171. ISSN: 0014-4851. DOI: 10.1007/s11340-011-9573-1. URL: https://dx.doi.org/10.1007/s11340-011-9573-1.

[40] A. Tabaković and E. Schlangen. “Self-Healing Technology for Asphalt Pavements”. In: *Advances in Polymer Science*. Advances in Polymer Science, 2015, pp. 285–306. DOI: 10.1007/12_2015_335.

[41] J. Qiu et al. “Evaluating Self Healing Capability of Bituminous Mastics”. In: *Experimental Mechanics* 52.8 (2012), pp. 1163–1171. ISSN: 0014-4851. DOI: 10.1007/s11340-011-9573-1. URL: https://dx.doi.org/10.1007/s11340-011-9573-1.

[42] Á. García et al. “A simple model to define induction heating in asphalt mastic”. In: *Construction and Building Materials* 31 (2012), pp. 38–46. ISSN: 0950-0618. DOI: https://doi.org/10.1016/j.conbuildmat.2011.12.046. URL: https://www.sciencedirect.com/science/article/pii/S0950061811007239.

[43] Q. Liu, S. Wu, and E. Schlangen. “Induction heating of asphalt mastic for crack control”. In: *Construction and Building Materials* 41 (2013), pp. 345–351. ISSN: 0950-0618. DOI: https://doi.org/10.1016/j.conbuildmat.2012.11.075. URL: https://www.sciencedirect.com/science/article/pii/S0950061812009117.

[44] B. H. Dinh, D-W Park, and T. H. M. Le. “Effect of rejuvenators on the crack healing performance of recycled asphalt pavement by induction heating”. In: *Construction and Building Materials* 164 (2018), pp. 246–254. ISSN: 0950-0618. DOI: https://doi.org/10.1016/j.conbuildmat.2017.12.193. URL: https://www.sciencedirect.com/science/article/pii/S0950061817325989.

[45] Q. Dai, Z. Wang, and M. Rosli Mohd Hasan. “Investigation of induction healing effects on electrically conductive asphalt mastic and asphalt concrete beams through fracture-healing tests”. In: *Construction and Building Materials* 49 (2013), pp. 729–737. ISSN: 0950-0618. DOI: https://doi.org/10.1016/j.conbuildmat.2013.08.089. URL: https://www.sciencedirect.com/science/article/pii/S0950061813008325.

[46] Ruiyang J. et al. “Optimization of induction heating parameters for improving Self-healing performance of asphalt mixture through partial least square model”. In: *Construction and Building Materials* 365 (2023), p. 130019. ISSN: 0950-0618. DOI: https://doi.org/10.1016/j.conbuildmat.2022.130019. URL: https://www.sciencedirect.com/science/article/pii/S0950061822036753.

[47] Q. Liu et al. “A comparative study of the induction healing behaviors of hot and warm mix asphalt”. In: *Construction and Building Materials* 144 (2017), pp. 663–670. ISSN: 0950-0618. DOI: https://doi.org/10.1016/j.conbuildmat.2017.03.195. URL: https://www.sciencedirect.com/science/article/pii/S0950061817305949.

[48] Pavetech Inc. *MD Maltene Reprint PPJ*. 2020. URL: https://www.pavetechinc.com/wp-content/uploads/2020/04/MD-Maltene-Reprint-PPJ.pdf.

[49] S. Xu et al. “The role of rejuvenators in embedded damage healing for asphalt pavement”. In: *Materials & Design* 202 (2021), p. 109564. ISSN: 0264-1275. DOI: https://doi.org/10.1016/j.matdes.2021.109564. URL: https://www.sciencedirect.com/science/article/pii/S0264127521001179.

[50] E. Schlangen and S. Sangadji. “Addressing Infrastructure Durability and Sustainability by Self Healing Mechanisms - Recent Advances in Self Healing Concrete and Asphalt”. In: *Procedia Engineering* 54 (2013). The 2nd International Conference on Rehabilitation and Maintenance in Civil Engineering (ICRMCE), pp. 39–57. ISSN: 1877-7058. DOI: https://doi.org/10.1016/j.proeng.2013.03.005. URL: https://www.sciencedirect.com/science/article/pii/S1877705813003597.

[51] Á. García, E. Schlangen, and M. van de Ven. “Properties of capsules containing rejuvenators for their use in asphalt concrete”. In: *Fuel* 90.2 (2011), pp. 583–591. ISSN: 0016-2361. DOI: https://doi.org/10.1016/j.fuel.2010.09.033. URL: https://www.sciencedirect.com/science/article/pii/S0016236110005041.

[52] A. Tabaković et al. “The reinforcement and healing of asphalt mastic mixtures by rejuvenator encapsulation in alginate compartmented fibres”. In: *Smart Materials and Structures* 25.8 (July 2016), p. 084003. DOI: 10.1088/0964-1726/25/8/084003. URL: https://dx.doi.org/10.1088/0964-1726/25/8/084003.

[53] S. Xu et al. “Calcium alginate capsules encapsulating rejuvenator as healing system for asphalt mastic”. In: *Construction and Building Materials* 169 (2018), pp. 379–387. ISSN: 0950-0618. DOI: https://doi.org/10.1016/j.conbuildmat.2018.01.046. URL: https://www.sciencedirect.com/science/article/pii/S0950061818300461.

[54] J-F Su, J. Qiu, and E. Schlangen. “Stability investigation of self-healing microcapsules containing rejuvenator for bitumen”. In: *Polymer Degradation and Stability* 98.6 (2013), pp. 1205–1215. ISSN: 0141-3910. DOI: https://doi.org/10.1016/j.polymdegradstab.2013.03.008. URL: https://www.sciencedirect.com/science/article/pii/S0141391013000621.

[55] S. Xu et al. “Optimization of the Calcium Alginate Capsules for Self-Healing Asphalt”. In: *Applied Sciences* 9.3 (2019), p. 468. ISSN: 2076-3417. DOI: 10.3390/app9030468. URL: https://dx.doi.org/10.3390/app9030468.

[56] H. Wang et al. “Self-Healing Properties of Asphalt Concrete with Calcium Alginate Capsules Containing Different Healing Agents”. In: *Materials* 15.16 (2022), p. 5555. ISSN: 1996-1944. DOI: 10.3390/ma15165555.

[57] ISO. “ISO Focus”. In: *Magazine of the International Standards Organisation* 3 (2006), pp. 1–48. ISSN: 1729-8709. URL: https://www.iso.org/files/live/sites/isoorg/files/news/magazine/ISO.

[58] G. Rebitzer et al. “Life cycle assessment: Part 1: Framework, goal and scope definition, inventory analysis, and applications”. In: *Environment International* 30.5 (2004), pp. 701–720. ISSN: 0160-4120. DOI: https://doi.org/10.1016/j.envint.2003.11.005. URL: https://www.sciencedirect.com/science/article/pii/S0160412003002459.

[59] Federal Highway Administration. *Pavement Life Cycle Assessment Framework*. https://www.fhwa.dot.gov/pavement/sustainability/hif16014.pdf. 2016.

[60] T. Bradley et al. “5.18 - Life Cycle Assessment (LCA) of Algae Biofuels”. In: *Comprehensive Renewable Energy (Second Edition)*. Ed. by Trevor M. Letcher. Second Edition. Oxford: Elsevier, 2022, pp. 387–404. ISBN: 978-0-12-819734-9. DOI: https://doi.org/10.1016/B978-0-12-819727-1.00067-4. URL: https://www.sciencedirect.com/science/article/pii/B9780128197271000674.

[61] A. A. Butt, B. Birgisson, and N. Kringos. “Optimizing the Highway Lifetime by Improving the Self Healing Capacity of Asphalt”. In: *Procedia - Social and Behavioral Sciences* 48 (2012). Transport Research Arena 2012, pp. 2190–2200. ISSN: 1877-0428. DOI: https://doi.org/10.1016/j.sbspro.2012.06.1192. URL: https://www.sciencedirect.com/science/article/pii/S1877042812029357.

[62] A. M. Rodríguez-Alloza et al. “Life Cycle Assessment of Self-healing Versus Traditional Maintenance Road Techniques”. In: *RILEM Bookseries*. RILEM Bookseries, 2022, pp. 1289–1295. DOI: 10.1007/978-3-030-46455-4_164.

[63] D. Garraín and Y. Lechón. “Environmental footprint of a road pavement rehabilitation service in Spain”. In: *Journal of Environmental Management* 252 (2019), p. 109646. ISSN: 0301-4797. DOI: https://doi.org/10.1016/j.jenvman.2019.109646. URL: https://www.sciencedirect.com/science/article/pii/S0301479719313647.

[64] Y. Yue et al. “A comparative life cycle assessment of asphalt mixtures modified with a novel composite of diatomite powder and lignin fiber”. In: *Construction and Building Materials* 323 (2022), p. 126608. ISSN: 0950-0618. DOI: https://doi.org/10.1016/j.conbuildmat.2022.126608. URL: https://www.sciencedirect.com/science/article/pii/S0950061822002999.

[65] R. Veropalumbo et al. “Environmental assessment of asphalt mastics containing plastic bottles and jet grouting waste”. In: *Environmental Impact Assessment Review* 93 (2022), p. 106736. ISSN: 0195-9255. DOI: https://doi.org/10.1016/j.eiar.2022.106736. URL: https://www.sciencedirect.com/science/article/pii/S0195925522000026.

[66] Q. Liu et al. “Induction heating of electrically conductive porous asphalt concrete”. In: *Construction and Building Materials* 24.7 (2010), pp. 1207–1213. ISSN: 0950-0618. DOI: https://doi.org/10.1016/j.conbuildmat.2009.12.019. URL: https://www.sciencedirect.com/science/article/pii/S0950061809004309.

[67] K. Blazejowski. “Stone Matrix Asphalt: Theory and Practice”. In: CRC Press, 2010, pp. 70–75. DOI: 10.1201/b10285.

[68] R. Vreeker et al. “Drying and Rehydration of Calcium Alginate Gels”. In: *Food Biophysics* 3.4 (2008), pp. 361–369. ISSN: 1557-1858. DOI: 10.1007/s11483-008-9087-2. URL: https://dx.doi.org/10.1007/s11483-008-9087-2.

[69] OneClick LCA. *Life Cycle Assessment for Buildings*. 2021. URL: https://www.oneclicklca.com/building-life-cycle-assessment-ebook/.

[70] F. Yin. “Performance and Life-Cycle Cost Benefits of Stone Matrix Asphalt”. In: *1st International Conference on Stone Matrix Asphalt*. 2018. URL: https://www.asphaltpavement.org/uploads/documents/EngineeringPubs/2018SMAConference/04.pdf.

[71] T. N. Ligthart, E. E. Keijzer, and A. M. M. Ansens. *LCA en MKBA van onderhoud ZOAB+ wegverhardingen met zelfherstel*. Tech. rep. TNO-060-UT-2012-01051. TNO, 2012.

[72] A. A. A. Molenaar, E. T. Hagos, and M. F. C. Van De Ven. “Effects of Aging on the Mechanical Characteristics of Bituminous Binders in PAC”. In: *Journal of Materials in Civil Engineering* 22.8 (2010), pp. 779–787. ISSN: 0899-1561. DOI: 10.1061/(asce)mt.1943-5533.0000021.

[73] H. Zhang et al. “Performance enhancement of porous asphalt pavement using red mud as alternative filler”. In: *Construction and Building Materials* 160 (2018), pp. 707–713. ISSN: 0950-0618. DOI: https://doi.org/10.1016/j.conbuildmat.2017.11.105. URL: https://www.sciencedirect.com/science/article/pii/S0950061817323152.

[74] Joost Vogtlander. *Eco-costs 2021, Idemat database*. https://nexus.openlca.org/search/query=milling!database=IDEMAT. 2023.

[75] Stichting Nationale Milieudatabase. *Assessment method*. Mar. 2022. URL: https://milieudatabase.nl/en/environmental-performance/assesment-method/.

[76] L.B. Stevens. *Road Surface Management for Local Governments – Resource Notebook*. Tech. rep. DOT-I-85-37. Washington, D.C.: Federal Highway Administration, May 1985.

[77] General Directorate of Techniques Road Infrastructure Department. *Guidelines for Routine Road Maintenance Using IRI*. Tech. rep. 12303939. Ministry of Public Works and Transport Japan, 2018.

[78] Eco-Costs Value. *Ashby Charts*. https://www.ecocostsvalue.com/data-tools-books/ashby-charts/. 2023.

[79] P. Galgani et al. “Fossil fuel and other non-renewable material depletion: Impact-specific module for true price assessment; True pricing method for agri-food products”. In: (2021).

A

Appendix A

LCA Background calculations

Table A.1: Impact categories as outlined by EN15804 + A2 methodology

Impact category	Abbreviation	Reference Unit
Acidification	AC	mol H+ eq
Climate change	CC	kg CO2 eq
Ecotoxicity, freshwater	EcTF	CTUe
Eutrophication, freshwater	EuF	kg P eq
Eutrophication, marine	EuM	kg N eq
Eutrophication, terrestrial	EuT	mol N eq
Human toxicity, cancer	HT-C	CTUh
Human toxicity, non-cancer	HT-nC	CTUh
Ionising radiation	IR	kBq U-235 eq
Land use	LU	Pt
Ozone depletion	OD	kg CFC11 eq
Particulate matter	PM	disease inc.
Photochemical ozone formation	PcOF	kg NMVOC eq
Resource use, fossil	RUf	MJ
Resource use, minerals and metals	RUmm	kg Sb eq
Water use	WU	m3 depriv.

Table A.2: Summary table of the required raw materials needed for the construction and maintenance procedures in each case.

REFERENCE				
Material	**Amount (kg)**	**Transport* (t.km)**	**Assumption**	**Frequency**
Aggregate	111.39	5.5695	(v)	2
Bitumen	6.87	0.3436	(w)	2
Rejuvenator**	0.21	0.01055	(x)	2

SELF-HEALING				
Material	**Amount (kg)**	**Transport (t.km)**	**Assumption**	**Frequency**
Aggregate	103.63	5.1815	(v)	1
Bitumen	6.61	0.3305	(w)	1
Steel Fibres	2.84	0.142	(y)	1
Capsules	0.23	0.0114	(z)	1

Assumptions

(v) ecoinvent 3.9 - market for limestone, crushed, washed
(w) ecoinvent 3.9 - bitumen adhesive compound, production, cold
*Transport on land via lorry of 16-32 metric tonnes, emission band EURO6 (ecoinvent 3.9)
(x) ecoinvent 3.9 - market for soybean oil, crude
**used in maintenance procedure
(y) steel production, electric, low alloy, production mix. Fibres formed by milling, at an energy of 0.77MJ/kgproduced by electricity from the grid [74]
(z) As outlined in table 5.2. Data taken from ecoinvent and agribalyse databases

Table A.4: Summary table of the required processes and flows needed for the construction and maintenance procedures in each case.

REFERENCE				
Process	**Amount**	**Unit**	**Assumption**	**Frequency**
Heat from natural gas	31.13	MJ	(a)	2
Electricity	0.64	kWh	(b)	2
Diesel burned, construction	3.328	MJ	(c)	2
Diesel burned, maintenance	1.77	MJ	(d)	2

SELF-HEALING				
Process	**Amount**	**Unit**	**Assumption**	**Frequency**
Heat from natural gas	31.13	MJ	(a)	1
Electricity	0.64	kWh	(b)	1
Diesel burned, construction	3.328	MJ	(c)	1
Diesel burned, maintenance vehicle	1.77	MJ	(d)	7
Diesel burned, induction machine	13.9	MJ	(e)	7

Assumptions
(a) Propane - 0.265MJ/kg needed to reach temperature of mixing and compaction
(b) Electricity of medium voltage, from grid
(c) Includes diesel burned in building machine, rolling and compaction
(d) Diesel burned in maintenance vehicle, per vehicle pass, consumption estimated to be 38L/km
(e) Diesel burned in electric generating set, of 30% efficiency

Table A.3: Capsule raw materials required for the optimum self-healing mixture

Capsule raw materials required per m^2		
Material	**Amount (kg)**	**Assumption and/or database used**
Brown seaweed	4.82	Optimised production of brown seaweed (agibalyse 3.0)
$CaCl_2$	0.60	Calcium chloride, Solvay process (ecoinvent 3.9)
Soda Ash	0.24	Sodium Carbonate, Solvay process (ecoinvent 3.9)
Hydrochloric acid	0.08	30% solution concentration (ecoinvent 3.9)
Soybean oil	0.51	see table 5.3 (x)
Deionised water	0.83	deionised water, at user (ecoinvent 3.9)

Process	**Amount**	**Assumption**
Drying and mixing	31.13 MJ	Electricity from grid medium voltage (ecoinvent 3.9)

Notes:

Table A.5: Unit environmental impacts for the impact categories of the EN 15804+A2 (2019) discussed in the LCA

IC	Reference unit	Aggregate kg	Bitumen kg	Transport t.km	Diesel (v) MJ	Diesel (g) MJ	Propane MJ	Electricity kWh
AC	mol H+ eq	6.09E-05	3.08E-03	5.01E-04	9.55E-04	1.31E-03	2.12E-04	2.11E-03
CC	kg CO2 eq	3.01E-03	3.94E-01	1.70E-01	9.20E-02	9.76E-02	8.99E-02	4.06E-01
EcT	CTUe	2.38E+00	1.36E+01	2.10E+00	7.17E-01	1.03E+00	6.66E-01	4.19E+00
EuF	kg P eq	3.89E-07	8.60E-05	1.29E-05	2.85E-06	5.67E-06	6.61E-06	3.92E-04
EuM	kg N eq	2.10E-05	4.19E-04	1.02E-04	4.23E-04	5.66E-04	6.13E-05	3.65E-04
EuT	mol N eq	2.92E-04	4.51E-03	1.11E-03	4.64E-03	6.19E-03	6.61E-04	3.18E-03
Ht-C	CTUh	1.55E-12	3.05E-10	6.37E-11	2.85E-11	3.04E-11	3.73E-11	1.10E-10
HT-nC	CTUh	4.96E-11	7.04E-09	2.03E-09	5.35E-10	1.33E-09	8.91E-10	3.64E-09
IR	kBq U-235 eq	1.83E-04	1.06E-01	1.15E-02	5.68E-03	5.76E-03	1.46E-03	2.27E-01
LU	Pt	1.15E-01	2.53E+00	1.55E+00	1.57E-01	1.67E-01	8.18E-02	1.10E+00
OD	kg CFC11 eq	4.71E-10	3.23E-07	3.67E-08	1.97E-08	1.95E-08	6.61E-09	1.94E-08
PM	disease inc.	8.72E-10	1.78E-08	1.07E-08	2.54E-08	2.27E-09	2.81E-09	5.78E-09
POF	kg NMVOC eq	6.31E-05	4.19E-02	4.17E-04	1.28E-03	1.62E-03	2.29E-04	8.69E-04
RUf	MJ	3.72E-02	2.38E+01	2.51E+00	1.26E+00	1.28E+00	9.66E-01	8.34E+00
RUmm	kg Sb eq	1.21E-08	2.59E-06	5.90E-07	4.73E-08	5.54E-07	3.13E-07	9.19E-07
WU	m3 depriv.	3.51E-03	1.60E-01	1.19E-02	2.92E-03	4.08E-03	4.19E-03	2.74E-01

Table A.6: Unit environmental impacts for the impact categories of the EN 15804+A2 (2019) discussed in the LCA. Includes extra flows and materials required for the self-healing mixture.

IC	Reference unit	Seaweed kg	CaCl2 kg	Soda Ash kg	HCl kg	Soybean Oil kg	Water kg	Steel kg
AC	mol H+ eq	1.73E-02	7.60E-03	4.99E-03	5.92E-03	6.70E-03	6.76E-06	2.67E-03
CC	kg CO2 eq	9.15E-01	4.83E-01	3.17E-01	6.31E-01	3.32E+00	1.17E-03	5.59E-01
EcT	CTUe	2.00E+01	7.03E+01	4.62E+01	1.66E+01	1.02E+02	8.65E-02	1.07E+01
EuF	kg P eq	3.29E-04	3.75E-04	2.46E-04	5.45E-04	6.87E-04	7.42E-07	3.37E-04
EuM	kg N eq	1.70E-03	6.65E-04	4.37E-04	7.58E-04	1.48E-02	1.04E-06	5.57E-04
EuT	mol N eq	1.71E-02	2.11E-02	1.38E-02	9.76E-03	2.35E-02	1.40E-05	5.69E-03
Ht-C	CTUh	8.06E-10	5.05E-10	3.32E-10	5.28E-10	2.57E-09	1.36E-12	2.70E-08
HT-nC	CTUh	1.45E-08	1.81E-08	1.19E-08	1.36E-07	5.85E-08	7.17E-11	1.49E-08
IR	kBq U-235 eq	1.84E-01	4.54E-02	2.98E-02	2.12E-01	3.42E-02	3.26E-04	1.51E-01
LU	Pt	2.41E+00	6.68E+00	4.39E+00	3.57E+00	8.25E+02	3.87E-03	2.50E+00
OD	kg CFC11 eq	1.72E-07	3.28E-08	2.15E-08	3.99E-07	9.62E-08	3.83E-10	3.42E-08
PM	disease inc.	1.19E-07	5.13E-08	3.36E-08	3.35E-08	5.47E-08	4.36E-11	5.05E-08
POF	kg NMVOC eq	5.44E-03	1.65E-03	1.08E-03	1.99E-03	7.77E-03	2.82E-06	1.62E-03
RUf	MJ	1.48E+01	3.12E+00	2.05E+00	9.75E+00	7.35E+00	1.19E-02	7.83E+00
RUmm	kg Sb eq	5.37E-06	8.78E-06	5.76E-06	6.79E-06	6.10E-06	3.75E-09	4.77E-06
WU	m3 depriv.	5.13E-01	1.01E+00	6.63E-01	8.26E-01	3.25E-01	4.43E-02	4.03E-01

Table A.7: LCA impacts Self-healing

A1-3 (Raw materials)

		Capsules	Steel fibres	Aggregate	Bitumen	Transport
IC	**Reference unit**					
AC	mol H+ eq	2.52E-02	7.58E-03	6.31E-03	2.04E-02	2.85E-03
CC	kg CO2 eq	2.41E+00	1.59E+00	3.12E-01	2.61E+00	9.68E-01
EcT	CTUe	1.08E+02	3.05E+01	2.46E+02	8.99E+01	1.19E+01
EuF	kg P eq	8.76E-04	9.56E-04	4.03E-05	5.68E-04	7.32E-05
EuM	kg N eq	7.15E-03	1.58E-03	2.18E-03	2.77E-03	5.80E-04
EuT	mol N eq	4.11E-02	1.61E-02	3.03E-02	2.98E-02	6.32E-03
Ht-C	CTUh	2.06E-09	7.68E-08	1.61E-10	2.01E-09	3.62E-10
HT-nC	CTUh	5.84E-08	4.23E-08	5.14E-09	4.65E-08	1.16E-08
IR	kBq U-235 eq	2.41E-01	4.28E-01	1.90E-02	7.01E-01	6.56E-02
LU	Pt	2.83E+02	7.09E+00	1.19E+01	1.67E+01	8.81E+00
OD	kg CFC11 eq	2.56E-07	9.72E-08	4.88E-08	2.14E-06	2.09E-07
PM	disease inc.	1.75E-07	1.43E-07	9.04E-08	1.18E-07	6.11E-08
POF	kg NMVOC eq	9.26E-03	4.60E-03	6.54E-03	2.77E-01	2.37E-03
RUf	MJ	1.99E+01	2.22E+01	3.86E+00	1.57E+02	1.43E+01
RUmm	kg Sb eq	1.44E-05	1.36E-05	1.26E-06	1.71E-05	3.36E-06
WU	m3 depriv.	1.47E+00	1.14E+00	3.63E-01	1.06E+00	6.75E-02

A4-5 Construction

		Propane	Electricity	Building machine
IC	**Reference unit**			
AC	mol H+ eq	6.40E-03	1.95E-03	2.45E-03
CC	kg CO2 eq	2.71E+00	3.75E-01	2.36E-01
EcT	CTUe	2.01E+01	3.88E+00	1.84E+00
EuF	kg P eq	1.99E-04	3.63E-04	7.32E-06
EuM	kg N eq	1.85E-03	3.38E-04	1.09E-03
EuT	mol N eq	1.99E-02	2.94E-03	1.19E-02
Ht-C	CTUh	1.12E-09	1.01E-10	7.32E-11
HT-nC	CTUh	2.69E-08	3.37E-09	1.37E-09
IR	kBq U-235 eq	4.41E-02	2.10E-01	1.46E-02
LU	Pt	2.47E+00	1.02E+00	4.02E-01
OD	kg CFC11 eq	1.99E-07	1.80E-08	5.05E-08
PM	disease inc.	8.47E-08	5.34E-09	6.52E-08
POF	kg NMVOC eq	6.89E-03	8.04E-04	3.28E-03
RUf	MJ	2.91E+01	7.71E+00	3.24E+00
RUmm	kg Sb eq	9.43E-06	8.50E-07	1.21E-07
WU	m3 depriv.	1.26E-01	2.54E-01	7.49E-03

B1-7 Use phase

		Induction machine	Vehicle (diesel)
IC	**Reference unit**	(diesel generator)	
AC	mol H+ eq	1.21E-02	1.27E-01
CC	kg CO2 eq	1.17E+00	9.49E+00
EcT	CTUe	9.09E+00	1.00E+02
EuF	kg P eq	3.61E-05	5.52E-04
EuM	kg N eq	5.36E-03	5.50E-02
EuT	mol N eq	5.87E-02	6.02E-01
Ht-C	CTUh	3.61E-10	2.96E-09
HT-nC	CTUh	6.78E-09	1.30E-07
IR	kBq U-235 eq	7.20E-02	5.61E-01
LU	Pt	1.98E+00	1.62E+01
OD	kg CFC11 eq	2.49E-07	1.90E-06
PM	disease inc.	3.21E-07	2.21E-07
POF	kg NMVOC eq	1.62E-02	1.58E-01
RUf	MJ	1.60E+01	1.25E+02
RUmm	kg Sb eq	5.99E-07	5.39E-05
WU	m3 depriv.	3.69E-02	3.97E-01

Table A.8

A1-3 (Raw materials incl. required for rehabilitation at t = 20)				
IC	**Reference unit**	Aggregate	Bitumen	Transport
AC	mol H+ eq	1.38E-02	4.24E-02	1.04E-02
CC	kg CO2 eq	6.84E-01	5.42E+00	3.52E+00
EcT	CTUe	5.39E+02	1.87E+02	4.33E+01
EuF	kg P eq	8.83E-05	1.18E-03	2.66E-04
EuM	kg N eq	4.77E-03	5.76E-03	2.11E-03
EuT	mol N eq	6.63E-02	6.20E-02	2.30E-02
Ht-C	CTUh	3.52E-10	4.19E-09	1.32E-09
HT-nC	CTUh	1.13E-08	9.67E-08	4.20E-08
IR	kBq U-235 eq	4.15E-02	1.46E+00	2.39E-01
LU	Pt	2.61E+01	3.48E+01	3.20E+01
OD	kg CFC11 eq	1.07E-07	4.44E-06	7.59E-07
PM	disease inc.	1.98E-07	2.45E-07	2.22E-07
POF	kg NMVOC eq	1.43E-02	5.75E-01	8.62E-03
RUf	MJ	8.45E+00	3.27E+02	5.19E+01
RUmm	kg Sb eq	2.75E-06	3.56E-05	1.22E-05
WU	m3 depriv.	7.96E-01	2.20E+00	2.45E-01

A4-5 Construction				
		Propane	Electricity	Building machine
AC	mol H+ eq	1.32E-02	3.91E-03	4.91E-03
CC	kg CO2 eq	5.59E+00	7.50E-01	4.73E-01
EcT	CTUe	4.14E+01	7.75E+00	3.69E+00
EuF	kg P eq	4.11E-04	7.25E-04	1.46E-05
EuM	kg N eq	3.82E-03	6.76E-04	2.17E-03
EuT	mol N eq	4.11E-02	5.89E-03	2.38E-02
Ht-C	CTUh	2.32E-09	2.03E-10	1.46E-10
HT-nC	CTUh	5.54E-08	6.73E-09	2.75E-09
IR	kBq U-235 eq	9.09E-02	4.20E-01	2.92E-02
LU	Pt	5.09E+00	2.04E+00	8.05E-01
OD	kg CFC11 eq	4.11E-07	3.59E-08	1.01E-07
PM	disease inc.	1.75E-07	1.07E-08	1.30E-07
POF	kg NMVOC eq	1.42E-02	1.61E-03	6.55E-03
RUf	MJ	6.01E+01	1.54E+01	6.48E+00
RUmm	kg Sb eq	1.95E-05	1.70E-06	2.43E-07
WU	m3 depriv.	2.61E-01	5.07E-01	1.50E-02

B1-7 Use phase			
		Vehicle (diesel)	Rejuvenator
AC	mol H+ eq	4.87E-03	2.83E-03
CC	kg CO2 eq	4.69E-01	1.40E+00
EcT	CTUe	3.66E+00	4.29E+01
EuF	kg P eq	1.45E-05	2.90E-04
EuM	kg N eq	2.16E-03	6.26E-03
EuT	mol N eq	2.36E-02	9.92E-03
Ht-C	CTUh	1.45E-10	1.08E-09
HT-nC	CTUh	2.73E-09	2.47E-08
IR	kBq U-235 eq	2.90E-02	1.44E-02
LU	Pt	7.99E-01	3.48E+02
OD	kg CFC11 eq	1.00E-07	4.06E-08
PM	disease inc.	1.29E-07	2.31E-08
POF	kg NMVOC eq	6.50E-03	3.28E-03
RUf	MJ	6.43E+00	3.10E+00
RUmm	kg Sb eq	2.41E-07	2.57E-06
WU	m3 depriv.	1.49E-02	1.37E-01

Table A.9: Eco cost as per the EN15804+A2 impact categories.

Impact category	Quantity and unit	Associated cost
Climate change	1 kg CO2 eq	0.12 €
Ozone Depletion	1 kg CFC 11 eq	0.00 €
Acidification	1 mol H+ eq	7.08 €
Eutrophication freshwater	1 kg P eq	15.32 €
Eutrophication marine	1 kg N eq	22.12 €
Eutrophication terrestrial	1 mol N eq	1.58 €
Photochemical ozone creation	1 kg NMVOS	5.67 €
ADP, metals and minerals	1 kg Sb	**note (a)**
ADP, fossil fuels	1 MJ	**note (b)**
Water use	1 m3 dep.	**note (c)**
Particulate Matter emissions (PM 2.5)	disease inc. (cases)	147,000 €
Ionizing radiation, human health	1 kBq U235 eq	**note (d)**
Eco-toxicity	1 CTUe	3.63E-03
Human toxicity cancer	1 CTUh	920,000 €
Human toxicity non-cancer	1 CTUh	216,000 €
Land Use	Pt (Production per time)	**note (e)**

(a) Different midpoint system for Abiotic depletion, metals and minerals
(b) Different midpoint system for Abiotic depletion, fossil.
(c) Different midpoint system: Baseline Water Stress
(d) as an energy carrier, it is considered separately
(e) Land-use and biodiversity considered separately, geographically sensitive

Databases used for LCI data and their geographic scope
limestone production, crushed, washed | limestone, crushed, washed 'Rest of world'
bitumen adhesive compound production, cold | bitumen adhesive compound, cold | Cutoff, U 'Europe'
market for transport, freight, lorry 16-32 metric ton, EURO6 | transport, freight, lorry 16-32 metric ton, EURO6 | Cutoff, U 'Rest of world'
market for diesel, burned in building machine | diesel, burned in building machine 'Global'

Databases used for LCI data and their geographic scope

market for propane, burned in building machine | propane, burned in building machine 'Global'

steel production, electric, low-alloyed | steel, low-alloyed | Cutoff, U 'Europe without Switzerland and Austria'

market group for electricity, medium voltage | electricity, medium voltage | Cutoff, U 'Europe without Switzerland'

market for diesel, burned in diesel-electric generating set, 18.5kW | diesel, burned in diesel-electric generating set, 18.5kW | Cutoff, U 'Global'

market for soybean oil, crude | soybean oil, crude 'Global'

seaweed, optimised production, 1kg algae, fresh weight 'Europe without Switzerland'

soda production, solvay process, calcium chloride, 'Global'

soda production, solvay process, soda ash, light-crystalline-heptahydrate, 'Global'

market for deionised water, from tap, at user 'Europe without Switzerland'

market for hydrochloric acid without water, 30% solution state, 'Global'

Table A.11: Contributions to the eco-cost per activity considered in this LCA for the Reference mixture

IC	€ per IC	C prod.	SF prod.	Agg. prod.	Bit. prod.	Transport	Construction	Maintenance
AC	0.66	-	-	0.10	0.30	0.07	0.14	0.05
CC	2.19	-	-	0.08	0.67	0.43	0.78	0.23
EcTF	3.14	-	-	1.96	0.68	0.16	0.17	0.17
EuF	0.04	-	-	0.00	0.02	0.00	0.01	0.00
EuM	0.60	-	-	0.11	0.13	0.05	0.14	0.19
EuT	0.40	-	-	0.05	0.10	0.04	0.11	0.05
HTc	0.01	-	-	0.00	0.00	0.00	0.00	0.00
HTn-c	0.05	-	-	0.00	0.02	0.01	0.01	0.01
PM	0.17	-	-	0.03	0.04	0.03	0.05	0.02
PcOF	3.57	-	-	0.08	3.26	0.05	0.12	0.78
	€ 10.82	**€ -**	**€ -**	**€ 2.46**	**€ 5.21**	**€ 0.84**	**€ 1.52**	**€ 0.78**

Table A.12: Contributions to the eco-cost per activity considered in this LCA for the Self-Healing Mixture

IC	Total € per IC	C prod.	SF prod.	Agg. prod.	Bit. prod.	Trans.	Construction	Maintenance
AC	1.52	0.18	0.05	0.04	0.14	0.04	0.07	0.99
CC	2.78	0.30	0.20	0.04	0.32	0.21	0.40	1.32
EcTF	2.29	0.39	0.11	0.89	0.33	0.08	0.09	0.40
EuF	0.06	0.01	0.01	0.00	0.01	0.00	0.01	0.01
EuM	1.73	0.16	0.04	0.05	0.06	0.02	0.07	1.34
EuT	1.30	0.06	0.03	0.05	0.05	0.02	0.05	1.05
HTc	0.08	0.00	0.07	0.00	0.00	0.00	0.00	0.00
HTn-c	0.07	0.01	0.01	0.00	0.01	0.00	0.01	0.03
PM	0.20	0.03	0.02	0.01	0.02	0.02	0.02	0.08
PcOF	2.76	0.05	0.03	0.04	1.57	0.02	0.06	0.99
	€ 12.78	**€ 1.20**	**€ 0.56**	**€ 1.13**	**€ 2.51**	**€ 0.40**	**€ 0.79**	**€ 6.20**